UNIVERSITY OF ILLINOIS
URBANA

AERONOMY REPORT NO. 85

ROCKET RADIO MEASUREMENT OF ELECTRON DENSITY IN THE NIGHTTIME IONOSPHERE

by
B. E. Gilchrist
L. G. Smith

April 1, 1979

Library of Congress ISSN 0558-0581

Aeronomy Laboratory
Department of Electrical Engineering
University of Illinois
Urbana, Illinois

Supported by
National Aeronautics and Space Administration

ABSTRACT

One experimental technique based on the Faraday rotation effect of radio waves is presented for measuring electron density in the nighttime ionosphere at midlatitudes. In the experiment high frequency linearly-polarized radio signals are transmitted to a linearly-polarized receiving system located in a spinning rocket moving through the ionosphere. Faraday rotation is observed in the reference plane of the rocket as a change in frequency of the detected receiver output. Computer analysis measures this frequency change and uses the information to obtain electron-density data. System performance is evaluated and some sources of error are identified. It is found that the dominant controlling factor for accuracy is signal-to-noise ratio. The data obtained from the above method has been useful in calibrating a Langmuir probe experiment for electron-density values of 100 cm^{-3} and greater. Data from two rocket flights are presented to illustrate the experiment.

TABLE OF CONTENTS

LIST OF TABLES

LIST OF FIGURES

1. INTRODUCTION

The University of Illinois rocket-radio propagation experiment was designed in 1963 and first used for the International Quiet Sun Year (IQSY) in 1964 and 1965. The propagation experiment is used in conjunction with a Langmuir probe to provide a detailed description of electron concentration versus altitude in the lower ionosphere. The Langmuir probe is able to follow the detailed variation (fine structure) of the ionosphere's electron concentration profile, but is unable to convert its measurement directly into electron density of sufficient accuracy. Therefore, the propagation experiment is required to provide an independent measure of average electron concentration that can be used tc calibrate the more detailed measurements of the Langmuir probe.

In general, it can be stated that for daytime launches at midlatitudes the propagation experiment, used since 1964 with only slight modification, has been very successful in providing the necessary calibration. For nighttime launches at midlatitudes, however, the propagation experiment has not been satisfactory. To overcome this problem and to help identify possible limiting sources of error, the original experiment has been modified and simplified. The original experiment measured both differential absorption and Faraday rotation; the modified experiment measures Faraday rotation only.

The modified experiment was first used for the flight of Nike Apache 14.534, launched on 10 August 1977. It was subsequently used for the flight of Nike Apache 14.533, launched on 5 January 1978. Both flights used the modified experiment at a frequency at 2.225 MHz. The flights also used the original experiment at 3.385 MHz in order to allow a comparison of the two experiments. The data from these flights are presented in this report.

The organization of this report will be to first present, in Chapter 2, the reasons for making measurements of electron density in the nighttime as well as a comparison between day and night profiles. The principle of Faraday rotation measurement and its application to both the original and modified experiment are presented in Chapter 3. Chapter 4 contains a description of the modified experiment system including the ground-based transmitter, the rocket payload and the necessary telemetry and data recording support. The data reduction process used in the experiment is presented in Chapter 5 where the final electron-density profiles are shown. The experimental limitations that have been identified in both the hardware

and software are discussed in Chapter 6. Finally, Chapter 7 contains a summary and makes conclusions about the modified propagation experiment. In addition, recommendations for future work are given.

It will be seen that both the original and modified experiments are capable of measuring electron densities as small as 100 cm^{-3}. The modified experiment is, however, easier to implement and is preferred for nighttime measurements.

2. THE NIGHTTIME *E* REGION

2.1 *General Properties and Reasons for Measuring Nighttime Profiles*

The ionosphere plays an important role in a variety of effects in radio propagation [*Lawrence et al.*, 1964] and in upper atmospheric physics [*Ratcliffe*, 1972]. Electron density and its altitude distribution are essential information in the analysis of these effects. As a result, electron-density profile measurements have been of fundamental importance. Further, considerable effort has been made in identifying and studying the sources of ionization production and the role of atmospheric dynamics as they affect these profiles. This effort has been quite successful in explaining the major features of daytime profiles, but work for nighttime profiles still remains.

The major hindrance has been the difficulty of obtaining detailed and accurate nighttime electron-density profiles. In addition to their importance in the analysis of other physical effects, these profiles can be used in revealing information about the ionosphere itself. *Smith et al.* [1974] used nighttime profiles to calculate ionization rates in the ionosphere, while *Voss and Smith* [1977] correlated certain profile characteristics with geomagnetic activity to identify energetic particles as a major source of nighttime ionization in the 120 to 200 km region under disturbed geomagnetic conditions.

A daytime ionosphere is shown in Figure 2.1 (profile 1). Electron densities in the daytime are determined by the solar radiation in the UV and X-ray parts of the spectrum. Typical electron densities are on the order of 10^5 cm^{-3} and are reproducible from day to day for a given solar zenith angle. One exception to this is the sporadic-*E* layers which can occur in both day and night profiles in the 90 to 110 km region. Figure 2.1 shows sporadic-*E* layers in profiles 1 and 2 at 100 and 106 km, respectively.

After sunset electron density falls off rapidly and within two hours reaches the typical nighttime value of 10^3 cm^{-3}. The nighttime ionosphere has been shown to have substantial amounts of temporal variations and complex altitude structure [*Smith*, 1970]. In addition, very little radiowave absorption is observed in the night [*Dickinson et al.*, 1976]. Figure 2.1 (profile 2) shows a nighttime electron-density profile taken near local midnight which demonstrates the more complex structure. As can be seen, in addition to the intense sporadic-*E* layer at 106 km a much wider layer is

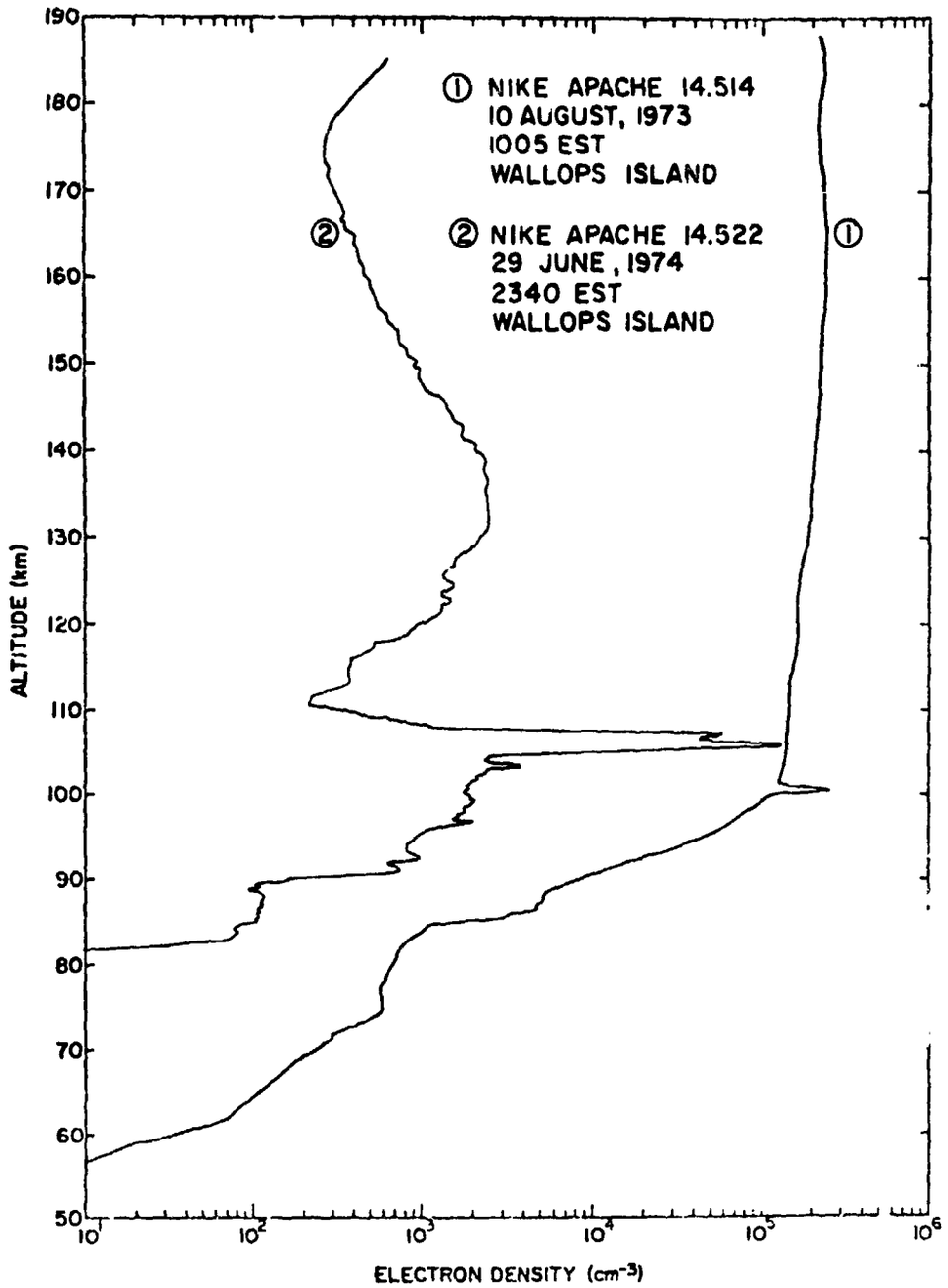

Figure 2.1 Profile 1 is representative of the daytime electron density (10^5 cm^{-3}). Towards night this electron density rapidly decays to a lower nighttime equilibrium level of 10^3 cm^{-3} (profile 2). The nighttime density profile shows much variability and structure [*Voss and Smith*, 1977].

present between 110 km and 175 km; this is the intermediate layer. The intermediate layer is located between the *E* and *F* layers with a vertical extent, typically, of tens of kilometers and is the result of a wind shear. Through the night this layer tends to move down in altitude following the atmospheric tide. The valleys below and above the layer may have electron concentrations as low as 200 cm^{-3}.

2.2 *Methods of Nighttime Profile Measurements using Rockets*

Knight [1972] has made a survey of published nighttime electron-density profiles. Of the profiles that were obtained using rocket measurements, most use versions of the Langmuir probe. However, the techniques used to calibrate the probe varied. By far the simplest procedure is to rely solely on ground-based experiments such as ionosondes. A second class of experiments is that which used an independent probing system to measure the electron density; for example, the resonance probe [*Hirao and Muraoka*, 1967] which measures plasma frequency, and the standing wave impedance probe [*Ulwick et al.*, 1967] which measures the input impedance of an antenna deployed in the ionospheric plasma.

A third class of experiments is that using rocket-borne radio propagation experiments. The major advantage of this method is that the radio signal propagates through a region of the ionosphere that has been unaffected by the passage of the rocket except for a localized region around the rocket [*Bowhill*, 1964]. Within this classification a variety of techniques have been used. In general, the radio propagation experiments can be divided into two categories according to which property of the propagated wave is measured: absorption and phase (or frequency). Many experimental systems incorporate methods to make measurements in both categories. The absorption measurement provides information on the imaginary part of the complex index of refraction for the ionosphere. Similarly, phase or frequency measurement yields information on the real part of the index of refraction. Both the real and imaginary parts can be used to calculate electron density. Further subdivision within each category is possible based upon the frequency of the propagated wave: VLF experiments have been reported that operate below the ionospheric plasma and gyrofrequencies; there are also HF and VHF experiments operating above these frequencies. Examples of these categories applied to the nighttime ionosphere will now be given.

Cartwright [1964] and *Kimura et al.* [1967] have demonstrated the use of VLF and LF Doppler frequency measurement techniques at 10.2 and 40 kHz, respectively. Each used a remotely situated transmitter with the signal propagating in the earth-ionosphere waveguide. By comparing the Doppler-shifted received signal with a stable local oscillator on board the rocket and telemetering the beat frequency to the ground, the Doppler shift is measured. Because Doppler shift is affected by the index of refraction of the medium, electron density can then be extracted. To amplify the Doppler shift before measurement, Kimura first multiplied the beat frequency by 200 thus increasing the effect. Cartwright's final electron-density profile is shown in Figure 2.2. This profile is significant as it is the first *in situ* observation of the intermediate layer in a nighttime electron-density profile.

A dispersive Doppler technique at much greater frequencies was used by *Aikin and Blumle* [1968] to measure nighttime profiles at the equator. Their experiment was based on the technique first introduced by *Seddon* [1953]. The experiment uses two harmonically related frequencies (at 24.5 and 73.5 MHz) transmitted from the rocket. These signals are received on the ground where the low frequency is multiplied up to the higher and their beat frequency determined. This frequency contains index of refraction information which can be used to give electron density. *Bowhill* [1964] gives a detailed description of this experimental technique.

Nighttime techniques to measure absorption have in general not been successful in obtaining accurate electron-density profiles. This is because of the low level of absorption present in the nighttime ionosphere and is further complicated by the presence of ionospheric reflections causing standing waves. Some success was reported by *Hall and Fooks* [1965] using a ground-based LF transmitter at 202 kHz and a rocket payload designed to sense the field strength of the signal. However, the presence of standing waves reduced the experiment's accuracy.

2.3 *Conclusion*

This chapter has discussed the characteristics of the nighttime ionosphere and presented some possible methods to measure the electron-density profiles. Experience with the rocket program of the Aeronomy Laboratory has shown that a Langmuir probe combined with a radio propagation experiment is very effective. As has been mentioned earlier, electron-density measurement using radio propagation is in general more difficult at night than during the

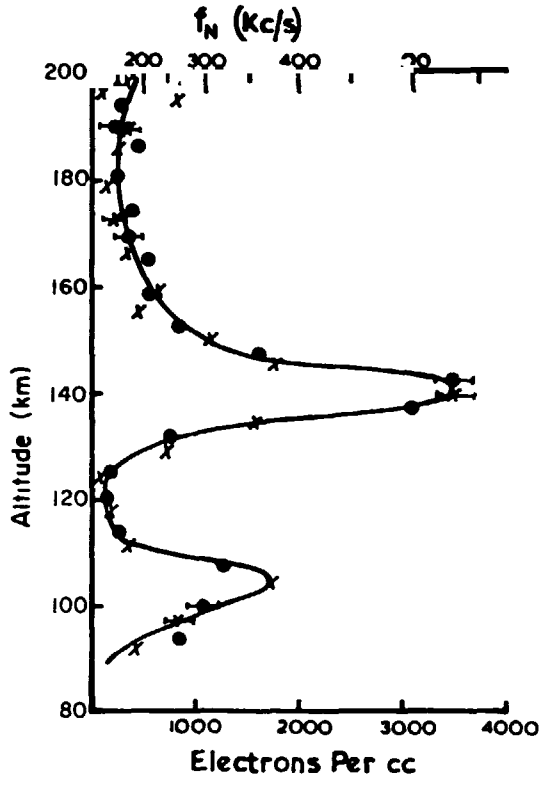

Figure 2.2 Nighttime electron-density profile as measured by *Cartwright* [1964] using VLF Doppler experiment. An intermediate layer is shown at 140 km.

day. The reasons for this can now be summarized. Firstly, the nighttime electron density is typically two orders of magnitude smaller than the daytime value, which causes a corresponding reduction in all radio ionospheric effects. Secondly, the more complex structure and regions of low electron density which occur in the nighttime *E* region require that the experiment has good altitude resolution and sensitivity. Finally, because of the possibility of strong reflections (in the virtual absence of absorption) any experiment must either be insensitive to them or account for their existence in the analysis of the results. The following chapters will present a relatively simple radio propagation experiment which appears to satisfy these nighttime requirements.

3. THE FARADAY ROTATION EXPERIMENT

3.1 *Introduction*

The original propagation experiment and the modified version for nighttime use, to be described in detail in a later chapter, both take advantage of the fact that a radio wave propagating through the ionosphere is modified in characteristic ways. If a rocket carrying a receiver can detect how the radio signal has been altered, information on electron concentration can be determined as a function of altitude. This chapter will discuss the use of Faraday rotation as a technique for measuring electron concentration.

Faraday rotation is a phenomenon in which a linearly polarized signal has its direction of polarization rotated as it travels. The use of this effect as a measurement technique for the ionosphere can be considered to be part of a general class of experiments designed to measure differential phase velocities between differing plane wave propagating modes or signals of different frequencies [*Ratcliffe*, 1972].

The chapter begins with a section discussing the general theory of Faraday rotation. This is followed by two sections describing how Faraday rotation is measured in both the original and the modified radio propagation experiments. Additionally, the section dealing with the original experiment contains a brief system description to provide a basis for comparing it with the modified experiment.

Although the particulars of the modified experiment are to be discussed in the following chapter, it will be useful at this point to briefly discuss the reasoning involved in modifying the original experiment, as this will illuminate why the particular choice of transmitted radio signal used in the modified experiment was made. As has been previously mentioned, the original propagation experiment had not been successful in providing usable nighttime data; this was because the errors internal to the experimental system were larger than the effects to be measured. However, because of the system's complexity, any significant sources of error could not be positively identified. It was felt that if the system's complexity could be reduced, some sources of error might be eliminated while simplifying the analysis of any remaining error sources. Further, because of time constraints prior to the launch of Nike Apache 14.534, no substantial hardware development for a

new experiment could be completed in time for this rocket flight. Therefore, it was concluded that the design of the new experiment must be based on existing equipment. Also, because the original experiment would still be used for daytime flights, this equipment could not be extensively modified.

There are two general areas that introduce operational complexity into the original experiment: these are the feedback amplitude control loop and its requirement for independent generation of both propagating modes. These are used in the measurement of differential absorption, which in the nighttime is negligible. Therefore, by not attempting to measure differential absorption and relying solely on Faraday rotation information, the related hardware for these two areas could be eliminated, greatly simplifying the system's operation. It will be shown that this new experiment can successfully measure the electron-density profile of the nighttime *E* region.

3.2 *Faraday Rotation*

Michael Faraday first demonstrated (in 1845) that the plane of polarization of a light beam is rotated when passed through certain substances having a magnetic field aligned along the light's direction of propagation. It was further found that the amount of rotation was proportional to the magnitude of the magnetic field and the distance traversed in the substance. This phenomenon of polarization rotation has since acquired the name of Faraday rotation or Faraday effect.

For the purposes of this report we are interested in describing the Faraday rotation of a radio wave in the lower ionosphere. To do this the necessary theoretical development begins with the work of *Appleton* [1932] and *Hartree* [1931]. By using the results of their work ionospheric Faraday rotation and the role electron concentration plays in this effect can be described.

The presence of a magnetic field in a region of free electrons, such as the ionosphere, causes a plane electromagnetic wave to split into two characteristic modes having different polarizations and indices of refraction. The Appleton-Hartree theory can be used to determine both the polarization and index of refraction for each mode. Their theory is based upon the following assumptions: the ionospheric medium is electrically neutral, electron-neutral collision frequency is independent of electron energy, the magnetic field is uniform, and a background of essentially stationary ions exists.

The Appleton-Hartree analysis begins by assuming that a plane electromagnetic wave (satisfying Maxwell's equations) is propagating in a positive z direction

$$\vec{E}(z,t) = \vec{E}\, e^{j(\omega t - kz)} \tag{3.1}$$

where k is the propagation constant and ω is the frequency of the radio signal. $\vec{E}$ is a complex vector containing amplitude and phase information for the directional components of the electric field

$$\vec{E} = \hat{x}\, E_x + \hat{y}\, E_y \tag{3.2}$$

Figure 3.1 presents a simplified diagram depicting the situation. Also indicated is the earth's magnetic field, $\vec{B}$, with an assumed direction, and the ionosphere with electron density, N_e.

The motion of ionospheric free electrons is affected both by the earth's magnetic field and by the travelling electromagnetic wave. This is reflected in the equation of motion for each electron

$$m \frac{d^2\vec{r}}{dt^2} + m\nu \frac{d\vec{r}}{dt} = -e \left(\frac{d\vec{r}}{dt} \times \vec{B} \right) - e\, \vec{E}(z,t) \tag{3.3}$$

where $\vec{r}$ is the electron displacement from some rest position, ν is the electron-neutral collision frequency and m and e are the mass and charge of the electron. The above equation makes the assumption that the magnetic field associated with the travelling wave is very much smaller than the earth's magnetic field.

By requiring that an electromagnetic wave simultaneously satisfy all Maxwell's equations as well as equation (3.3) the work of Appleton and of Hartree demonstrated that only two possible travelling waves of the form in equation (3.1) could propagate through the ionosphere. Each of these has a unique polarization and index of refraction; before these can be given the following standard symbols must be introduced:

$$X = \frac{\omega_N^2}{\omega^2} = \frac{N_e\, e^2}{m\epsilon_o \omega^2} \tag{3.4}$$

$$Y = \frac{\omega_H}{\omega} = \frac{e|\vec{B}|}{m\omega} \tag{3.5}$$

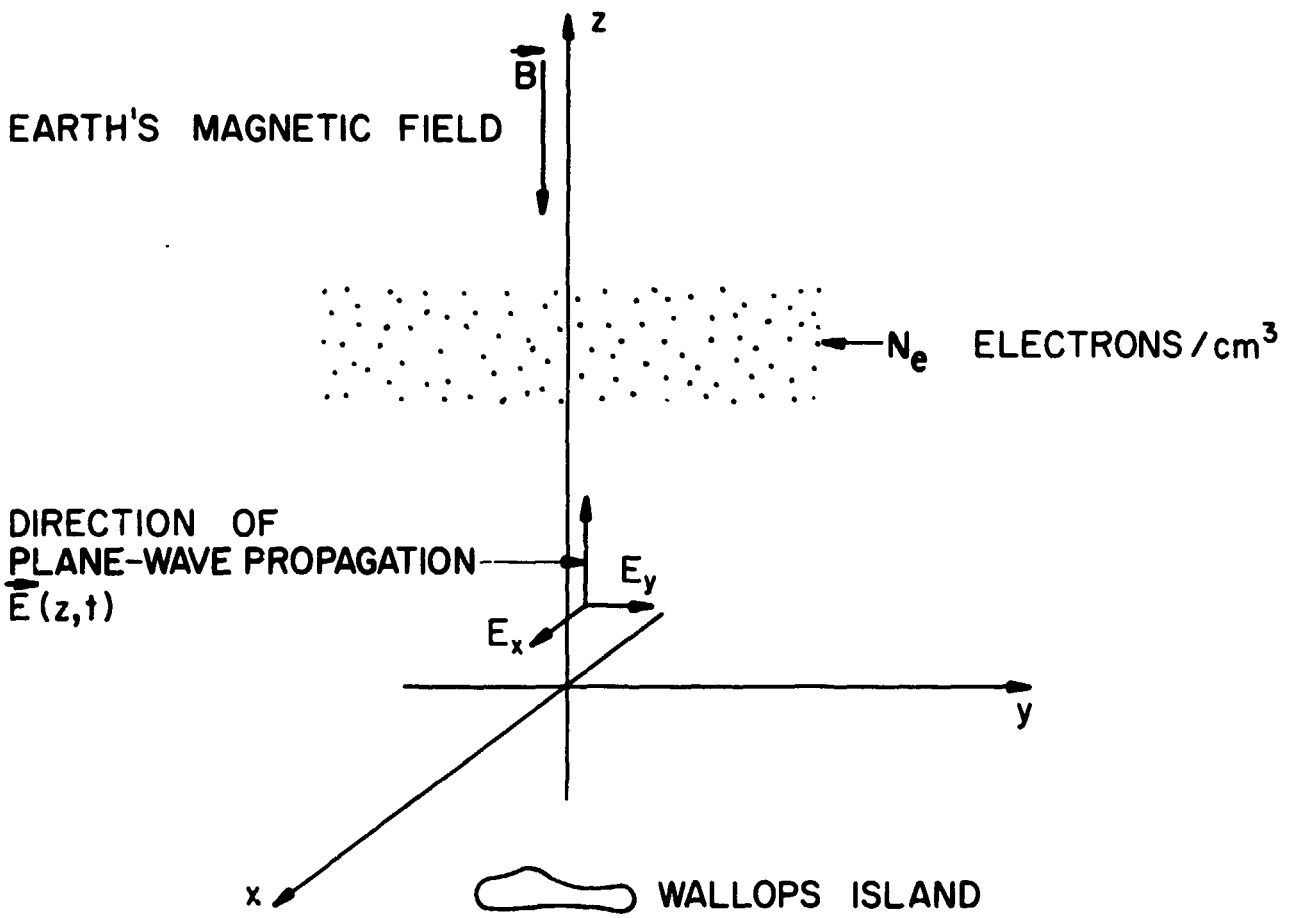

Figure 3.1 Simplified model at midlatitudes (Wallops Island) for plane-wave propagation through a region with electron density, N_e, and magnetic field, $\vec{B}$. At midlatitudes the earth's magnetic field is nearly antiparallel to the z axis.

$$Z = \frac{\nu}{\omega} \tag{3.6}$$

where ω_N is the plasma frequency and ω_H is the gyrofrequency. Also, $Y_L = Y\cos\theta$ and $Y_T = Y\sin\theta$, where θ is the angle between the magnetic field and the direction of propagation.

Using the above defined terms, the allowed propagating modes have two possible polarizations given by the equation

$$R = \frac{E_x}{E_y} = -j\left[\frac{Y_T^2/2Y_L}{(1-X-jZ)} \mp \left(1 + \frac{Y_T^4/4Y_L^2}{(1-X-jZ)^2}\right)^{\frac{1}{2}}\right] \tag{3.7}$$

Further, the index of refraction (n) is given by

$$n^2 = \frac{k^2}{\omega^2\varepsilon_o\mu_o} = 1 - \frac{X}{1-jZ-jY_LR} \tag{3.8}$$

Equation (3.8) is known as the Appleton-Hartree formula. The above equations define a unique pair of values of polarization and index of refraction for each travelling wave mode.

For the midlatitude launches from Wallops Island, Virginia, the earth's magnetic field is only 20° from a downward orientation (i.e., the $-z$ direction). This implies that the propagating wave is nearly longitudinal with respect to the magnetic field. It follows that

$$\left|\frac{Y_T^2}{2Y_L}\right| << |1-X-jZ| \tag{3.9}$$

Using this fact equations (3.7) and (3.8) can be simplified, yielding

$$R = \pm j \tag{3.10}$$

$$n^2 = 1 - \frac{X}{1-jZ\pm Y_L} \tag{3.11}$$

This is known as the quasi-longitudinal approximation. A further approximation can also be made in equation (3.11) when the local plasma frequency is much lower than the radio frequencies used in the propagation experiment, thus from equation (3.4) it follows that

$$X << 1 \tag{3.12}$$

Taking advantage of this fact, equation (3.11) becomes, by binomial expansion,

$$n = 1 - \frac{\frac{1}{2} X}{1 - jZ \pm Y_L}$$

or, on rationalizing,

$$n = \left[1 - \frac{1}{2} \frac{X(1 \pm Y_L)}{(1 \pm Y_L)^2 + Z^2} \right] - j \left[\frac{1}{2} \frac{XZ}{(1 \pm Y_L)^2 + Z^2} \right] \tag{3.13}$$

Equations (3.10) and (3.13) when used with the minus sign represent the parameters for the ionospheric mode called the ordinary mode. Similarly with the plus sign these equations represent the parameters for the second mode called the extraordinary mode. The ordinary mode has right-handed circular polarization while the extraordinary has left-handed. Equation (3.13) has the form of

$$n_R = \mu_R - j \chi_R \qquad \text{(for the ordinary mode)} \tag{3.14}$$

$$n_L = \mu_L - j \chi_L \qquad \text{(for the extraordinary mode)} \tag{3.15}$$

When these are substituted in equation (3.1), the travelling waves become

$$\vec{E}_R(z,t) = \vec{E}_R \, e^{-\chi_R k_o z} \, e^{j(\omega t - \mu_R k_o z)} \tag{3.16}$$

$$\vec{E}_L(z,t) = \vec{E}_L \, e^{-\chi_L k_o z} \, e^{j(\omega t - \mu_L k_o z)} \tag{3.17}$$

where k_o is the free space propagation constant. It is seen that χ represents attenuation per unit length and μ represents phase per unit length.

Using the above analysis, Faraday rotation in the ionosphere can now be explained. To begin, assume that a linearly-polarized plane wave is propagating in the $+z$ direction as in Figure 3.1. Also assume that it is incident on a semi-infinite ionospheric region of free electrons having a uniform magnetic field directed in the $-z$ direction. Because the magnetic field is longitudinal to the direction of propagation, the travelling wave must be decomposed into the modes defined in equations (3.16) and (3.17) as

it travels through the ionosphere. Any linearly-polarized wave may be directly decomposed into the vector sum of equal amplitude right- and left-handed polarized electric field vectors, which are the ordinary and extra-ordinary modes, respectively. Figure 3.2(a) shows this situation graphically where it is assumed the two polarized waves are initially in phase at $z = 0$. After the two modes have propagated a small distance, Δz, they are no longer in phase because their propagation constants are different. The effect of this is to cause the axis of polarization to rotate, which is the Faraday effect and is shown in Figure 3.2(b). The amount of rotation caused by this incremental change in position is

$$\Delta\Omega = \frac{k_o}{2} (\mu_R - \mu_L)\Delta z \tag{3.18}$$

where a positive sign indicates rotation in a left-handed sense.

For the purposes of the rocket radio propagation experiment the above analysis is not complete until the effect of the moving rocket is included. For a rocket moving in a $+z$ direction, this can be done by expressing equation (3.18) in a differential form

$$\frac{d\Omega}{dt} = \frac{k_o}{2} (\mu_R - \mu_L) \frac{dz}{dt} \tag{3.19}$$

Equation (3.19) can be rewritten in the following form

$$F = \frac{1}{2\pi} \frac{d\Omega}{dt} = \frac{1}{4\pi} (k_R - k_L) v \tag{3.20}$$

where F is the Faraday rate in deg s^{-1}, v is the rocket velocity in m s^{-1}, and

$$k_R = k_o \mu_R \tag{3.21}$$

$$k_L = k_o \mu_L \tag{3.22}$$

It follows from equations (3.4), (3.13), and (3.20) that Faraday rate is directly proportional to electron density. Therefore, experimentally measuring Faraday rate as a function of altitude can provide information on electron density also as a function of altitude.

It should be pointed out here that although approximations have been made in the preceding analysis to allow relatively simple formulation of

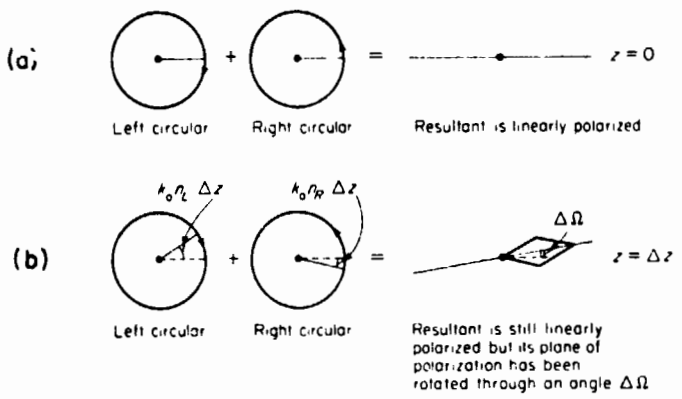

Figure 3.2 Illustration of the rotation of the plane of polarization of the resultant wave as it propagates from a) $z = 0$ to (b) $z = \Delta z$ along the magnetic field [*Yeh and Liu*, 1972].

Faraday rotation, these approximations are *not* used in the actual experiment.

3.3 *Measurement Technique of the Original Propagation Experiment*

This section describes the Faraday rotation measurement used in the original radio propagation experiment. Also a general system and operational description is presented that will be useful later in understanding the details of the modified experiment.

The original propagation experiment measures both Faraday rotation and differential absorption to obtain electron-density information [*Mechtly et al.*, 1967]. To accomplish this the experiment uses a transmitted radio signal that easily allows both effects to be identified. This is done by independently generating two signals having the polarizations of the ionospheric ordinary and extraordinary modes and then combining them to form a composite transmitted signal. Figure 3.3 graphically describes the signals which are transmitted from a location near the launch site. This diagram represents what is seen at the rocket looking back towards the transmitting source. Figure 3.3(a) is the right-hand polarized (RHP) ordinary mode signal while Figure 3.3(b) is the left-hand polarized (LHP) extraordinary mode signal. It will be noted that the ordinary mode has a larger amplitude. The ordinary to extraordinary power ratio is adjusted to be 10 db; the reason for this will be discussed later in the section. Also, the extraordinary mode signal is adjusted to be nominally 500 Hz higher in frequency than the ordinary mode.

When the electric fields from these two signals are added, the resultant shown in Figure 3.3(c) is obtained. This composite signal, seen at the rocket, is an electric field vector that spins in a right-handed sense at the mean of the ordinary and extraordinary frequencies. Because the amplitudes of the two circularly polarized signals are different, the composite signal is elliptically polarized. Further, since the two signals have different frequencies, the polarization ellipse spins in a left-handed sense at a rate of 250 Hz. As this composite signal propagates through the ionosphere, Faraday rotation will cause the phase of the polarization ellipse to increase with altitude according to the electron-density profile. In the reference plane of the moving rocket this change in phase appears as a change in frequency of the polarizati rotation rate. By measuring the frequency of polarization rotation and extracting the contribution due to Faraday effect the electron density can be determined.

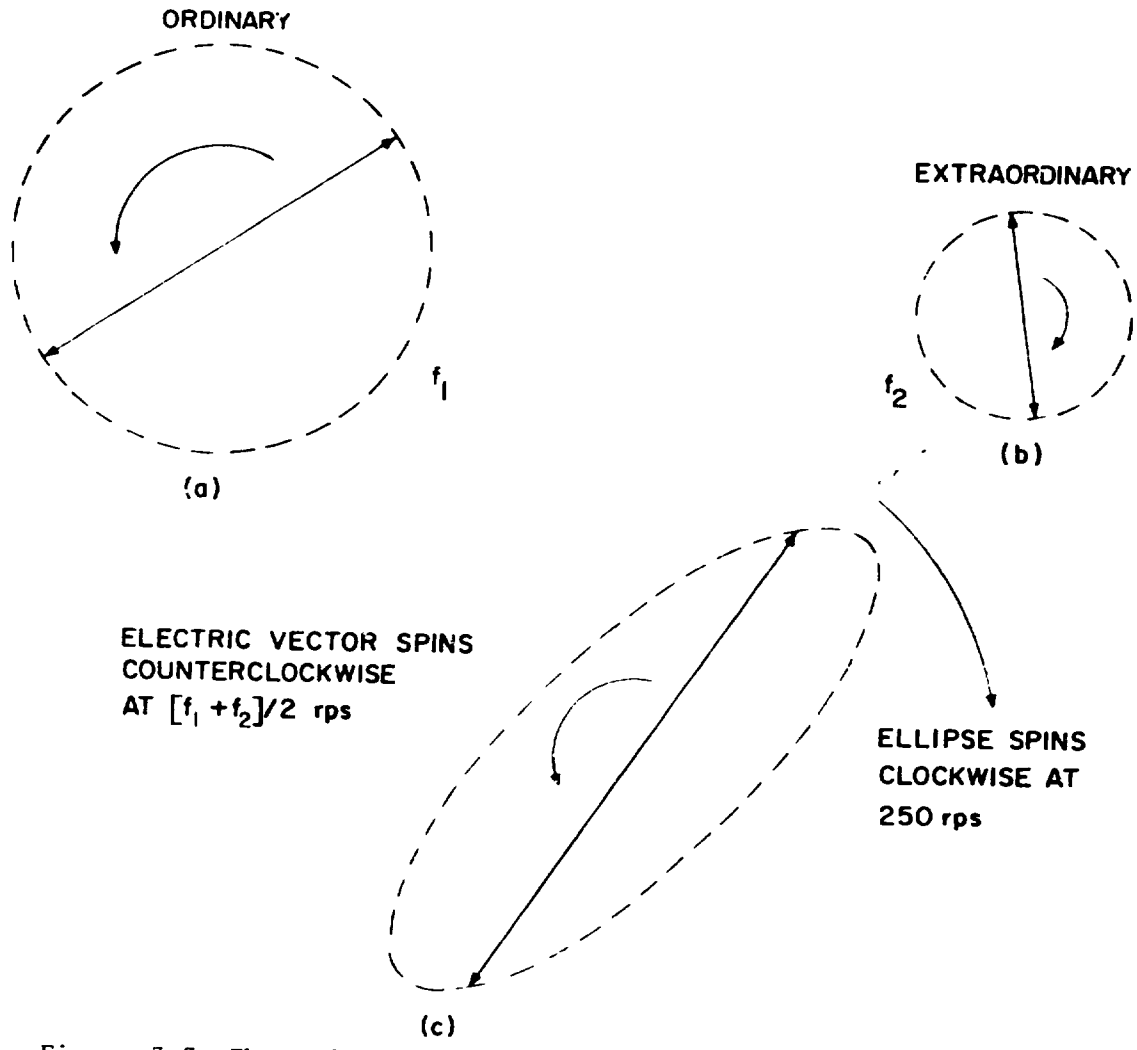

Figure 3.3 The ordinary mode signal (a) and the extraordinary mode signal (b) combine to form the polarization ellipse (c) [*Salah and Bowhill*, 1966].

The complete propagation experiment consists of two systems operating simultaneously, but on separate radio frequencies. The choice of operating frequencies is made to provide significant daytime differential absorption while still leaving sufficient signal for Faraday rotation measurements; the 2 to 5 MHz range has been found to adequately satisfy the above requirements. Typically one system operates at 2.225 MHz, while the other operates at either 3.385 or 5.040 MHz. The criterion for choosing between the latter two frequencies is based upon which frequency combination is expected to give the best tradeoff between measurement sensitivity and highest attainable measurement altitude. Measurement sensitivity is inversely related to the square of the frequency, but lower frequencies have lower reflection heights beyond which the experiment ceases to operate. In general 3.385 MHz is used at night and 5.040 MHz in the day.

The design of the original experiment was based on the best available technology of the early 1960's. The approach taken was to keep the rocket payload simple at the expense of a more complicated ground transmitting system. The resulting design was capable of supplying Faraday rotation resolution to ±5 deg s^{-1} and absorption resolution to ±0.2 dB. When combined with Langmuir probe data, electron-density profile accuracy of better than ±10% could be obtained [*Mechtly*, 1974]. However, the above results could only be obtained during the daytime.

The rocket payload equipment required to receive the composite transmitted signal of Figure 3.3(c) includes a linearly polarized ferrite loop antenna feeding an AM-type receiver. That is, the receiver detector is of the envelope detection type and follows the carrier's envelope. For the original experiment this type of receiver works well with the composite signal because the 10 dB power ratio between ordinary and extraordinary modes (32% modulation) prevents the signal, as seen at the spinning rocket, from ever undergoing any deep modulation nulls. If a modulation null did occur, the envelope detector would cause intermodulation of the signal preventing proper operation of the experiment.

The receiver output consists of DC and 500 Hz signals having an amplitude ratio corresponding to the 10 dB power ratio of the two modes. As seen in Figure 3.4, the output of the receiver is telemetered to the ground where it is recorded and also sent to the transmitter van location.

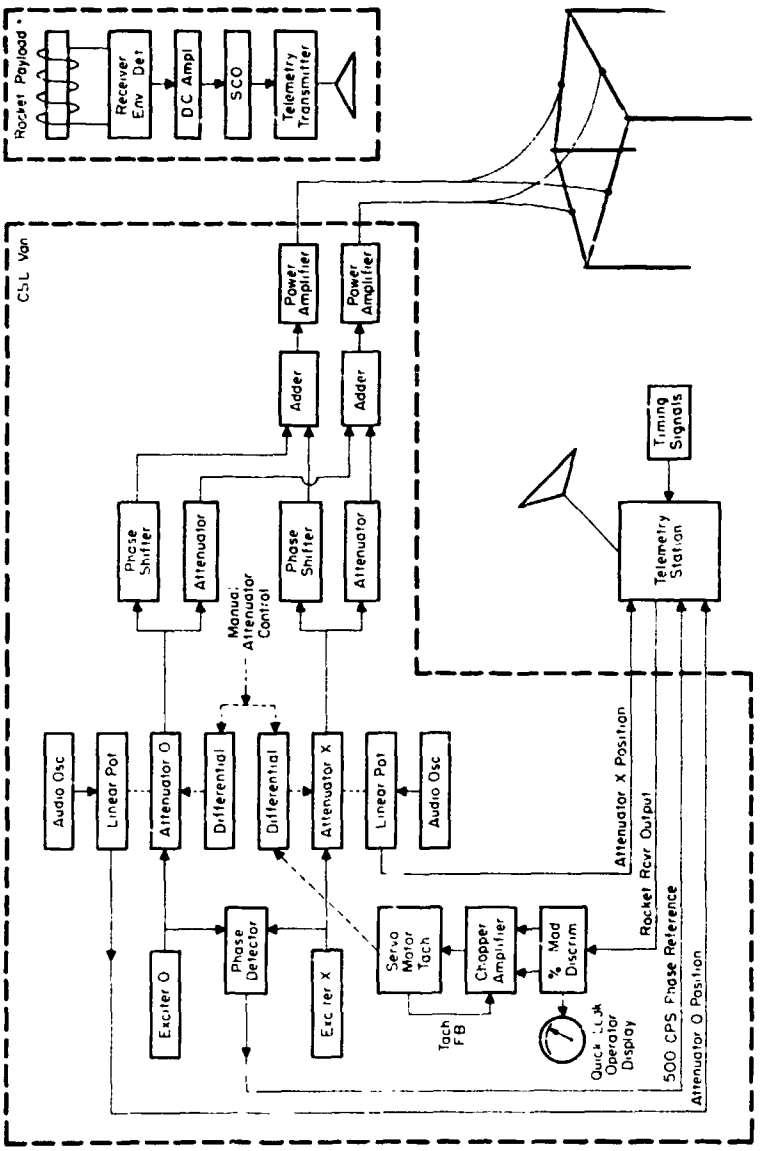

Figure 3.4 Radio propagation experiment system block diagram [*Knoebel et al.*, 1965].

At the van, the percent modulation of the receiver output is measured. Under conditions of differential absorption the extraordinary mode is absorbed more than the ordinary mode which causes the percent modulation to decrease below its nominal 32% value. When this is observed in the van, the extraordinary transmitter power is automatically increased to compensate for it. Power levels are recorded during the flight providing a measure of differential absorption.

In addition to recording the transmitter power levels and the receiver outputs, the 500 Hz difference frequencies observed in the transmitter van and the rocket spin rate are also recorded. Faraday rate is measured from each system after the flight by measuring the 500 Hz difference frequency, f_d, the rocket spin rate, f_s, and the receiver output frequency, f_o, and using the relation

$$F = \tfrac{1}{2}[f_o - f_d - 2f_s] \tag{3.23}$$

where F is the Faraday rate.

Several techniques have been used through the years to make the necessary frequency measurements. Initially a mechanical system was used to directly obtain the Faraday rate [*Gooch et al.*, 1966]. Later a technique of counting zero crossings was used for frequency measurement [*Slekys and Mechtly*, 1970]. Recently, to give better discrimination against noise, a method of using spectral measurements from Fourier analysis has been used. This later approach is also used in the modified propagation experiment and is described in a later chapter. Further information on the original experiment can be found in *Knoebel et al.* [1965], *Gooch et al.* [1966], *Knoebel and Skaperdas* [1966], and *Morrison* [1966].

3.4 *Principle of Measurement Using Modified Propagation Experiment*

This section contains a general description of the modified radio propagation experiment; the details will be given in the following chapters. The purpose here is first to describe the signal that is transmitted from the ground installation to the rocket and to show how ionospheric effects modify this signal as received at the rocket. Then the modification of the signal by the receiver in the rocket payload will be discussed.

3.4.1 *Signal at the input of the receiver.* The rocket, while it is ascending in the region of interest, has a velocity vector, $\vec{v}$, that to a

good approximation lies along the line of sight from the ground transmitting installation; see Figure 3.5(a). The receiving antenna is sensitive to electric field components that are perpendicular to the rocket axis, which is usually nearly parallel to $\vec{v}$. Figure 3.5(b) shows the field components, of the modified experiment, as they are observed from the rocket's location looking back towards the transmitter. The two linearly polarized CW signals emanating from the same dipole antenna are decomposed into right- and left-hand polarized electric field vectors; these are shown in the figure as A_R and A_L, respectively. The numerical subscripts differentiate between the two signals, which are at slightly different frequencies, f_1 and f_2 where $(f_1-f_2) \cong 500$ Hz as in the original experiment. Because the two CW sources are incoherent, their respective right- and left-hand mode vectors coincide along the polarization axis at different times. However, because both signals are transmitted from the same antenna and with the assumption that their frequencies are close enough, they both share the same polarization axis. As the rocket ascends through the ionosphere, this polarization axis will rotate due to Faraday rotation; in the northern hemisphere an observer positioned as shown in Figure 3.5(a) will see the polarization axis rotate in a left-hand sense as the rocket ascends. Finally, a phasor is included in Figure 3.5(b) that represents the rocket receiving antenna with effective length, l. This antenna rotates at the rocket spin rate, f_s, in a right-hand sense. It is only sensitive to that component from each of the four electric field vectors that is parallel to the antenna phasor at each instant of time.

A mathematical description of the rocket receiver input voltage, $V(t)$, can now be derived. To do this, the transmitted signal will be modified in stages to include the rocket's spin, forward velocity, and the ionospheric effects to be measured. This is begun by providing a mathematical description of the two independent CW signals as seen by a stationary observer positioned at some far-field altitude, z.

As was stated previously each of the linearly polarized CW signals can be described as the sum of right- and left-hand polarized waves. In the immediate vicinity of the observer, these can be approximated as plane waves travelling with propagation constants, k_R and k_L, for right- and left-hand polarization, respectively. Mathematically, the electric fields of the two independent CW signals can be described as:

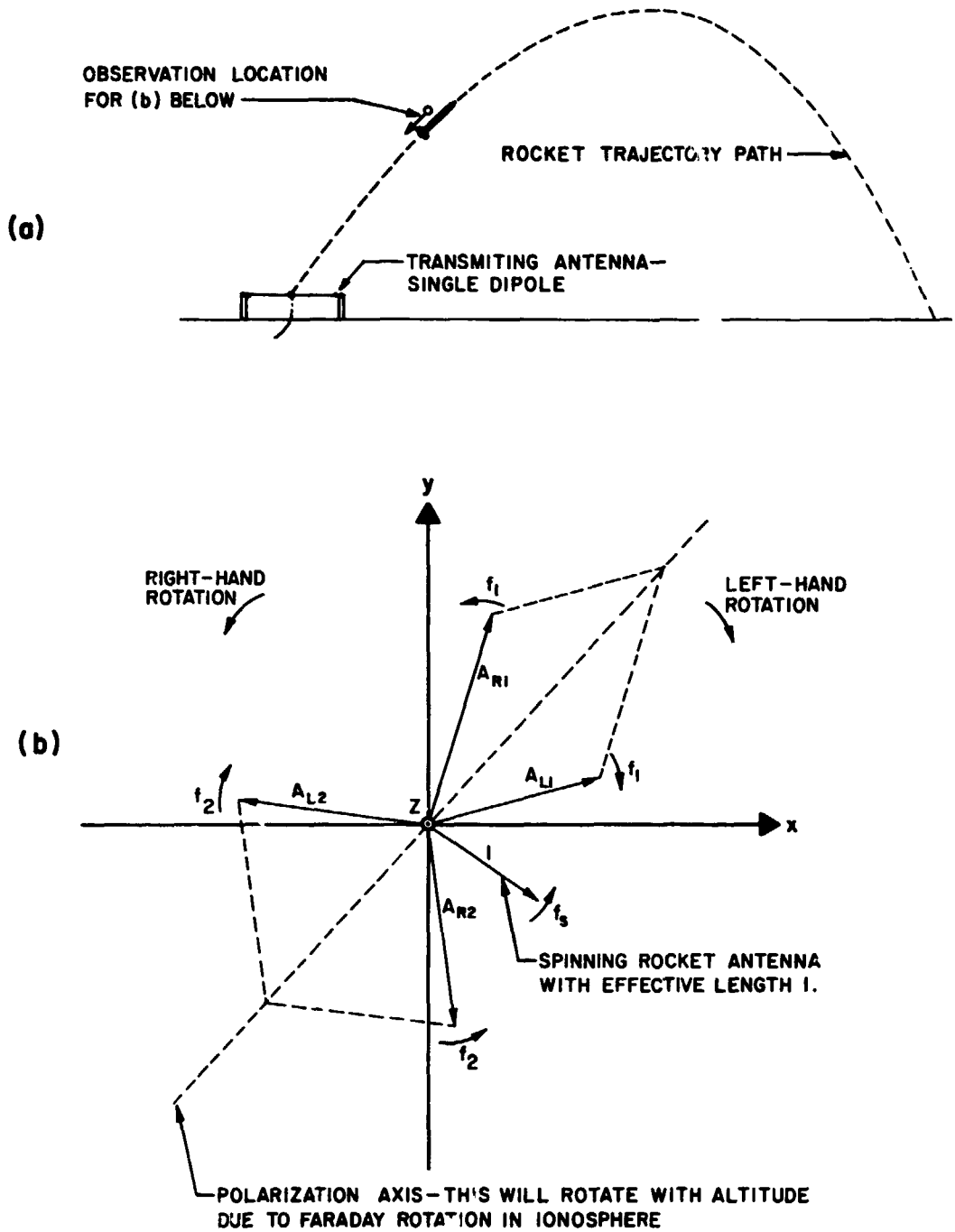

Figure 3.5 Transmitted signal decomposed into right- and left-hand polarized components at frequencies f_1 and f_2 as seen from the rocket. No differential absorption case ($A_R = A_L$) shown. f_s is the roll rate of the rocket.

$$\vec{E}_1 = A_{R1}[\hat{x}\cos(\omega_1 t - k_R z + \theta_1) + \hat{y}\sin(\omega_1 t - k_R z + \theta_1)]$$
$$+ A_{L1}[\hat{x}\cos(\omega_1 t - k_L z + \theta_1) - \hat{y}\sin(\omega_1 t - k_L z + \theta_1)]$$

and

$$\vec{E}_2 = A_{R2}[\hat{x}\cos(\omega_2 t - k_R z + \theta_2) + \hat{y}\sin(\omega_2 t - k_R z + \theta_2)]$$
$$+ A_{L2}[\hat{x}\cos(\omega_2 t - k_L z + \theta_2) - \hat{y}\sin(\omega_2 t - k_L z + \theta_2)]$$

where

$\omega_1 = 2\pi f_1$ and $\omega_2 = 2\pi f_2$ are the carrier frequencies

k_R is the right-handed (ordinary) mode propagation constant

k_L is the left-handed (extraordinary) mode propagation constant

θ_1 and θ_2 are the carrier phases

A_{R1} and A_{R2} are the right-handed amplitudes

A_{L1} and A_{L2} are the left-handed amplitudes

It was assumed above that since $f_1 \simeq f_2$, then $k_{R1} \cong k_{R2} = k_R$ and $k_{L1} \cong k_{L2} = k_L$. The error caused by this assumption is at least an order of magnitude smaller than the desired accuracy.

The total transmitted signal is

$$\vec{E}_T = \vec{E}_1 + \vec{E}_2$$

The frequency spectrum of $\vec{E}_T$ is shown in Figure 3.6(a) where the amplitudes of the spectral components are shown. It can be seen that the ordinary and extraordinary modes for $\vec{E}_1$ and $\vec{E}_2$ are at the same frequency.

The spinning rocket antenna can be described mathematically as

$$\vec{A} = l[\hat{x}\cos(\omega_s t + \phi) + \hat{y}\sin(\omega_s t + \phi)]$$

where

l is the antenna effective length

$\omega_s = 2\pi f_s$ is the rocket spin rate

ϕ is the rocket spin phase constant

(a) Spectrum as seen by stationary observer

(b) Spectrum seen by rotating observer below the ionosphere (f_s = rotation rate in ccw direction)

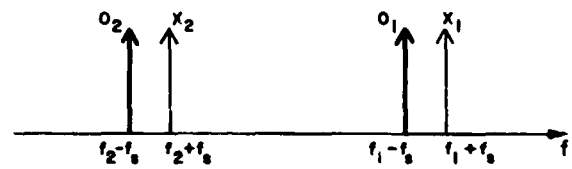

(c) Spectrum seen by rotating and linearly moving (away from source) observer

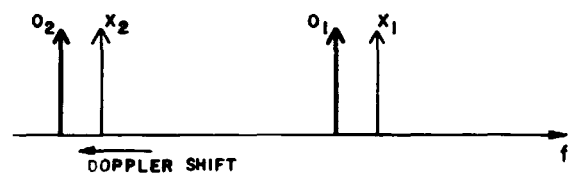

(d) Same as (c) above, but with O and X experiencing different phase velocities, as in the ionosphere

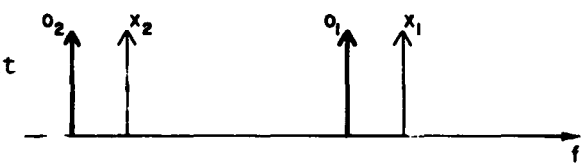

(e) Final spectra from original experiment

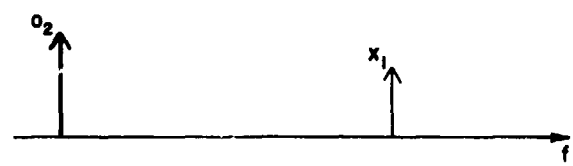

Figure 3.6 The signals received at the rocket are frequency shifted due to: (b) rocket spin, (c) Doppler shift and (d) dispersive (or differential) Doppler shift. In the original experiment only the O_2 and X_1 components are transmitted.

It has been assumed above that the rocket antenna spins in a right-handed sense with respect to its direction of travel, which in this case is in a positive-z direction, at a spin rate f_s.

The RF voltage at the input to the receiver is simply the projection of $\vec{E}_T$ along $\vec{A}$, that is

$$V(t) = \vec{E}_T \cdot \vec{A}$$

Therefore

$$\begin{aligned} V(t) = \ell\{&\cos(\omega_s t+\phi)[A_{R1}\cos(\omega_1 t-k_R z+\theta_1) + A_{L1}\cos(\omega_1 t-k_L z+\theta_1) \\ &+ A_{R2}\cos(\omega_2 t-k_R z+\theta_2) + A_{L2}\cos(\omega_2 t-k_L z+\theta_2)] \\ &+ \sin(\omega_s t+\phi)[A_{R1}\sin(\omega_1 t-k_R z+\theta_1) - A_{L1}\sin(\omega_1 t-k_L z+\theta_1) \\ &+ A_{R2}\sin(\omega_2 t-k_R z+\theta_2) - A_{L2}\sin(\omega_2 t-k_L z+\theta_2)]\} \end{aligned}$$

Using trigonemetric identities $V(t)$ can be put into a form that shows its spectral components

$$\begin{aligned} V(t) = \ell\{&A_{R1}\cos[(\omega_1-\omega_s)t-k_R z+\theta_1-\phi] + A_{L1}\cos[(\omega_1+\omega_s)t-k_L z+\theta_1+\phi) \\ &+ A_{R2}\cos[(\omega_2-\omega_s)t-k_R z+\theta_2-\phi) + A_{L2}\cos[(\omega_2+\omega_s)t-k_L z+\theta_2+\phi]\} \end{aligned}$$

The frequency spectrum of $V(t)$ is shown in Figure 3.6(b). As can be seen, the effect of a right-handed (counter-clockwise) spinning observer is to pull the ordinary mode down in frequency and the extraordinary mode up in frequency by the spin rate, f_s.

To complete this mathematical description of the modified experiment, one must also include the effects of the rocket's motion. Typically, the rocket velocity, v, is between 1.0 and 1.5 km s^{-1} at the altitudes of interest. There are two important effects that should be included. First, assuming that the rocket moves in a positive-z direction, it follows that z in the above equations, becomes a function of time, i.e., $z = vt$. Second, since the rocket is moving away from the transmitter, there will be a downward Doppler shift in the received frequencies.

The relation between the transmitted frequencies f_1 and f_2 and the received Doppler-shifted frequencies, f_1' and f_2', can be quantified. For an observer receding from a source, the equation relating f to f' is

$$f' = f(1 - \frac{v}{c})$$

where c is the speed of light. For typical rocket velocities and operating frequencies, the observed frequency is lowered by 10 to 20 Hz. This absolute shift in carrier frequency is of little consequence because the experiment is based on comparison of signals having nearly the same frequency which are all Doppler shifted. However, the differential Doppler shift between signal components may be of concern. The formula relating the difference frequency, $f_M = f_1 - f_2$, to its differential Doppler counterpart, $f'_M = f'_1 - f'_2$, is

$$f'_M = f_M(1 - \frac{v}{c})$$

For f_M = 500 Hz and v between 1.0 and 1.5 km s^{-1}, f'_M would be between 499.9983 and 499.9975 Hz. If, as in the original experiment, it is assumed that $f_M \cong f'_M$ the measured Faraday rate will be low by 1 to 3 mHz. This can cause an error of 10 to 100 cm^{-3} in electron concentration, which can be of significance in the nighttime ionosphere. The effect of Doppler shift on the signal spectra is shown in Figure 3.6(c); the small differential Doppler shift cannot be observed on this scale.

When the above effects are included in the analysis, $V(t)$ becomes:

$$V(t) = \mathcal{L}\{A_{R1}\cos[(\omega'_1-\omega_s-k_R v)t+\theta_1-\phi] + A_{L1}\cos[(\omega'_1+\omega_s-k_L v)t+\theta_1+\phi]$$
$$+ A_{R2}\cos[(\omega'_2-\omega_s-k_R v)t+\theta_2-\phi] + A_{L2}\cos[(\omega'_2+\omega_s-k_L v)t+\theta_2+\phi]\} \quad (3.24)$$

The ionospheric phase velocity information, which will be used to retrieve electron-density information, is now contained in the frequency parameters of each of the sinusoidal arguments as $k_R v$ and $k_L v$. This spectral modification is included in Figure 3.6(d); as is implied, the nighttime ionosphere provides only small changes in the observed spectra.

When a similar mathematical analysis is done for the original experiment, its spectra are ideally as shown in Figure 3.6(e) where there is only one ordinary and one extraordinary spectral component present, having different amplitudes. It is interesting to point out that a practical limitation of the original experiment has been its inability to generate perfect circular polarization at each frequency. The result of this is that in practice, O_1 and X_2 components present in Figure 3.6(d) were also present, with reduced

amplitudes, in the spectra of the original experiment; at times this has caused problems in the experiment's operation.

3.4.2 *Signal at the output of the receiver.* The preceding section presented a graphical and mathematical description of the signal in the modified experiment as it appears at the input of the receiver included in the rocket payload. In this section the analysis is extended to the output of the receiver. It is this signal which is telemetered to the ground and Fourier analyzed to give the Faraday rotation rates from which electron concentration is deduced.

The receiver's detector is of the envelope detection type. Envelope detectors are primarily designed for applications where the received signal is amplitude modulated (AM). For other modulation types, such as single-sideband (SSB) and double-sideband (DSB), the envelope detector cannot be used without introducing non-linear intermodulation effects; for the case where the modulating signal is a complex waveform, such as voice, this intermodulation would have disastrous effects. Even so, if the received signal has a spectrum with discrete spectral components, as is the case for the modified radio propagation experiment, it is still possible to identify the spectral components at the output of the detector. This is because a discrete spectrum in turn generates another discrete spectrum, albeit more complicated, and providing adequate frequency resolving techniques are utilized, this more complicated spectrum can still be used for Faraday rotation analysis.

To understand how the receiver input signal, derived in Section 3.4.1, is modified in the detection process, the envelope detector's operation must be explained. As the name implies, this type of detector is designed to follow the carrier envelope. The modulated carrier can be represented by the general expression

$$V(t) = K(t) \cos(\omega t) \tag{3.25}$$

The output of the envelope detector is proportional to the carrier's time varying amplitude, i.e., $|K(t)|$.

It will be noted from the above, that the carrier envelope is such that

$$\text{carrier envelope} = \begin{cases} K(t), & K(t) \geq 0 \\ -K(t), & K(t) < 0 \end{cases}$$

This implies that sign ambiguities can result, without additional information, when attempting to extract $K(t)$ from the carrier envelope, $|K(t)|$. This situation is illustrated in Figure 3.7 where the carrier envelopes for the particular examples of AM and DSB modulation are identified; the modulating source is a pure sine wave. As can be seen $K(t)$ cannot be directly obtained from the DSB carrier envelope. However, because the envelope detector modifies $K(t)$ in a predictable fashion, it is still possible to obtain pertinent information about $K(t)$ from the detector output, such as amplitude and frequency, since it is already known that $K(t)$ is a pure sinusoid. In a similar fashion, because the receiver input for the modified experiment is known, it is possible to identify its carrier envelope, which is the envelope detector output. In doing this, the spectral components at the detector output can be identified, which will allow the extraction of the needed Faraday rate information.

To determine the carrier envelope of the receiver input signal equation (3.24) must be modified to have the form of expression (3.25). This can be done, in two steps, using trigonometric identities and the fact that $\omega_2' = \omega_1' - \omega_M'$. First, equation (3.24) is modified as follows

$$V(t) = \mathcal{L}\{[A_{R1}\cos\theta_{R1}+A_{L1}\cos\theta_{L1}+A_{R2}\cos\theta_{R2}+A_{L2}\cos\theta_{L2}]\cos(\omega_1' t) + [A_{R1}\sin\theta_{R1}-A_{L1}\sin\theta_{L1}+A_{R2}\sin\theta_{R2}+A_{L2}\sin\theta_{L2}]\sin(\omega_1' t)\} \tag{3.26}$$

where

$$\theta_{R1} = (\omega_s + k_R v)t - \theta_1 + \phi$$

$$\theta_{L1} = (\omega_s - k_R v)t + \theta_1 + \phi$$

$$\theta_{R2} = (\omega_M' + \omega_s + k_R v)t - \theta_2 + \phi$$

$$\theta_{L2} = (\omega_M' - \omega_s + k_L v)t - \theta_2 + \phi$$

Second, two new functions, $K(t)$ and $\alpha(t)$, are defined as follows

$$K(t)\cos\alpha(t) = A_{R1}\cos\theta_{R1}+A_{L1}\cos\theta_{L1}+A_{R2}\cos\theta_{R2}+A_{L2}\cos\theta_{L2} \tag{3.27}$$

$$K(t)\sin\alpha(t) = A_{R1}\sin\theta_{R1}-A_{L1}\sin\theta_{L1}+A_{R2}\sin\theta_{R2}+A_{L2}\cos\theta_{L2} \tag{3.28}$$

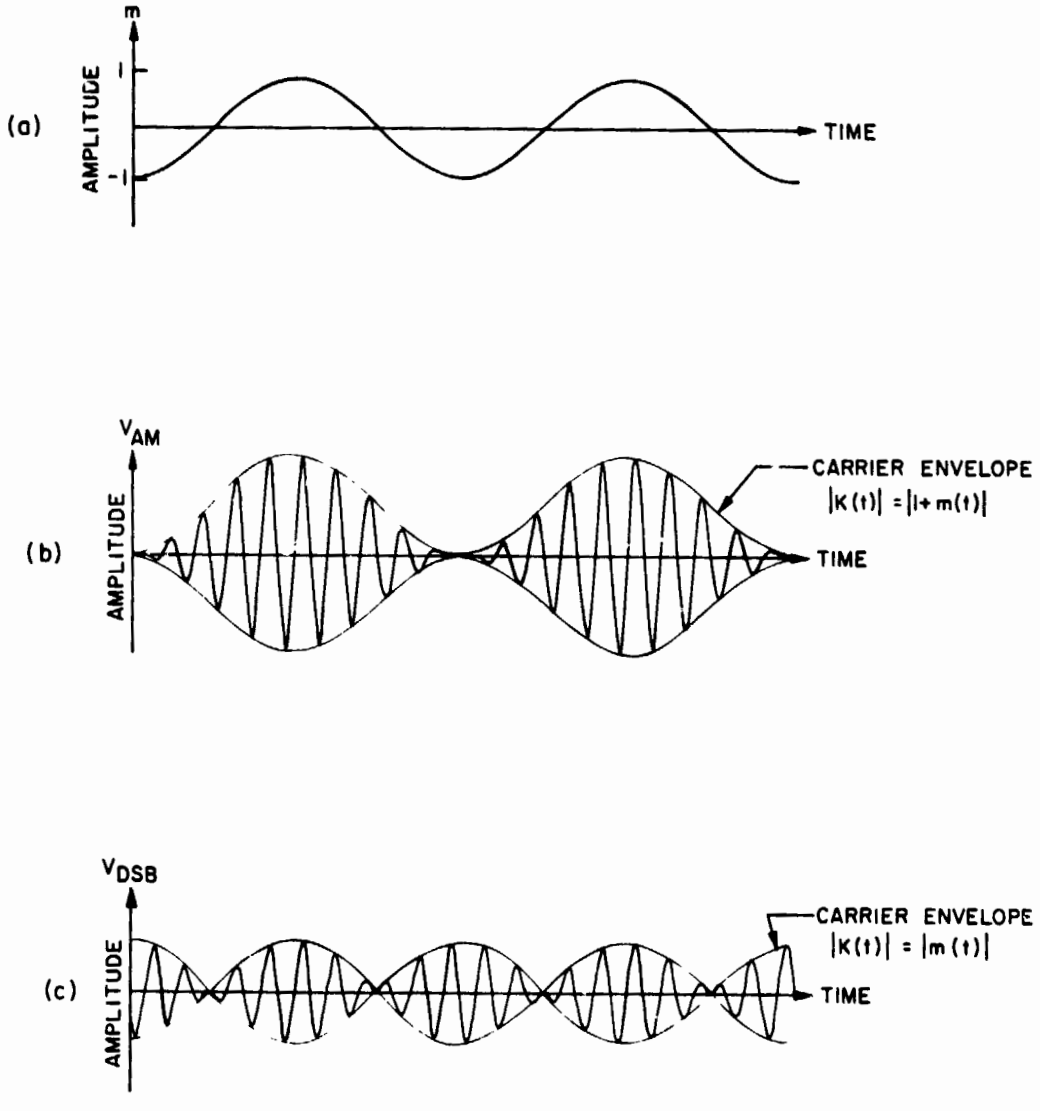

Figure 3.7 Carrier envelope, $|K(t)|$, for AM and DSB modulation. (a) Modulation signal, $m(t)$; (b) AM modulated signal, $V_{AM}(t) = [1+m(t)]\cos(\omega t)$; (c) DSB modulated signal, $V_{DSB}(t) = m(t)\cos(\omega t)$.

If equation (3.27) is substituted into equation (3.26), the result is

$$V(t) = \mathcal{L}k(t)\cos[\omega_1' t - \alpha(t)] \tag{3.29}$$

As can be seen, except for a multiplicative constant that is not critical to the analysis, the carrier envelope can now be identified as $|K(t)|$. The phase modulation term, $\alpha(t)$, is of no consequence to the envelope detector which is not sensitive to phase or frequency modulation effects about the carrier frequency.

From this analysis a specific equation for the detector output can be derived. Combining equations (3.27) and (3.28) it follows that

$$\begin{aligned} K^2(t) &= [K(t)\cos\alpha(t)]^2 + [K(t)\sin\alpha(t)]^2 \\ &= [A_{R1}^2 + A_{L1}^2 + A_{R2}^2 + A_{L2}^2] + 2A_{R1}A_{L1}\cos(\theta_{R1}+\theta_{L1}) \\ &\quad + 2A_{R1}A_{R2}\cos(\theta_{R2}-\theta_{R1}) + 2A_{R1}A_{L2}\cos(\theta_{L2}\ \theta_{R1}) \\ &\quad + 2A_{L1}A_{R2}\cos(\theta_{L1}+\theta_{R2}) + 2A_{L1}A_{L2}\cos(\theta_{L1}+\theta_{L2}) \\ &\quad + 2A_{R2}A_{L2}\cos(\theta_{R2}-\theta_{L2}) \end{aligned} \tag{3.30}$$

By further algebraic manipulation we have

$$\begin{aligned} K^2(t) &= [A_{R1}+A_{L1}+A_{R2}+A_{L2}]^2 + 2A_{R1}A_{L1}[\cos(\theta_{R1}+\theta_{L1})-1] \\ &\quad + 2A_{R1}A_{R2}[\cos(\theta_{R2}-\theta_{R1})-1] + 2A_{R1}A_{L2}[\cos(\theta_{L2}-\theta_{R1})-1] \\ &\quad + 2A_{L1}A_{R2}[\cos(\theta_{L1}+\theta_{R2})-1[+ 2A_{L1}A_{L2}[\cos(\theta_{L1}+\theta_{L2})-1] \\ &\quad + 2A_{R2}A_{L2}[\cos(\theta_{R2}-\theta_{L2})-1] \end{aligned} \tag{3.31}$$

The next step is to determine the square root of $K^2(t)$. An appropriate method to do this is by using a binomial expansion of $K^2(t)$. The particular form of $K^2(t)$, shown in equation (3.31), was chosen because it satisfies the necessary convergence conditions of the square-root binomial expansion. It is only necessary to carry out the expansion to the second degree ($[1+X]^{\frac{1}{2}} = 1 + X/2 - X^2/8 + \ldots$) to demonstrate and identify the relevant features of the detector output spectrum. However, because of the length of

even this much expansion, the final analytic expression for the detector output will not be given here; instead, a partial listing of the output's spectral components, resulting from the second degree expansion, is given in Table 3.1. For each frequency listed, its corresponding phase and approximate amplitude is given. The amplitude information is only approximate because each degree of the expansion has terms that contribute to these amplitudes; therefore, only the dominant amplitude term is shown for each spectral component in the tabulation.

Table 3.1 shows that the spectral components with the largest amplitudes are f_b and f_f. The components at multiples of $[2f_s + (1/2\pi)(k_R-k_L)v]$ away in frequency from these have decreasing amplitudes. Figure 3.8 graphically presents an actual receiver output spectrum taken from early in the flight of Nike Apache 14.533. As can be seen, the predicted spectrum is quite evident.

Table 3.1 Partial frequency spectrum of detector output

	FREQUENCY	PHASE	APPROXIMATE AMPLITUDE*
f_a	DC	---	$B - \frac{1}{B}(A_{R1}A_{L1} + A_{R1}A_{R2} + A_{R1}A_{L2} + A_{L1}A_{R2} + A_{L1}A_{L2} + A_{R2}A_{L2}) + \cdots$
f_b	$2f_s + \frac{1}{2\pi}(k_R - k_L)v$	$\pm 2\phi$	$\frac{1}{B}(A_{R1}A_{L1} + A_{R2}A_{L2}) + \cdots$
f_c	$4f_s + 2\frac{1}{2\pi}(k_R - k_L)v$	$4\phi + \pi$	$\frac{1}{B^3}(A_{R1}A_{L1}A_{R2}A_{L2}) + \cdots$
f_d	$f_M' - 4f_s - 2\frac{1}{2\pi}(k_R - k_L)v$	$-\theta_2 + \theta - 4\phi + \pi$	$\frac{1}{2}\frac{1}{B^3}(A_{R1}^2A_{L1}A_{L2} + A_{R1}A_{R2}A_{L2}^2) + \cdots$
f_e	$f_M' - 2f_s - \frac{1}{2\pi}(k_R - k_L)v$	$-\theta_2 + \theta_1 - 2\phi$	$\frac{1}{B}(A_{R1}A_{L2}) + \cdots$
f_f	f_M'	$-\theta_2 + \theta_1$	$\frac{1}{B}(A_{R1}A_{R2} + A_{L1}A_{L2}) + \cdots$
f_g	$f_M' + 2f_s + \frac{1}{2\pi}(k_R - k_L)v$	$-\theta_2 + \theta_1 + 2\phi$	$\frac{1}{B}(A_{L1}A_{R2}) + \cdots$
f_h	$f_M' + 4f_s + 2\frac{1}{2\pi}(k_R - k_L)v$	$-\theta_2 + \theta_1 + 4\phi + \pi$	$\frac{1}{2}\frac{1}{B^3}(A_{R1}A_{L1}^2A_{R2} + A_{L1}A_{R2}^2A_{L2}) + \cdots$
	$\vdots$		

* where $B = A_{R1} + A_{L1} + A_{R2} + A_{L2}$

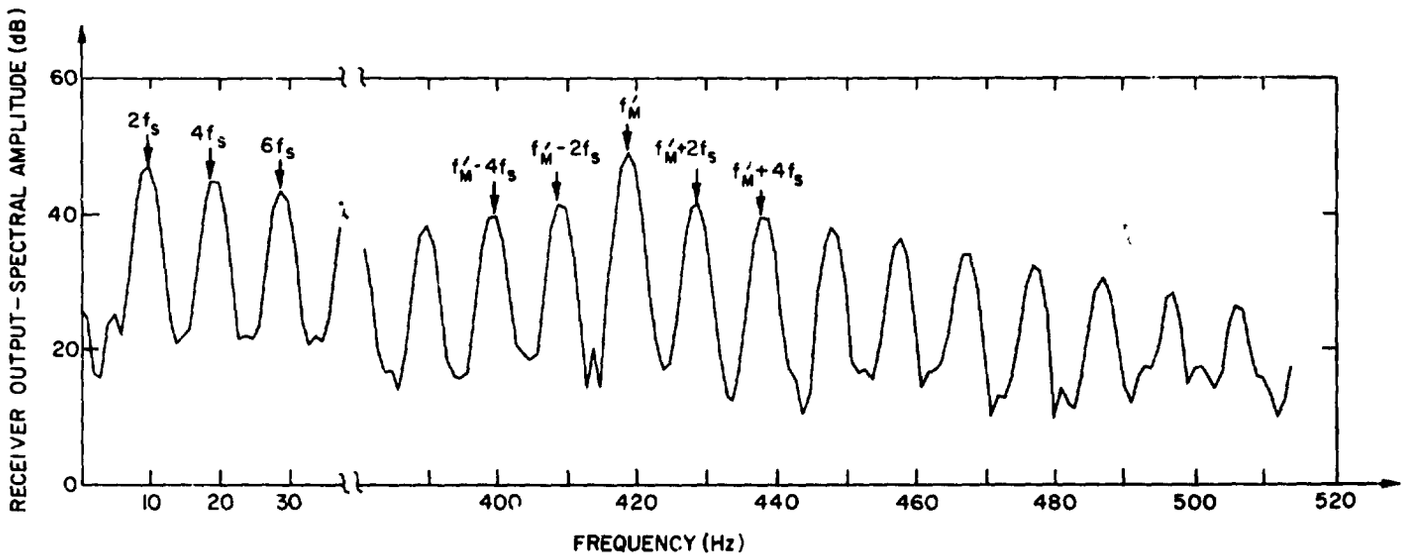

Figure 3.8 The spectrum of the receiver output for the frequency range 0 to 40 Hz and 380 to 520 Hz. These data are from Nike Apache 14.534. The principal frequencies are identified in terms of the rocket spin rate, f_s, and the Doppler-shifted difference frequency, f'_M.

4. MODIFIED PROPAGATION EXPERIMENT

This chapter is divided into three sections, corresponding to the three major parts of the experimental system. First, the ground-based transmitter system will be described. Second, the experiment payload package will be presented. Finally, the telemetry and data recording systems will be briefly explained.

4.1 *Ground-Based Transmitter*

The transmission source for the dual CW signal described in the previous chapter will be detailed in this section. As in the original experiment, two systems are simultaneously operated at different frequencies; system 1 operates at 2.225 MHz while system 2 operates at either 3.385 or 5.040 MHz. The two systems are not identical, as they were developed for the original experiment at different times. Therefore, there is some difference in system configuration between systems 1 and 2 for the modified experiment; pertinent differences will be identified in the following discussion.

Block diagrams for systems 1 and 2 are shown in Figures 4.1 and 4.2, respectively. When compared with the block diagram of the original experiment (Figure 3.4), the reduction in system complexity is apparent. The fundamental difference between systems 1 and 2 is the method used to generate the independent carrier signals, at frequencies f_1 and f_2. Once these signals are generated and combined, both systems operate identically by providing power amplification and transmission using a half-wave dipole.

The technique used in system 1 to generate the carrier signals is to use two separate crystal oscillator stages. Both crystals are housed in the same linear-proportional crystal oven. Placement of the crystals in the same oven helps reduce relative drift between the two frequencies. The use of a linear-proportional oven is preferred to an on-off type, as the latter causes sudden jumps in the frequency difference, $f_M = f_1 - f_2$, whenever the oven is switched on or off. The output of each oscillator is used to drive a buffer-amplifier stage before being combined. Additionally, the oscillator outputs are sampled and then mixed together to form the 500 Hz reference difference frequency, f_M. This reference frequency is both monitored at the transmitter and sent, on data lines, to the main base telemetry station where it is recorded on analog and digital magnetic tapes for later analysis.

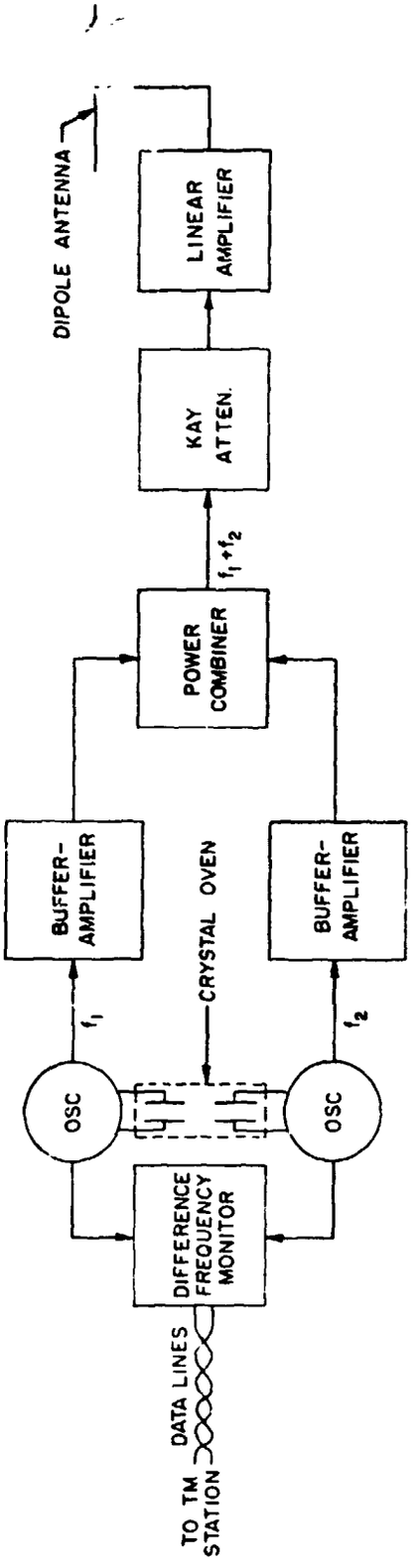

Figure 4.1 System 1 configuration.

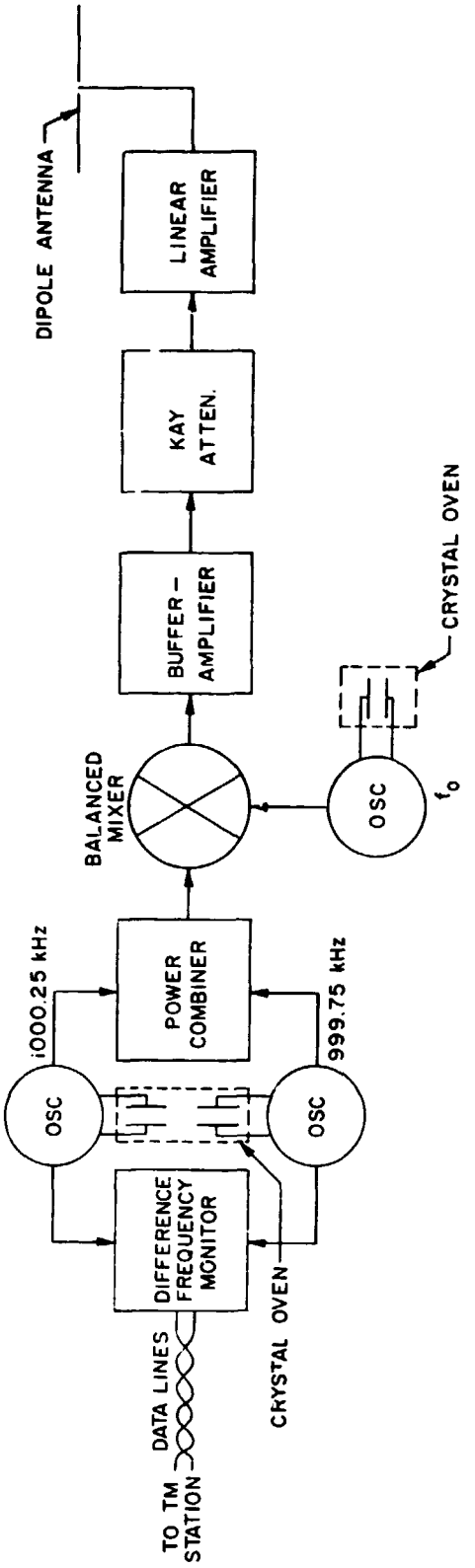

Figure 4.2 System 2 configuration.

System 2 follows a slightly different approach to generate f_1 and f_2. As shown in Figure 4.2 there are again two independent crystal oscillator stages whose crystals are located together in a crystal oven; their frequencies are 1000.250 kHz and 999.750 kHz. The outputs are directly added together, using a power combiner. As in system 1, the difference frequency is also generated for monitoring and recording purposes. The power-combined signal is then balance-mixed with another local oscillator. The local oscillator frequency, f_o, is chosen so that the sum frequency, f_o+1 MHz, is either at 3.385 or 5.040 MHz, whichever is desired. The output of the balance-mixer goes to a buffer-amplifier stage, which in turn is used to drive the linear power amplifier.

Up to this point, the value of the reference difference frequency, f_M, has been quoted as 500 Hz. However, for the modified propagation experiment any frequency between 400 and 530 Hz would be acceptable, as it is not critical to the experiment that f_M is exactly 500 Hz. It has been found to be critical though, that the difference frequencies from systems 1 and 2 should not be the same. The reason for this is because there is cross-talk interference in either the data lines or equipment at the main base telemetry station prior to recording the reference frequencies for each system. If the frequencies are nearly the same, they can introduce error in the post-flight measurement of these reference frequencies for data analysis purposes. It has been established that there should be a minimum 35 Hz separation between the two reference frequencies to provide adequate protection against cross-talk on any of the recorded data.

The power combiner, used in both systems is a Merrimac Industries power splitter/combiner. It is a broad-band device specified to cover 2 to 32 MHz, although tests demonstrated that it worked satisfactorily at the 1 MHz frequency used in system 2. These units were also specified to have a 1 W maximum input power; they were found to also operate satisfactorily at a 2 W power level in system 1. The signal level was adjusted from each oscillator so that equal signal levels were observed, on an oscilloscope, at the output of the combiner.

The original propagation experiment used two linear amplifiers in each system to provide the necessary transmitted power level; the modified experiment uses only one amplifier in each system. These amplifiers are specified to deliver 1 kW for an input of 100 mW; in practice, however,

the maximum output is about 500 W. Each amplifier has an adjustable automatic level control, which is set at its minimum sensitivity position to prevent any amplifier-induced distortion. The input level to each amplifier is controlled by a Kay step attenuator and it is adjusted for maximum output power without overdriving the amplifier.

The output of the amplifier from each system is used to feed a half-wave dipole. The dipole for each system is placed between telephone poles approximately 90 feet high and is fed with RG-8 coaxial cable. A balun (matching transformer) is used at the center of the dipole to help prevent radiation from the coaxial cable which would distort the far-field antenna pattern. The antenna input impedance as seen through the coaxial feedline is typically 50 to 60 Ω at an angle of ±20°.

4.2 *Payload Instrumentation*

The rocket payload used in the modified radio propagation experiment is identical to that used in the original experiment. The payload section, used in the propagation experiment, will now be described.

The primary payload section, related to the propagation experiment, consists of two receivers used to receive the ground-based transmitted signals from systems 1 and 2; the receiver in current use was developed at the University of Illinois Aeronomy Laboratory by G. W. Henry, Jr. A photograph of three completed receivers is shown in Figure 4.3; note that one has its covers removed to show the electronic circuits. These receivers were designed to provide good selectivity with a linear detector and AGC response over a wide dynamic range in a rocket environment. Receiver specifications are shown in Table 4.1 and its detector characteristics are shown in Figure 4.4.

The antennas used by the payload receivers are magnetic dipoles, and their design is typical of that used in transitorized portable broadcast-band radios. Each antenna consists of two ferrite rods used in the core of a Litz wire coil which is in parallel resonance with variable capacitors. A shielded one-turn symmetrical loop is used to couple the antenna to the receiver input. A schematic of the antenna circuit is shown in Figure 4.5. The payload section, housing the two antennas is shown in Figure 4.6. It will be noted from this photograph that each antenna is placed to maintain symmetry between the two ferrite rods; this is done to keep the antenna pattern as symmetrical as possible.

Table 4.1 Receiver performance data

Input:	Frequency	2.0 to 5.0 MHz
	Level	-110 to +10 dBm
	Impedance	To match ferrite antenna (600 Ω nominal)
Selectivity:	-6 dB bandwidth	2.811 kHz
	-60 dB bandwidth	4.490 kHz
	Shape factor (60/6)	1.597 : 1
Spurious responses (for 2.225 MHz f_c): (2.0 to 5.0 MHz range)		2122 kHz -103 dB 2156 kHz -103 dB 2451 kHz -102 dB 2470 kHz -100 dB 3135 kHz - 50 dB (Image)
AGC Characteristics:		
	Detector Output Flatness:	±0.2 V, -110 to +10 dBm input
	AGC Voltage Range:	+5.0 V (minimum signal) 0.8 V (maximum signal)
	AGC Output Impedance	2.2 kΩ
Detector Characteristics:		
	Nominal dc Output	2.0 ±0.2 V
	Linearity	±2 dB, 0.15 to 4.0 V
	Temperature Stability (-10 to +50°C)	Gain: ±3 dB Offset: ±0.05 V
	Output Impedance	Less than 10 Ω
Power Requirements:		+20 to +35 V @ 55 mA -20 to -35 V @ 15 mA
Environment:	Temperature	-10 to +50°C
	Shock and Vibration	0 to 15 g, sinusoidal 30g, random

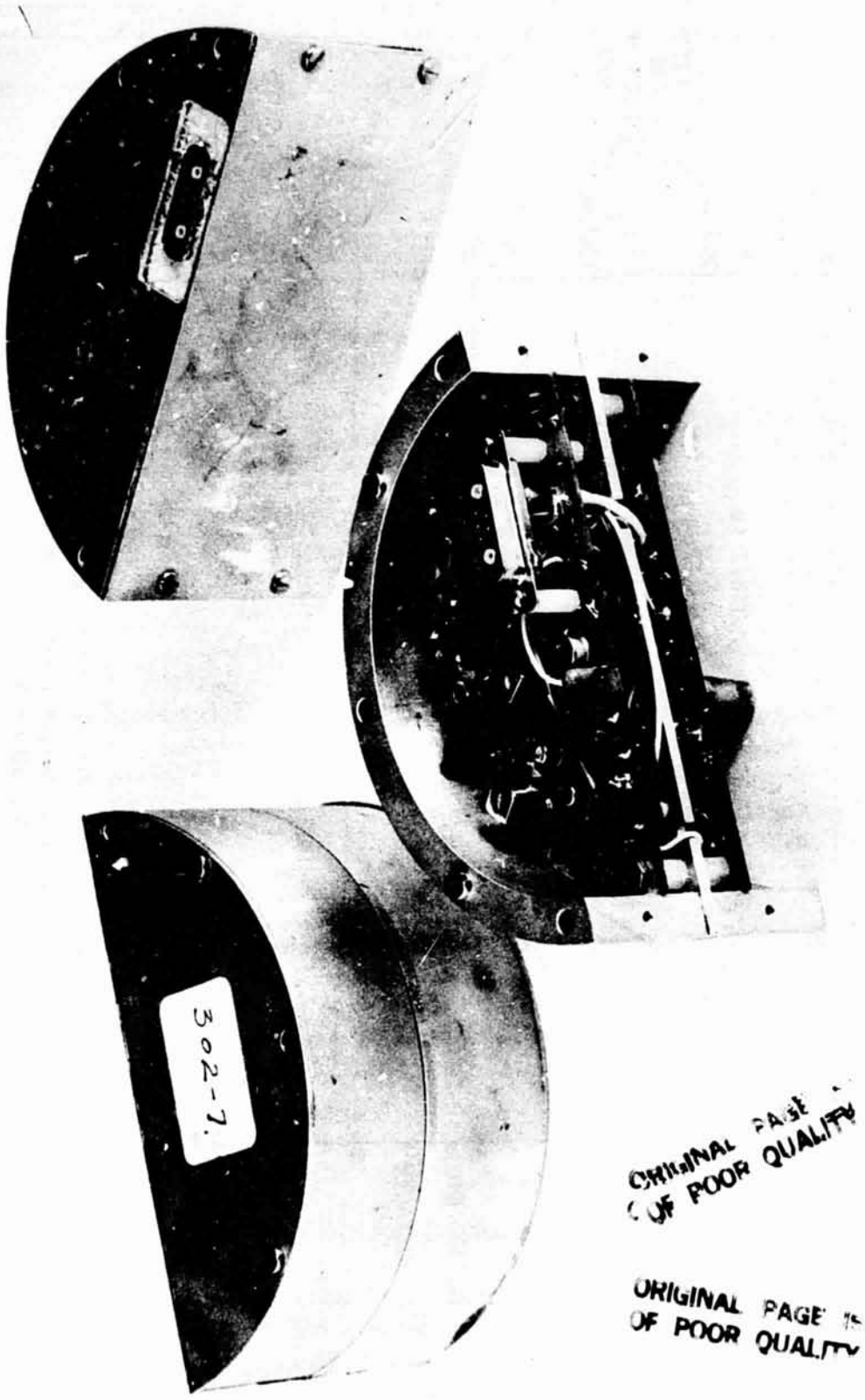

ORIGINAL PAGE IS
OF POOR QUALITY

Figure 4.3 Three completed receivers, one with cover plates removed.

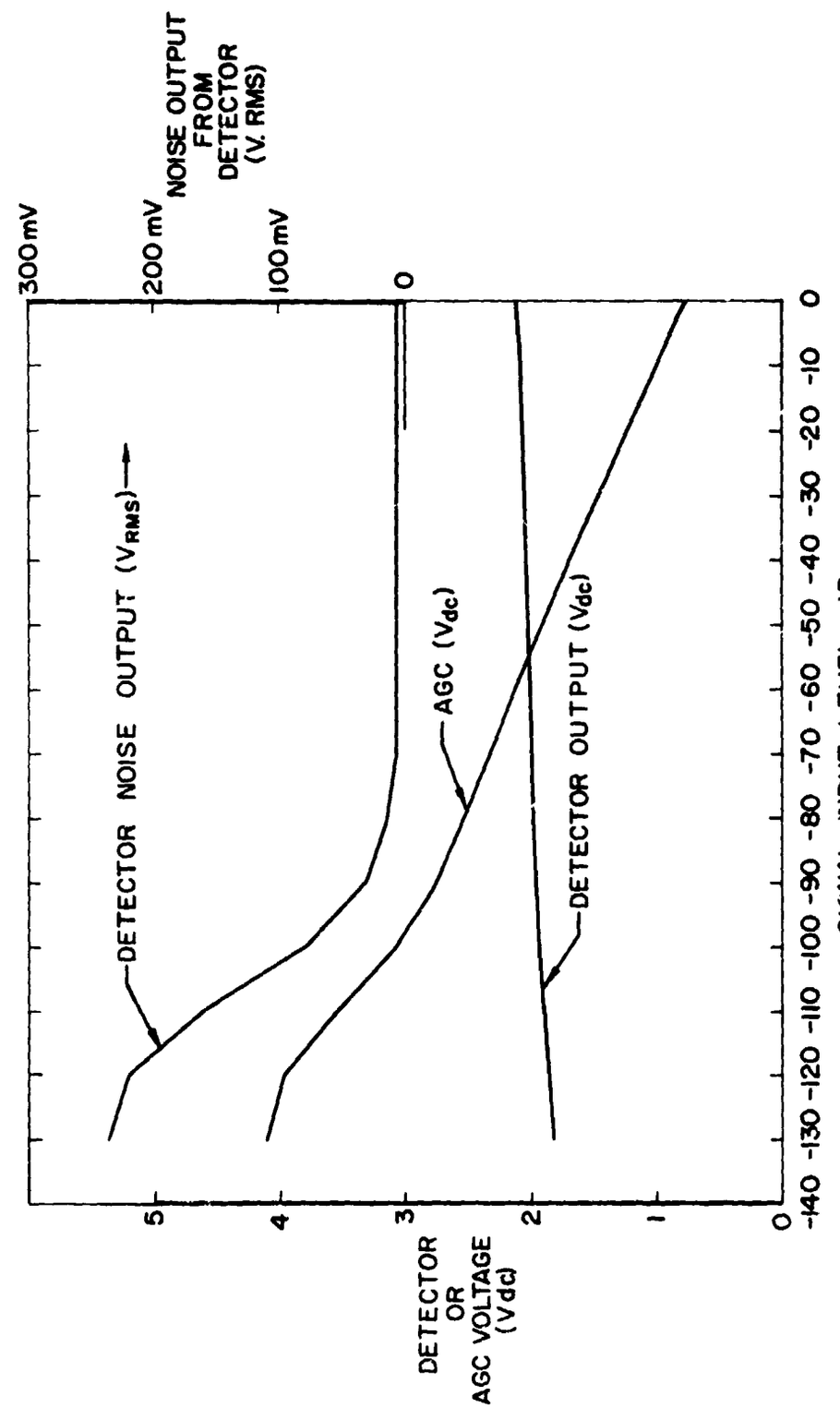

Figure 4.4 Detector characteristics versus input signal level.

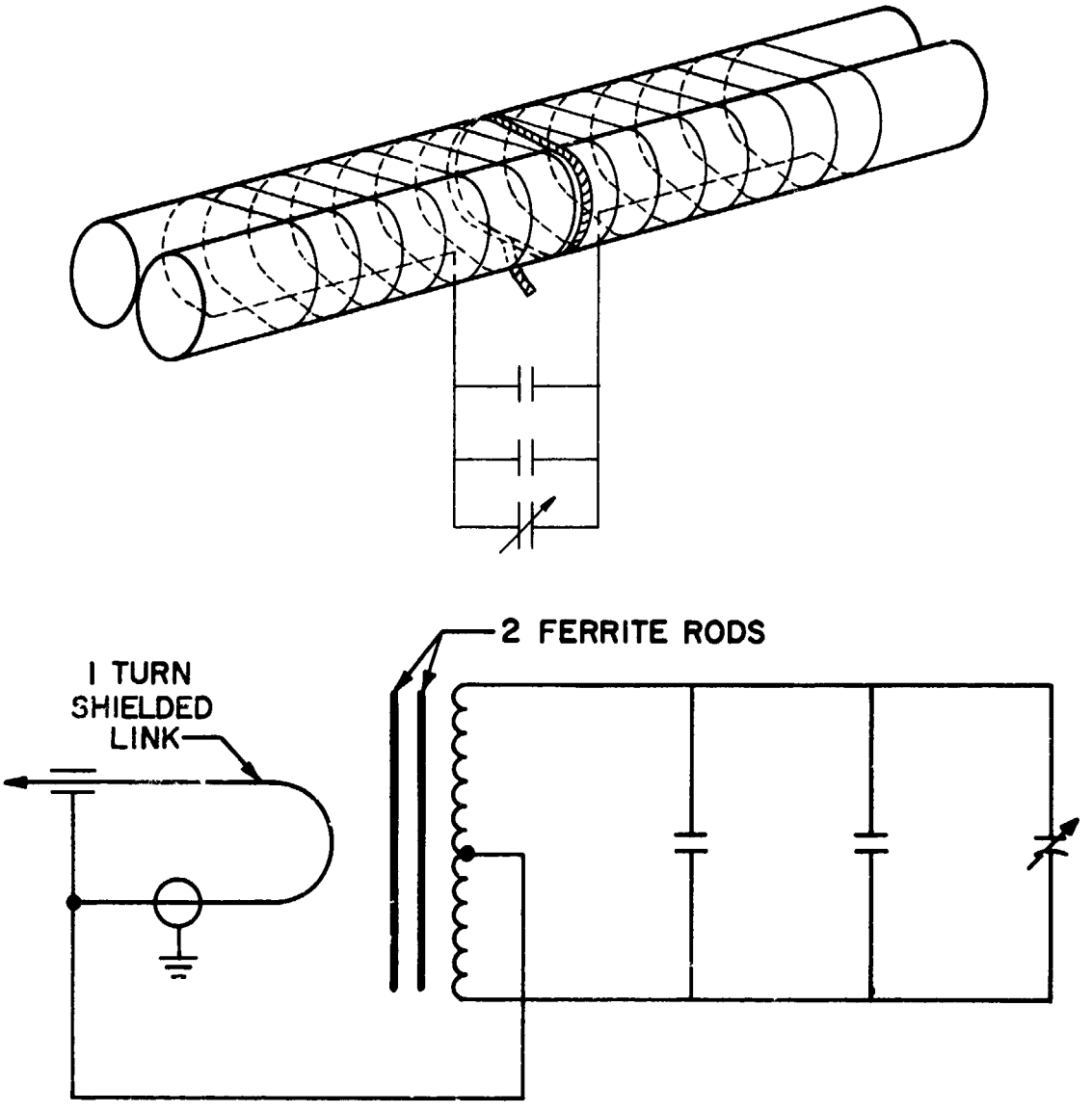

Figure 4.5 Schematic of the rocket receiving antenna [*Fillinger et al.*, 1976].

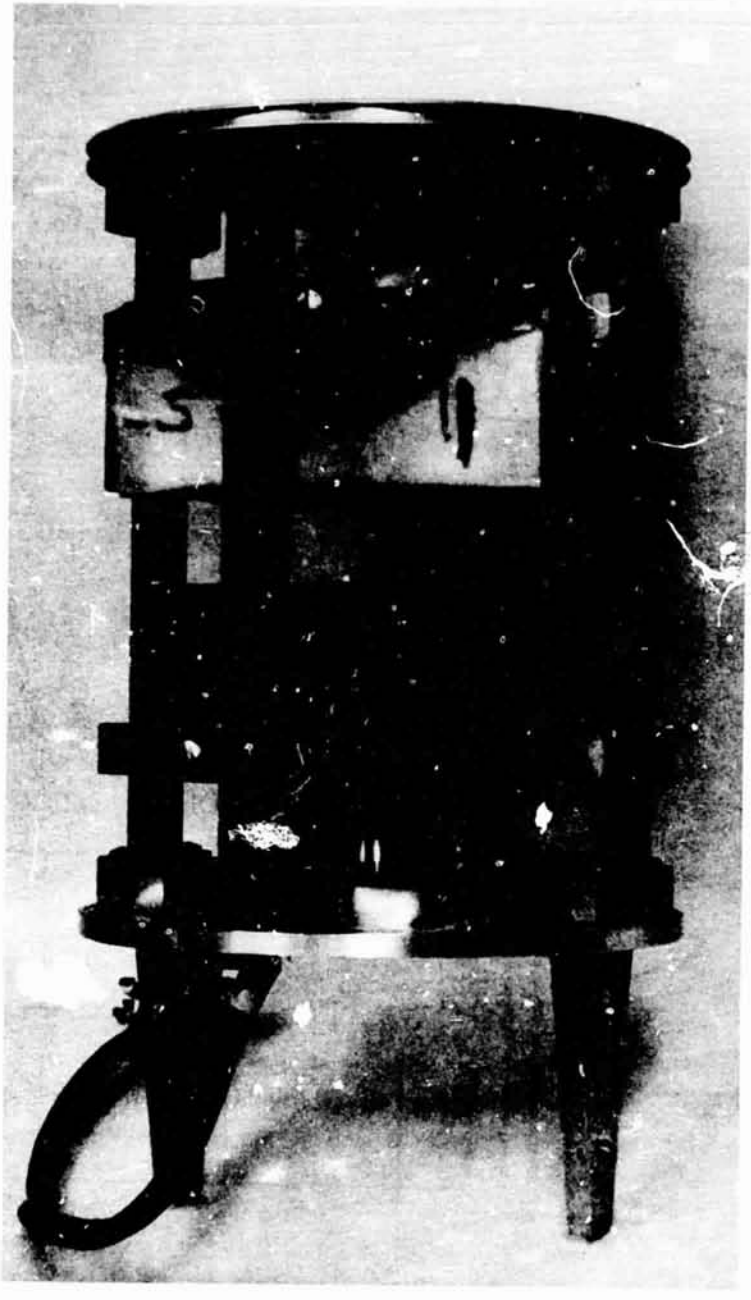

Figure 4.6 Linearly polarized receiving antenna [*Fillinger et al.*, 1976].

In addition to these payload receivers, the propagation experiment makes use of a magnetometer to measure the rocket spin rate. The magnetometer is an instrument sensitive to the earth's magnetic field. Using this field as a reference, the magnetometer has a sine wave output with frequency equal to the rocket spin rate.

Both receiver outputs and the magnetometer signal are telemetered to the ground where they are recorded for later analysis. The telemetry and data recording system will be described in the following section.

4.3 *Telemetry and Data Recording Systems*

For the purposes of data analysis, it is required that the two rocket receiver outputs, the magnetometer signal, and the two reference frequencies from the transmitters be recorded throughout the duration of the rocket flight. Therefore a telemetry and data recording system must support the experiment; details of both these systems are presented in this section.

The telemetry data from the rocket is transmitted using a frequency-modulated (FM) carrier system where the modulating signal is a composite of all the data channels. To form this composite modulating signal, each data channel first is used to FM a voltage-controlled oscillator (VCO). Each VCO operates at a different center frequency with enough separation so that the FM spectra from any one VCO does not interfere with the others. The VCO center frequencies are chosen from twenty-one standardized frequency channels (IRIG subcarrier channels: 1 to 21). Higher numbered channels require proportionally more bandwidth, but can carry higher frequency information. Therefore, the particular channel number chosen for a data channel is determined by its highest frequency component to be transmitted. The two rocket receiver outputs use IRIG channels 16 and 17 which can pass frequencies up to 600 and 790 Hz, respectively. The 5 to 10 Hz rocket spin (magnetometer) signal used IRIG channel 6, that passes frequencies up to 25 Hz. Once all the FM subcarriers are generated, they are simply linearly combined to form a composite modulating signal. The RF carrier frequency used at NASA-Wallops Island is in the vicinity of 2.25 GHz (S-band). The transmitted power output is typically 2 to 3 W.

Once received, the rocket telemetry signal is FM detected to obtain the composite modulating signal. An analog magnetic tape recording is made of this composite signal. Also recorded, on different tracks of the same tape,

are various multiplex signals containing time code information and the reference frequency signals from the transmitters. Additionally, a precision 100 kHz reference oscillator signal is recorded on the analog tape. This reference signal is used to compensate for the variations in tape speed during playback of the tape. Recording typically begins two minutes prior to launch and continues until splashdown.

The analog tape is not generally used in the processing of propagation experiment data. Instead a digital tape recording is made in real-time that records digital samples from the five previously mentioned data channels

a. system 1 receiver output (IRIG channel 17)
b. system 1 reference signal
c. system 2 receiver output (IRIG channel 16)
d. system 2 reference signal
e. magnetometer signal (IRIG channel 6)

Since the signals from the two rocket receivers and the magnetometer are contained in the detected composite telemetry signal, they must be extracted using frequency discriminators tuned to the proper IRIG channels. The discriminator outputs have low-pass 600 Hz filters for the rocket receivers and a 25 Hz filter for the magnetometer.

All five of the above data channels, a through e, are sampled sequentially. A complete set or sequence of samples is defined as one data frame. Five thousand data frames are recorded each second, which is equivalent to 5000 samples per data channel per second. The analog-to-digital converter has a resolution of 12 bits per sample.

The tape format is such that the digital information on the tape is divided into groups (called records). There are three different types of records: header records, calibration records, and data records. The tape begins with 4 header records which provide rocket identification information; each header record contains not more than 45 words, i.e., 45 digital values. This is followed by five telemetry discriminator calibration records, each containing 1005 words. Data records begin after the header and calibration records. Each data record contains 2008 words, of which 2000 are data samples and they are located in words 6 to 2005. Words 2006 through 2008 contain time code information, in Universal Time, to the

nearest tenth of a millisecond that corresponds to the time of the first sample of the following data record; see Table 4.2.

Occasionally a real-time digital tape is not possible. When this occurs, a post-flight digital tape is made from the analog tape. To eliminate the effects of tape speed variation from the analog tape playback, the sampling period is derived from the recorded 100 kHz reference signal. Also on occasion, the above described format is not achieved, therefore it is recommended that proper tape organization be confirmed prior to the tape's use. This can be easily done using a digital tape reading program developed by K. L. Fries, of the Aeronomy Laboratory Rocket Program. This program is documented in Appendix I.

Table 4.2 Coding of time words [*Fillinger et al.*, 1976]

Word 2006	bits	
	13 - 16	hundreds of milliseconds
	9 - 12	tens of milliseconds
	5 - 8	ones of milliseconds
	1 - 4	tenths of milliseconds

Word 2007	bits	
	13 - 15	tens of minutes
	9 - 12	ones of minutes
	5 - 7	tens of seconds
	1 - 4	ones of seconds

Word 2008	bits	
	15 - 16	hundreds of days
	11 - 14	tens of days
	7 - 10	ones of days
	5 - 6	tens of hours
	1 - 4	ones of hours

5. DATA REDUCTION

The data collected from the radio propagation experiment is used to calibrate the Langmuir probe mentioned in Chapter 1. To accomplish this, several data reduction steps must be performed in sequence. These steps include the extraction of Faraday rates, the conversion of Faraday rate information to electron concentration, and the calibration of probe current. This chapter discusses each of these steps.

5.1 *Fourier Spectral Analysis*

In Section 3.4 it was shown that the desired Faraday rotation information is embedded in the frequency arguments of certain sinusoidal terms from the rocket receiver output. Further, it was shown that the receiver output contained a large number of discrete spectral components with an approximate frequency spacing of $2f_s$. Therefore, to extract the Faraday information, a technique is required that can distinguish and measure the frequencies of particular spectral components.

From Table 3.1, the receiver output frequencies of most interest are f_c and f_g, where

$$f_c = f_M' - 2f_s - \frac{1}{2\pi}(k_R - k_L)v \tag{5.1}$$

$$f_g = f_M' + 2f_s + \frac{1}{2\pi}(k_R - k_L)v \tag{5.2}$$

This is because the amplitudes of these spectral components are the largest of all the frequencies containing ionospheric information. Equations (5.1) and (5.2) each contain Faraday rate information as well as the Doppler-shifted reference frequency and the rocket spin rate. It will be noted that by subtracting f_c from f_g the reference frequency is eliminated leaving only the rocket spin rate and the Faraday rate. The spin rate is separately obtained from the magnetometer channel. Using the above frequencies, an expression can be given to determine the desired Faraday rate, F.

$$F = \frac{1}{4}\left[f_g - f_c - 4f_s\right] \tag{5.3}$$

Fillinger et al. [1976] have described a procedure for deriving the frequency information from spectra of the signals. To understand how this is done consider an analog signal, $x(t)$, having a general spectrum defined by its continuous Fourier transform (CFT)

$$X(f) = \int_{-\infty}^{\infty} x(t)e^{-j2\pi ft}\,dt \tag{5.4}$$

This definition, however, is not practical for the present situation because it provides no information on how the frequencies of equation (5.3) vary with time. A more useful definition is available for situations where the signal is quasi-stationary, i.e., for a signal composed of frequency terms that vary slowly with time, which is the case for the receiver signal. For the above condition, a short-term spectrum, $X(f,t)$ can be defined as

$$X(f,t) = \int_{-\infty}^{\infty} w(t-\tau)\; x(\tau)e^{-j2\pi f\tau}\,d\tau \tag{5.5}$$

where $w(t)$ is a weighting or window function that has non-zero value for only a finite duration near $t = 0$ [*Allen*, 1977]; more will be said about this window function later. This new spectral definition allows for the possibility of observing spectral frequencies as they vary with time.

Equation (5.5) has two equivalent but distinct interpretations [*Allen and Rabiner*, 1977]. One view is shown graphically in Figure 5.1(a) where (5.5) has been decomposed into two cascaded sections. The first section is a complex mixing operation, which has the effect of shifting the spectrum of $x(t)$ down by an amount f. The second section is a linear filter with impulse response, $w(t)$. In general, $W(f)$, the CFT of $w(t)$, has a low pass characteristic with some cutoff frequency, f_c. The output from the combined system is a complex time varying signal that is sensitive only to the spectral energy from the input that is present in the frequency interval $(f-f_c,\ f+f_c)$. By altering the frequency parameter, f, the entire short-term spectrum can be determined.

The second interpretation of equation (5.5) is that it represents the CFT of the new signal

$$y(\tau) = w(t-\tau)x(\tau) \tag{5.6}$$

where t is now a fixed parameter. The transform of $y(\tau)$ is related to the transforms of x and w by the complex convolution of the two.

$$y(f) = [e^{-j2\pi ft}\; W(-f)] * X(f) \tag{5.7}$$

This point of view demonstrates that the short-term transform $X(f,t) = Y(f)$ is greatly influenced by the choice of window function. This interpretation

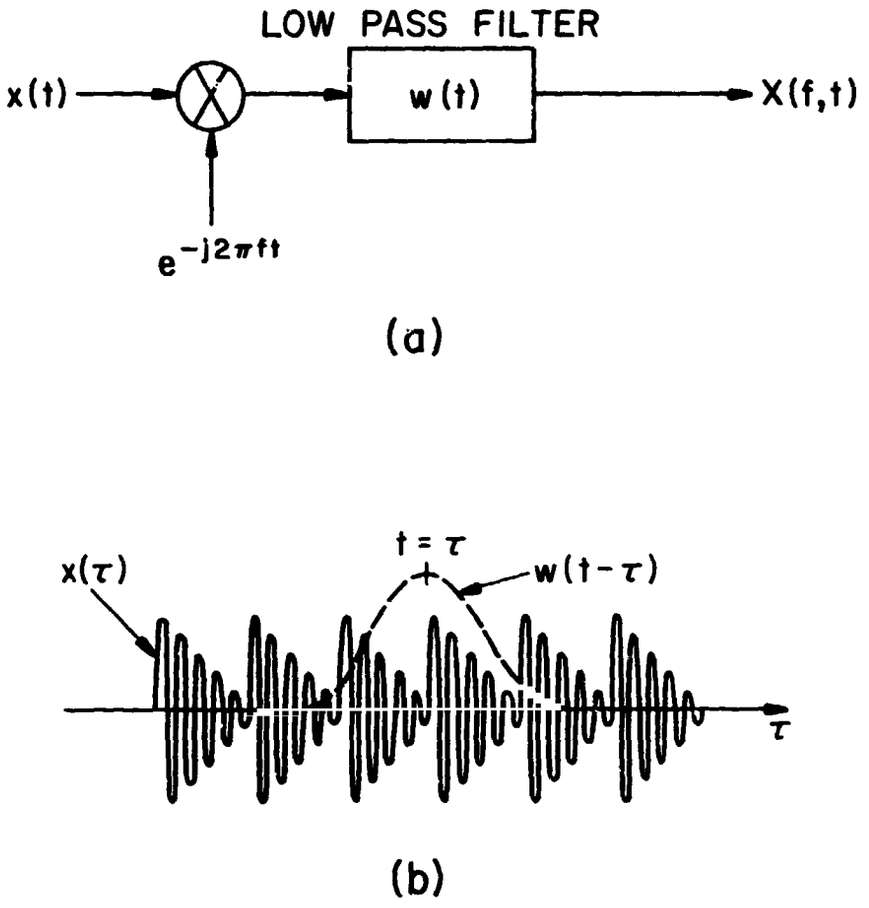

Figure 5.1 Two interpretations of the short-term spectrum defined in equation (5.5). (a) System interpretation using a mixer and linear filter, where $\omega(t)$ is assumed to be low pass. (b) Short-term spectrum is interpreted as the normal Fourier transform of $x(\tau)$ multiplied by the sliding window, $\omega(t-\tau)$.

is shown graphically in Figure 5.1(b) where an arbitrary sliding window function is shown superimposed on $x(\tau)$; the product of these two is then Fourier transformed.

When the signal to be analyzed has been sampled to form discrete digital values, an alternative to the CFT must be used, this is known as the discrete Fourier transform (DFT). The DFT is defined as

$$X(e^{j\omega}) = \sum_{n=-\infty}^{\infty} x(nT)e^{-j\omega n} \tag{5.8}$$

where $x(nT)$ is the sampled signal with sampling period, T [*Oppenheim and Schafer*, 1975]. The ω term in equation (5.8) is the standard convention for the radian frequency transform variable which has dimension of radians. This should not be confused with the sinusoidal angular frequency term having dimension of radians per second. The relation between radian frequency and the corresponding sinusoidal frequency, f, is

$$\omega = 2\pi fT \tag{5.9}$$

Also note that because the complex exponential is periodic, so also is the DFT defined by equation (5.8). In a similar fashion, a discrete equivalent to the short term spectrum can also be defined.

$$X_n(e^{j\omega}) = \sum_{m=-\infty}^{\infty} w[(n-m)T]x(m)e^{-j\omega m} \tag{5.10}$$

Here again it can be seen that the window, $w(nT)$, determines what portion of $x(nT)$ is to be spectrally analyzed. Once a window function is chosen, equation (5.10) can be used to obtain the necessary spectral information from the receiver and magnetometer channels.

Direct application of equation (5.10) to measure a signal's entire spectrum would require that it be repeatedly used, as each computation of (5.10) returns information for only one spectral frequency. To avoid this complication the actual procedure used for the propagation experiment data analysis uses a fast Fourier transform (FFT) to perform the DFT in equation (5.10) [*Bergland*, 1969]. The FFT is an efficient algorithm for computing the DFT that takes advantage of certain properties possessed by complex exponentials. By using the FFT there is a substantial reduction in processing time below what would be needed for direct DFT computation. The FFT uses an even number, N, of signal samples selected by the window function to calculate

N uniformly spaced components of the spectrum defined in equation (5.10); these components are at integer multiples [$-N/2$, ..., -1, 0, 1, ..., ($N/2$ -1)] of $\omega = 2\pi/N$. This corresponds to sampling the short-term spectrum at multiples of $f = (NT)^{-1}$; for example, sampling at a 5 kHz rate and using 5000 samples would mean sampling the spectrum at 1 Hz intervals.

Proper operation of the short-term spectrum analysis, using the FFT algorithm, requires that proper consideration be given to the data sampling rate, digital quantization effects, and the choice of window function. To satisfy the Nyquist sampling rate criterion, discrete samples must be taken at a rate that is at least twice as high as the highest frequency present in the spectrum of the signal being sampled. This implies that since the receiver channels have 600 Hz low pass filters, the sampling rate should be at least 1200 Hz. In practice since the low pass filters do not completely attenuate all frequencies above 600 Hz, a guard band must be provided, therefore, the experiment uses a sampling rate of 5000 Hz. If a signal is sampled below its Nyquist rate, a distorting effect (aliasing) results and causes high spectral frequencies to appear as low spectral frequencies.

Some consideration should be given to the accuracy and resolution of the digital samples. The act of digitizing the data inherently introduces noise into the data and is known as quantization noise. The question of accuracy is less critical as absolute amplitude information is not necessary to the Fourier analysis. However, the analog-to-digital conversion should not introduce any non-linear compressional effects that might alter the signal spectrum. The present digitizing system used at the Wallops Flight Center (NASA) has a 12-bit resolution.

The choice of window function is very critical to the success of the short term spectrum analysis. This can be noted by the predominant role that the window function plays in the short-term spectrum d inition, both continuous and discrete. Although the particular window chosen has several effects [*Allen*, 1977] the predominant consideration for spectral analysis is the window's ability to reduce spectral leakage. Spectral analysis of finite extent data with duration NT requires that a projection of the data be made on a basis set spanning the observation interval. For Fourier analysis this basis set consists of trigonometric functions that have periods which are submultiples of NT. If the signal being analyzed contains only frequencies from the basis set, they will project onto individual basis

vectors. However, if the signal contains frequencies other than those from the basis set, then the signal is not periodic in the interval NT and will thus have discontinuities at the ends of the interval. These discontinuities are cause for the signal to project over the entire basis set; this is referred to as spectral leakage. The purpose, therefore, of the window function is to reduce these discontinuities and thus spectral leakage so that a signal will have significant contribution on only those basis vectors that are near the frequency of the signal. This is done by choosing a window that brings the signal to zero as smoothly as possible or, conversely, that has a transform with a good low-pass characteristic and low side-lobes. A large number of possible windows have been described in the literature, each satisfying the above criterion to varying degrees. An excellent survey and study of window functions for harmonic analysis using the DFT is given by *Harris* [1978]. In general it can be stated that the shape of the window function will determine the peak side-lobe level while the window duration will determine the transition length between passband and stopband.

The actual window function used for the spectral analysis of the propagation experiment data is the Gaussian window [*Fillinger et al.*, 1976]. This window shows the desired low-pass frequency response of a concentrated main lobe at dc with low level side-lobes at higher frequencies. Theoretically, the Fourier transform of a Gaussian function is another Gaussian and, therefore, has no side-lobes in the frequency domain. However, because the FFT uses finite extent data, the Gaussian window function must be truncated at some point. This truncation causes the Fourier transform of the Gaussian to be slightly modified introducing the side-lobes. This situation is shown in Figure 5.2 where a 50 sample Gaussian window is shown with its DFT. The actual Gaussian window used for the data analysis has a duration of 5000 samples and combined with the 5 kHz sampling rate, allows the FFT to sample the spectrum at 1 Hz intervals.

The frequencies required for equation (5.3) must be known more accurately than are provided by the 1 Hz sample interval of the FFT. E. K. Walton has developed an algorithm to accurately interpolate between spectrum samples to determine the frequency of the spectral peak [*Fillinger et al.*, 1976]. His algorithm uses the fact that the Gaussian window modifies the spectrum of any signal having discrete frequencies or having a spectrum that is already Gaussian, in a known and predictable fashion. By using three spectral samples

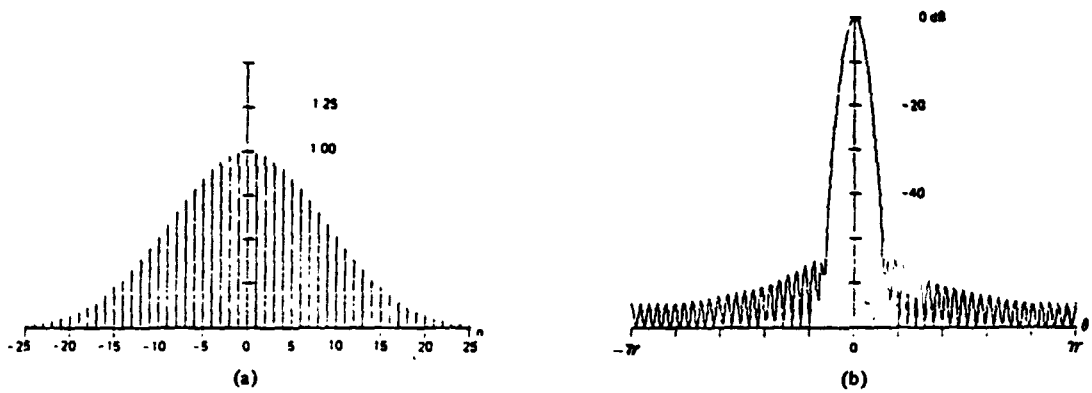

Figure 5.2 (a) Fifty sample Gaussian window. (b) Log-magnitude of its corresponding discrete Fourier transform [*Harris*, 1978].

about the peak, this algorithm is able to return the spectral peak frequency to within an experimentally determined accuracy of ±2.5 mHz.

A computer program incorporating the FFT with Gaussian window and Walton's algorithm is used to extract the frequency information needed for equation (5.3). This program is documented in Appendix II. The program is used to separately measure both frequencies (f_e and f_g) from the receiver channels as well as the rocket roll rate (f_s) from the magnetometer signal. As examples of the application of the analysis Figures 5.3 and 5.4 show the measured Faraday rate versus seconds after launch for Nike Apaches 14.533 and 14.534 determined from both system 1 (2.225 MHz) and system 2 (3.385 MHz).

5.2 *Calculation of Electron Density*

Once the Faraday rate is obtained using the analysis of the previous section, the corresponding electron concentration value may be calculated. To accomplish this, an iterative computer analysis procedure is used [*Mechtly et al.*, 1970]. This procedure is based on the complete Sen-Wyller theory [*Sen and Wyller*, 1960], which is an extension of the Appleton-Hartree analysis from Section 3.1. The principal change is the way that the velocity distribution of the electrons is treated. In practice the difference between the two theories is unimportant in the ionosphere at altitudes above about 80 km. The Sen-Wyller theory is used here because the computer program was developed originally for use in the daytime ionosphere.

Figure 5.5 shows a block diagram of the computer analysis procedure. Initially an assumption of electron concentration is made. Then using the Sen-Wyller equations and Burke-Hara polynomials [*Mechtly et al.*, 1967] the refractive index is calculated for each ionospheric mode at the frequency of the experiment. With these indices of refraction and the rocket velocity the corresponding Faraday rate is calculated. This calculated rate is compared with the actual measured Faraday rate to determine a better assumed electron concentration value by using the equation from the final block of Figure 5.5. With the new value of electron concentration, the above procedure is repeated. This iteration is repeated up to six times to determine the actual electron concentration value corresponding to the measured Faraday rate. This analysis makes the assumptions that the direction of radio propagation and the rocket's direction of travel are along the line of sight between the launch site and the rocket. The first of these assumptions is in danger of failing when the

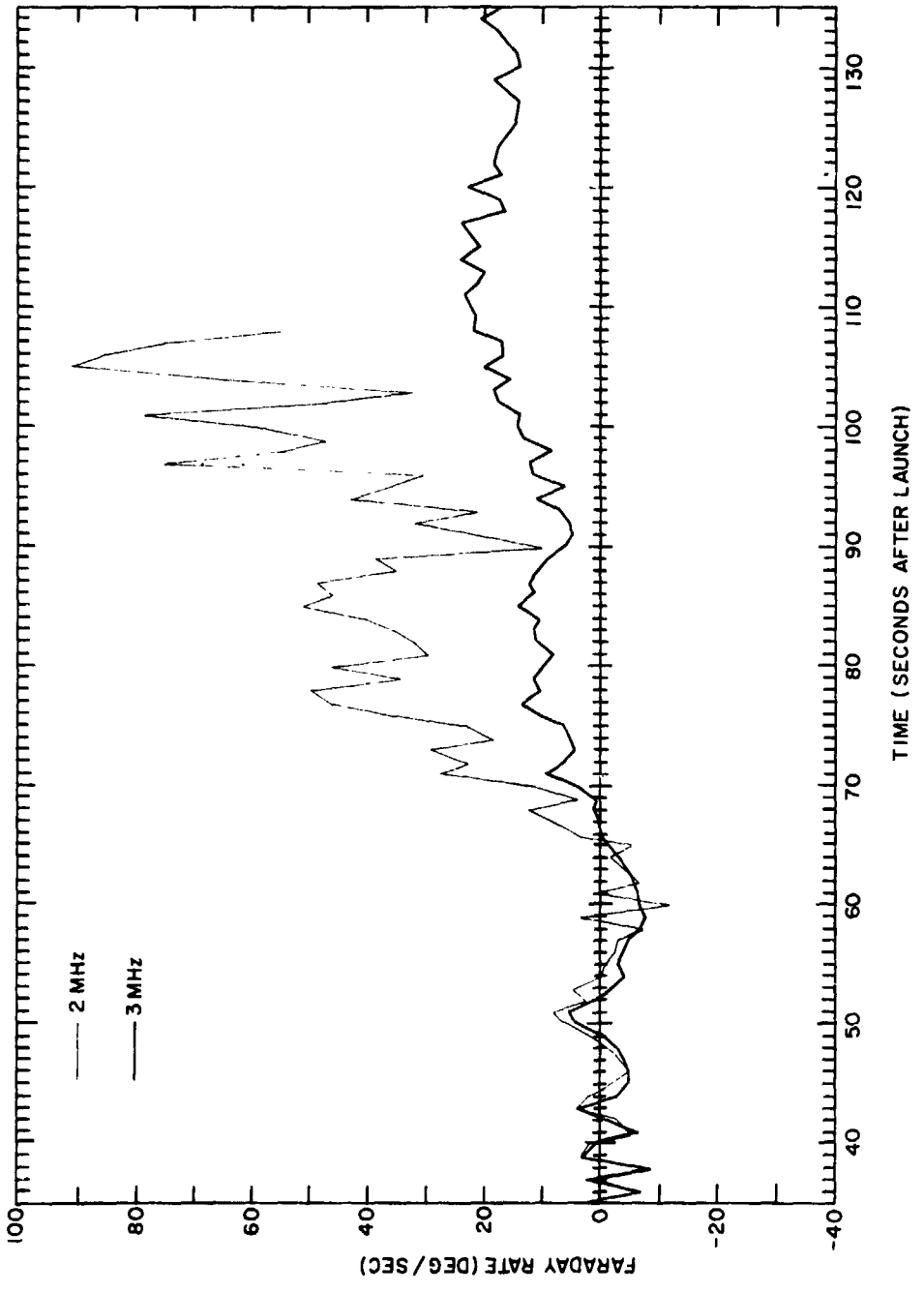

Figure 5.3 Faraday rate for Nike Apache 14.533.

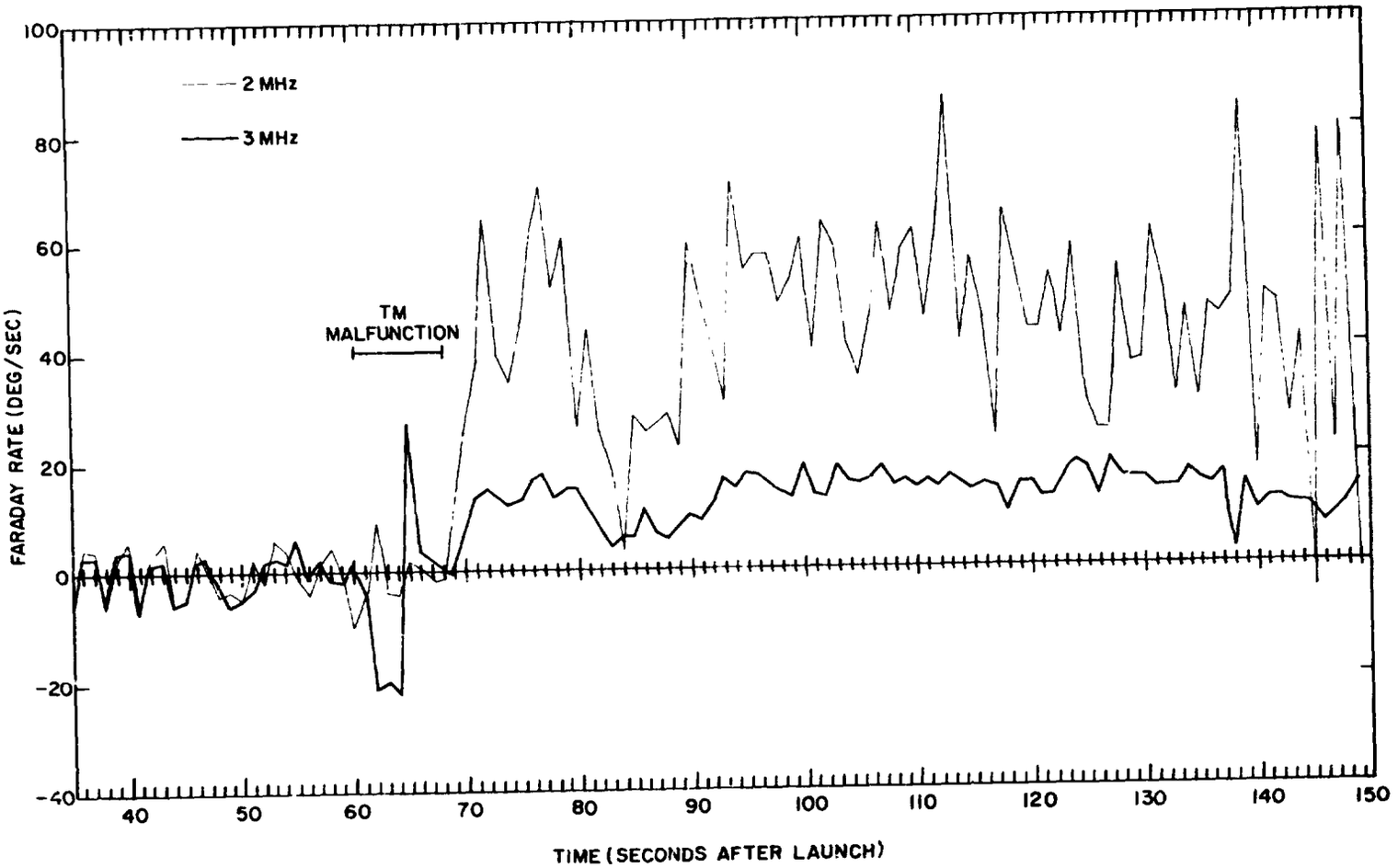

Figure 5.4 Faraday rate for Nike Apache 14.534. A telemetry malfunction occurred between 60 and 68 seconds after launch.

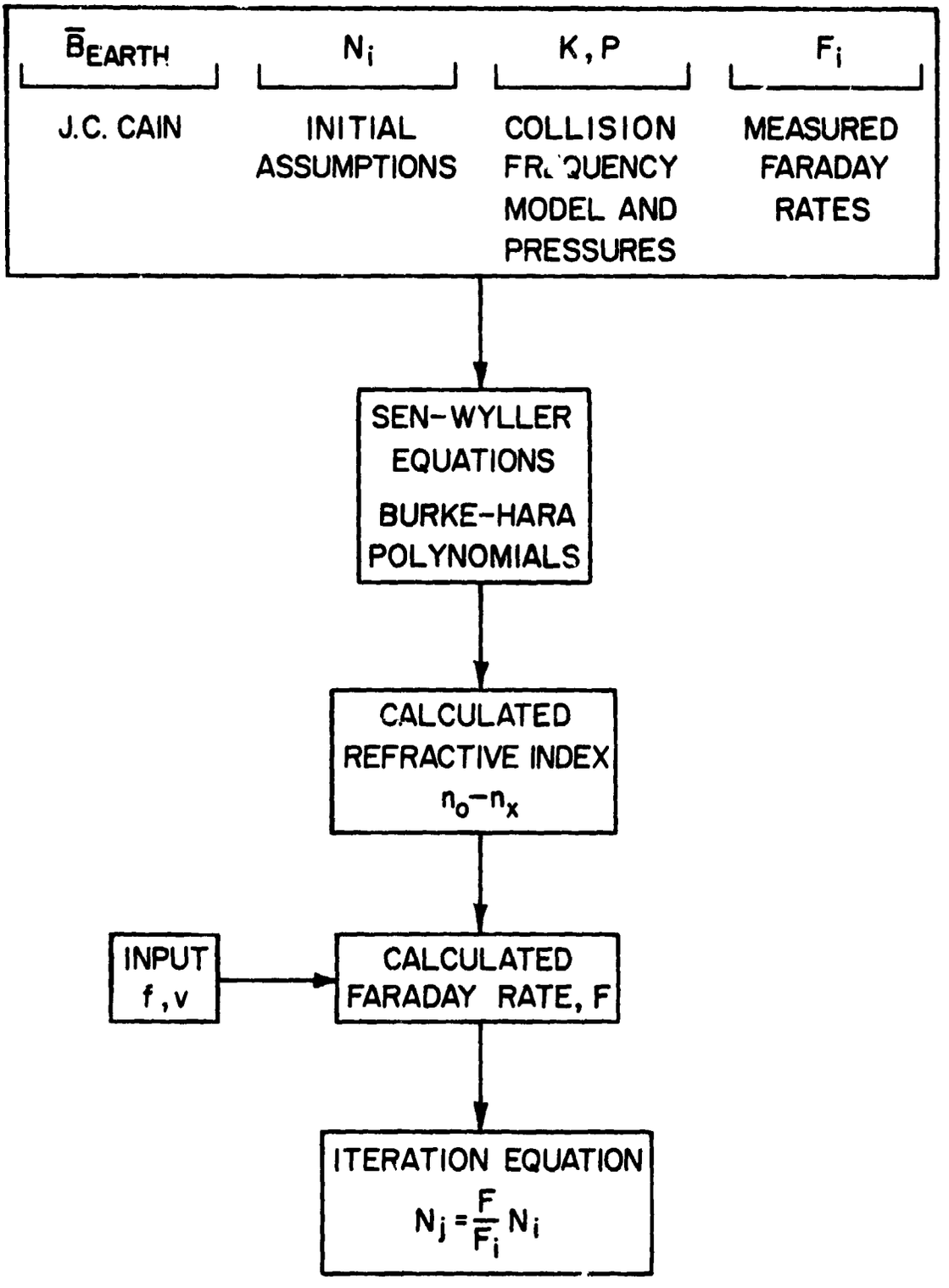

Figure 5.5 Procedure for analyzing Faraday rotation rates [*Fillinger et al.*, 1976].

rocket is near the radio wave reflection height as there may be significant bending of the propagation path at this altitude. The second assumption fails near rocket apogee.

When no differential absorption is measured, as at night, a collision frequency model must also be supplied. This model makes the assumption that collision frequency is proportional to the neutral atmosphere pressure, p. That is

$$\nu = K \cdot p$$

where K is the proportionality constant with units of s^{-1} Pa^{-1} and is assumed to have a value of 6.3×10^5 s^{-1} Pa^{-1} [*Smith et al.*, 1978]. The atmospheric pressures are obtained from the COSPAR International Reference Atmosphere Model [*CIRA*, 1972]. The program that calculates the electron concentration is documented in Appendix III.

The electron concentration values versus altitudes that were calculated for the flights of Nike Apaches 14.533 and 14.534 are shown in Figures 5.6 and 5.7, respectively. Shown in each figure are the independent results obtained from the 2 MHz system and the 3 MHz system. Also shown in each figure, for clarity, is a partial plot of the calibrated probe current. This calibration procedure is presented in the following section.

5.3 *Calibration of Probe Current*

The current from the Langmuir probe follows the detailed variation of the electron-density profile [*Mechtly et al.*, 1967]. However, because no accurate equations exist that relate probe current I to electron concentration, N_e, the probe data must be calibrated by comparison with the results from the propagation experiment. To accomplish this, the ratio N_e/I_{AVG} is calculated for each electron concentration value. A listing of this computer program is presented in Appendix IV. The required inputs include up to sixty seconds of electron concentration values and the corresponding probe current data. The probe current must start one second before the time of the first electron concentration value and must have all probe sweeps that occur above 130 km removed.

A semi-log plot is next made of N_e/I_{AVG} versus altitude. This is shown in Figures 5.8 and 5.9 for Nike Apaches 14.533 and 14.534, respectively. In general N_e/I_{AVG} need not be a constant, however, any change is expected to be slowly varying with altitude. Therefore, an average N_e/I_{AVG} value is

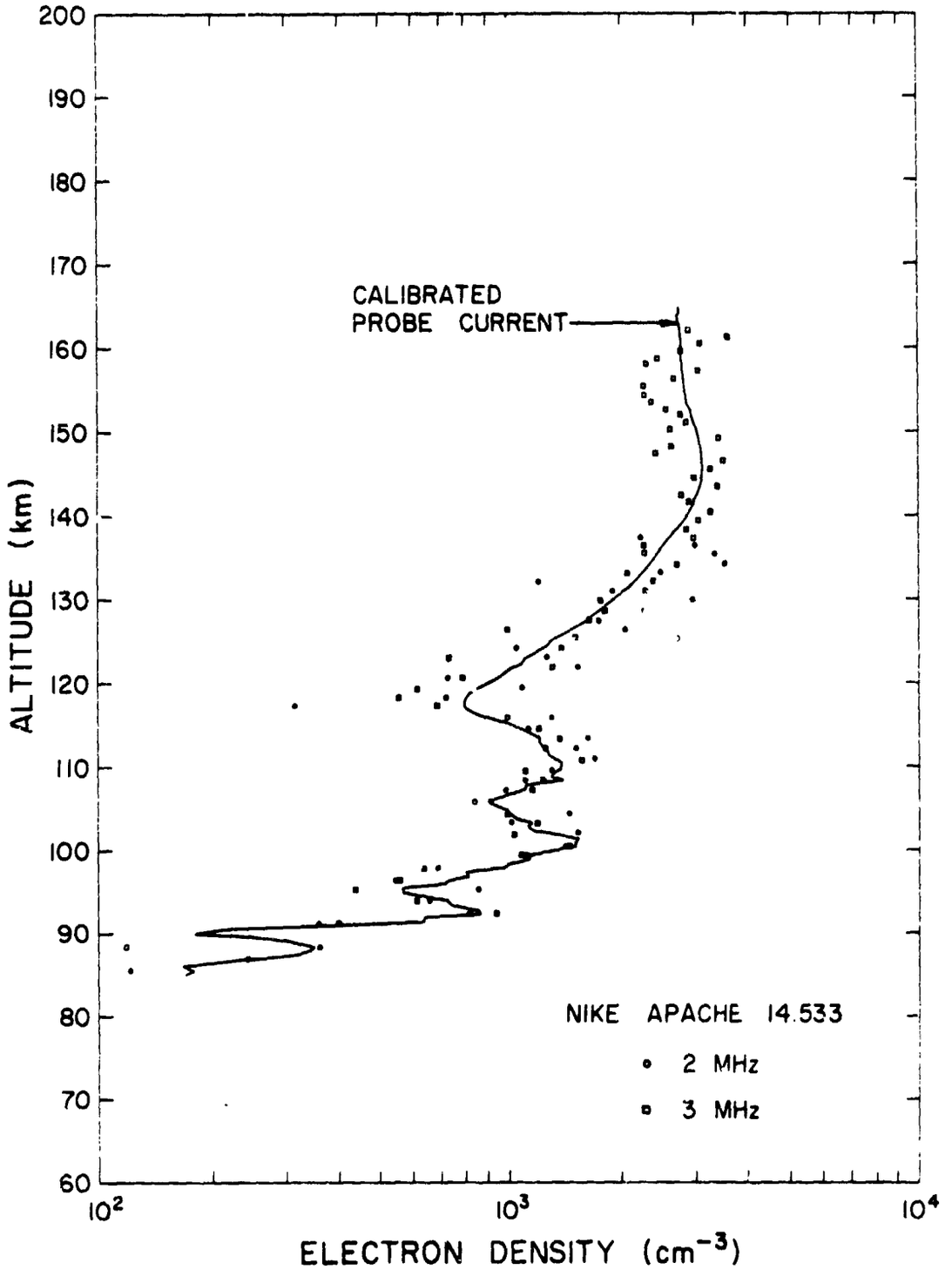

Figure 5.6 Electron-density values from the propagation experiments (individual points) compared with the calibrated probe current for Nike Apache 14.533.

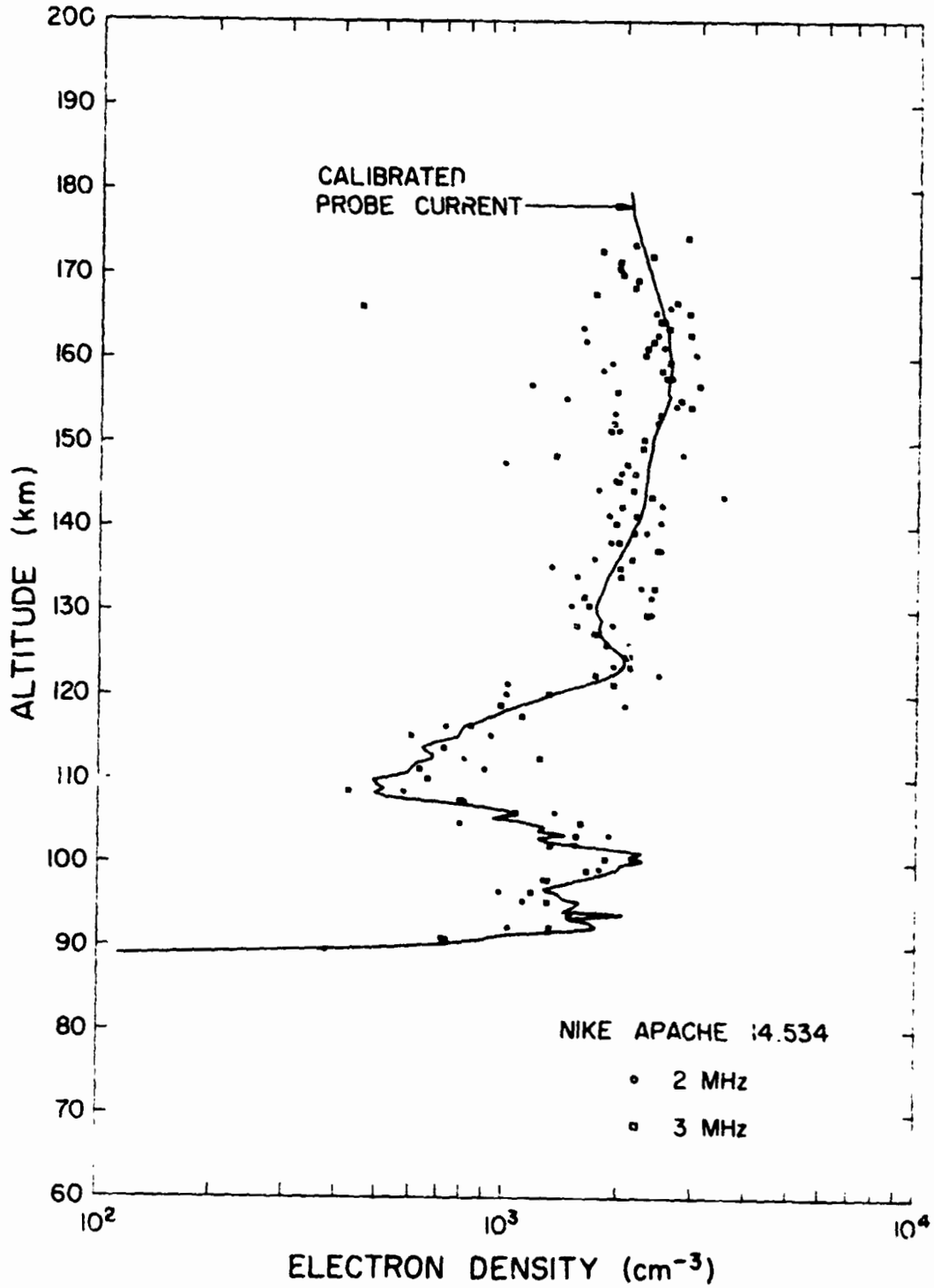

Figure 5.7 Electron-density values from the propagation experiments (individual points) compared with the calibrated probe current for Nike Apache 14.534.

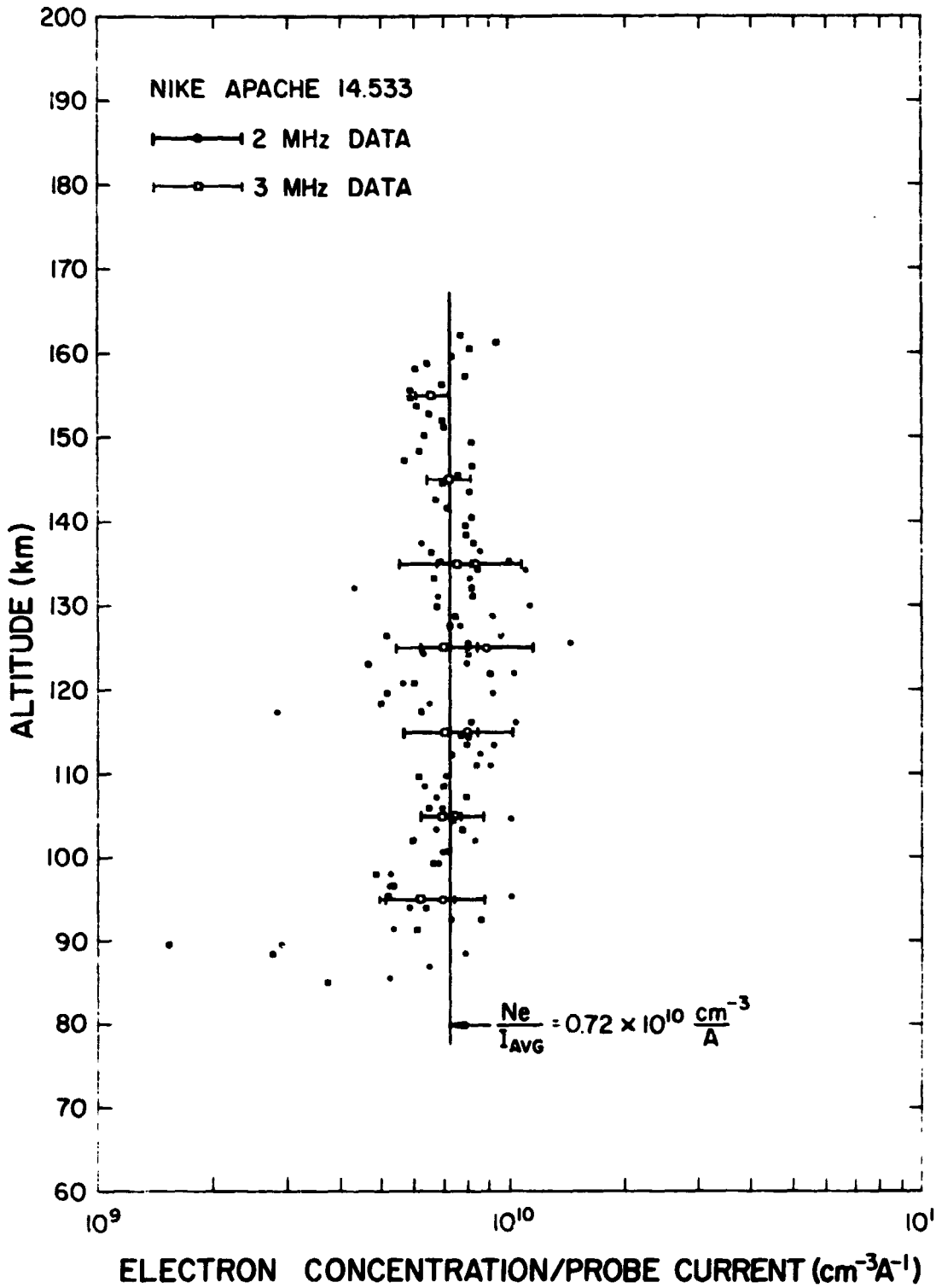

Figure 5.8 The probe calibration for Nike Apache 14.533.

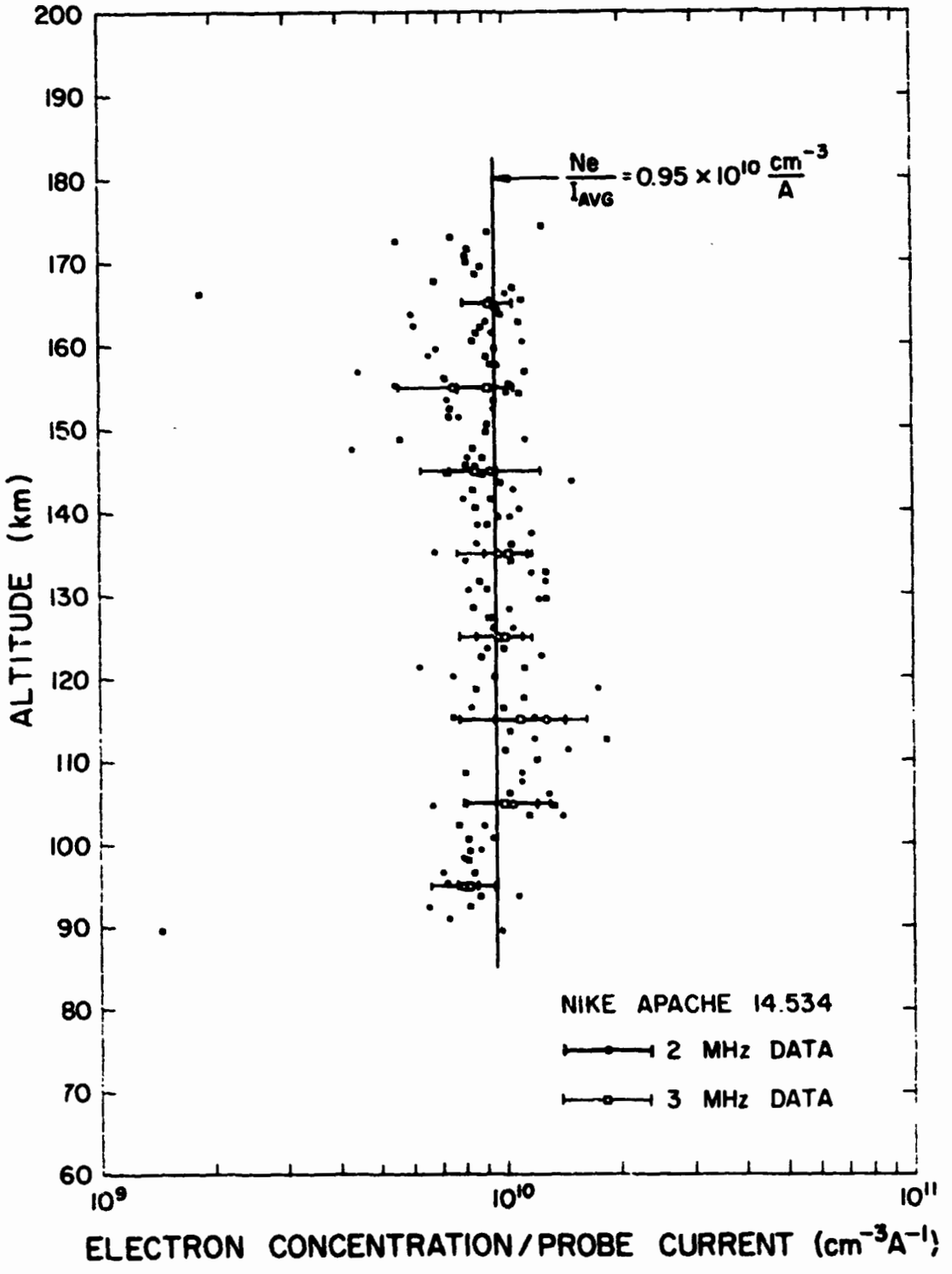

Figure 5.9 The probe calibration for Nike Apache 14.534.

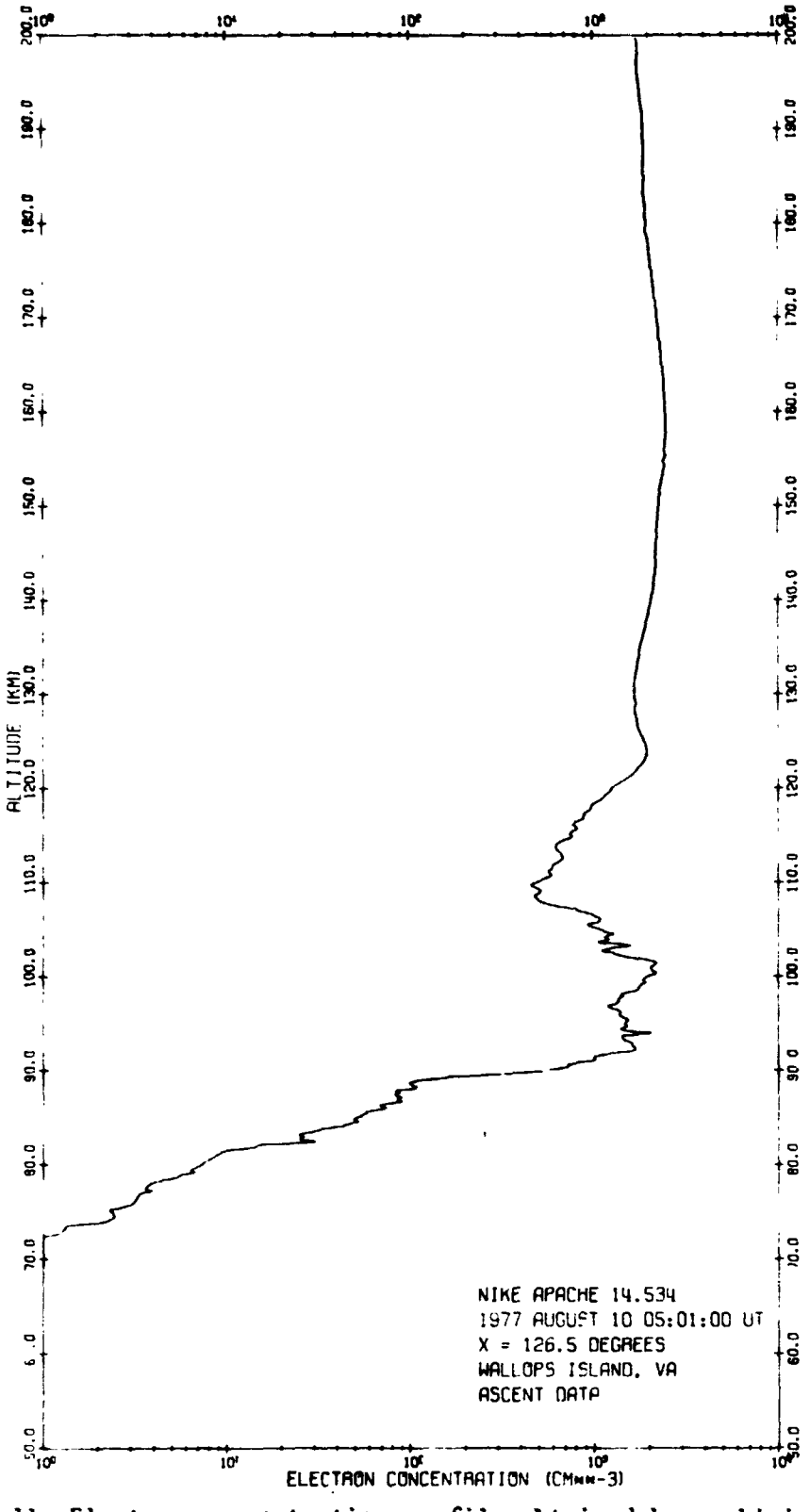

Figure 5.11 Electron concentration profile obtained by combining data from the probe and propagation experiments on Nike Apache 14.534.

 65-66

6. EVALUATION OF SYSTEM PERFORMANCE

6.1 *Introduction*

The purpose of this study is to identify sources of experimental error that presently limit the accuracy of the propagation experiment. The main discussion refers specifically to the modified version of the propagation experiment. However, much of the discussion is also relevant to the original experiment.

The experiment, in both versions, is fundamentally concerned with the measurement of two receiver frequencies and the rocket roll rate included in equation (5.3), thus any sources of noise or anomalous behavior that affect these measurements are of importance. The results of this study are divided into those errors related to the hardware and those connected with the software frequency measurement procedures.

6.2 *Hardware*

6.2.1 *Noise sources.* Noise is an inherent component of any electrical signal and can be loosely defined as any unwanted random or periodic effect that distorts the desired response. Noise of some form and magnitude is generated in all electrical components, including those that make up the propagation experiment. Further, radio frequency noise from a variety of naturally occurring sources is present in the reception of all free space radio propagation. It is, therefore, of interest here to identify any noise sources that are of sufficient amplitude to affect the accuracy of the experiment. Towards this end a series of system checks have been carried out at Wallops Island. These checks included an evaluation of the dependence of experimental accuracy on signal-to-noise ratio (SNR) and checks of noise effects which frequency modulate the reference signal. The checks have been made at various locations along the experimental system.

6.2.2 *Signal-to-noise ratio.* Intuitively it may be expected that experimental accuracy must be dependent on SNR. In particular the relative level of signal compared with noise as observed at the telemetry station is of interest since this is where analog data is recorded for later processing. Possible noise sources that can contribute to the total noise level include those in the ground transmitting equipment, atmospheric noise, receiver noise, noise in the telemetry equipment, as well as noise in the data recording process. To test the dependence of accuracy on SNR, the propagation experiment system was set up to simulate pre-launch conditions. The radio trans-

mitter was adjusted for the typical power of 250 W, the rocket was mounted on the launcher in proper launching position and the telemetry signal was transmitted to the telemetry station. With this configuration digital and analog data recordings were made from the received telemetry signal for periods of 30 seconds using the procedure of Section 4.3. At the end of each period of 30 seconds the transmitted power was reduced by 10 dB and another 30 seconds of data were recorded. This was continued until the transmitted power had been reduced by a total of 70 dB. The effect of reducing transmitted power is to decrease SNR although it may not be in the same steps of 10 dB because of the action of the rocket receiver AGC. Since the rocket was stationary, the output of the rocket receiver only consisted of the reference frequency, harmonics of the reference frequency, and noise. By using the frequency analysis procedure described in Chapter 5, the measured reference signal frequency from the receiver could be compared with that measured from the corresponding reference signal channel. The difference between these two measured frequencies is an indication of possible error in Faraday rate that would result from various SNR levels.

Figure 6.1 shows the results of this test for system 1 (2.225 MHz) as far as the 40 dB level of power reduction. As is indicated, the peak magnitude of the random error increased as the transmitted power was reduced. This fact is also represented numerically, in Figure 6.1, by the standard deviation (σ) for the error in the frequency which is calculated for each one-second interval. The standard deviation typically increases two to three times for each 10 dB reduction in transmitted power.

During the test just described the ground transmitter was located approximately 1 km from the rocket. However, the experiment is primarily designed to operate with the rocket at an altitude of the order of 100 km (the range is typically 50 to 150 km). The additional free space propagation path loss between 1 km and 100 km is approximately 26 dB. Therefore, it would be expected that if the rocket could be placed at a 100 km distance from the transmitter and the SNR system test repeated with full power, the standard deviation of the error in the frequency measurement would be about 9 mHz; that is, from Figure 6.1, between the 20 dB standard deviation level of 6.0 mHz and the 30 dB level of 10.5 mHz. Further as the rocket moved to greater distances it would also be expected that the magnitude of error would continue to increase. This type of behavior is indicated in Figure 6.2 which

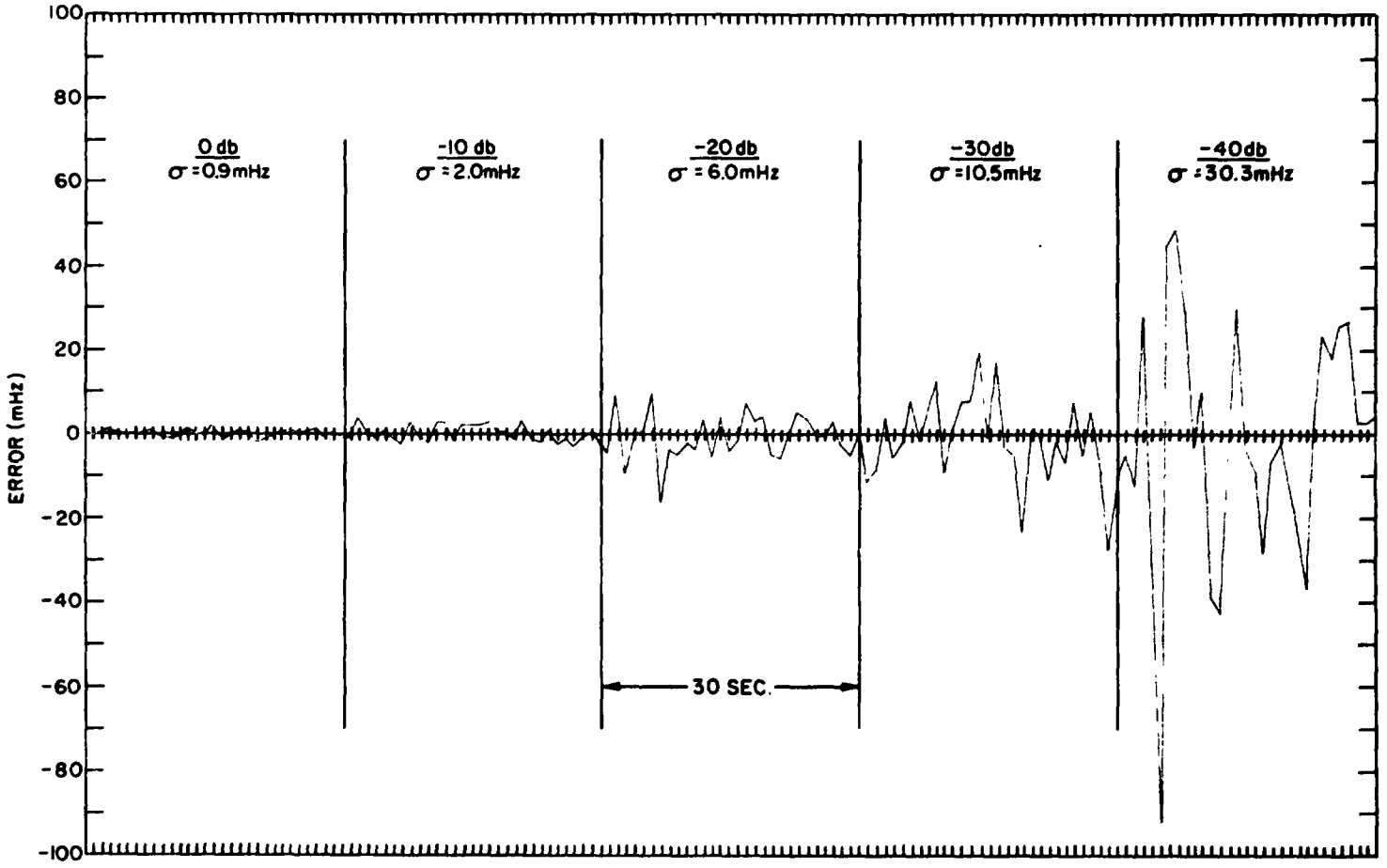

Figure 6.1 Effect of SNR on experimental error. SNR is decreased in approximate 10 dB steps and error is observed for 30 seconds. The standard deviation for each interval is also shown.

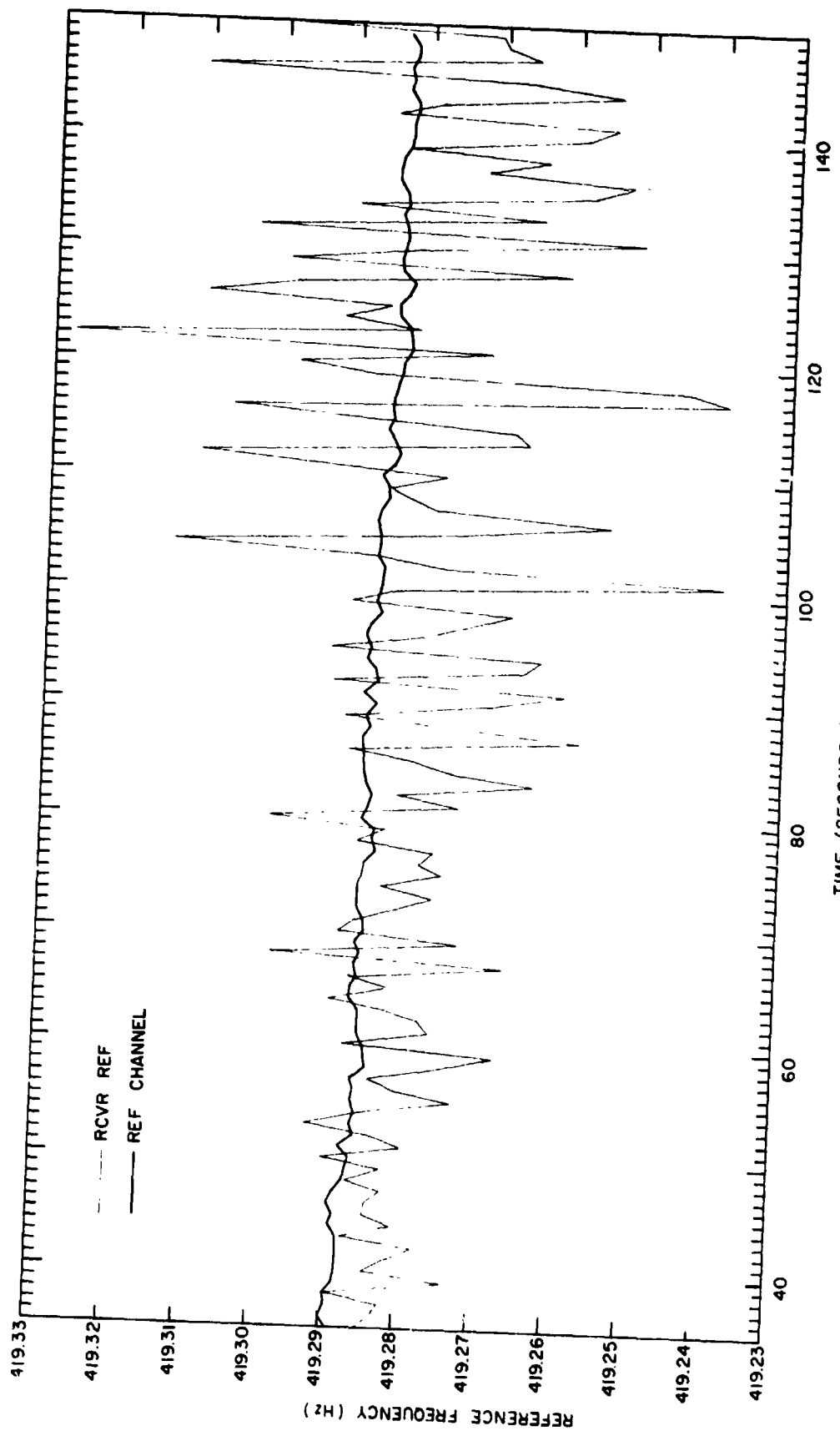

Figure 6.2 Reference signal frequency as measured from both the reference channel and receiver channel.

is actual data from the flight of Nike Apache 14.534, system 1. In this figure the frequency of reference signal measured from the reference channel (i.e., direct line to the TM station) and from the receiver channel (i.e., through the transmitter/receiver/telemetry system) is shown as a function of time after launch. As this figure indicates the frequency of the reference channel remains well-behaved during the flight while the frequency measured from the receiver channel increasingly becomes more erratic. This is interpreted to be a direct result of decreasing SNR.

The standard deviations for the measurement of receiver frequency given in Figure 6.1 cannot be directly compared with uncertainty in electron density. This is because electron density is only indirectly related to the frequency measurement through Faraday rotation and equation (5.3). However, since two receiver signal frequencies are required in equation (5.3), the standard deviations for frequency measurement error can be used in this equation to indicate an uncertainty for Faraday rate. By assuming, in equation (5.3), that the errors in both measurements of receiver frequency are statistically independent, the corresponding error in Faraday rate can be estimated. For a standard deviation of 9 mHz, the expected error at 100 km, the uncertainty in Faraday rate is 4.5 mHz. By calculation an uncertainty in Faraday rate of 5.7 mHz at the 2.225 MHz transmitting frequency corresponds to an electron-density uncertainty of 100 cm^{-3}. Therefore, when this uncertainty has been combined with other possible errors, it should be expected that the electron-density error will be about 100 cm^{-3}. Figures 5.6 and 5.7 show that the measured electron-density values for Nike Apaches 14.533 and 14.534, respectively, both have an uncertainty on the order of 100 cm^{-3} for the final calibrated probe current in the lower portions of the profile (i.e., near 100 km). By increasing SNR it is expected that this uncertainty would be decreased.

The SNR system test also provides detailed information about the receiver output spectrum as a function of input signal level. In general it is found that as the transmitted signal level is reduced, the output signal decreases very slowly and the noise level increases rapidly. Table 6.1 shows this result numerically by giving the relative amplitude of the reference signal as well as the peak noise level observed within a 30 Hz bandwidth centered at the reference frequency. The noise level at frequencies near that of the reference signal is an indication of the level of noise present

Table 6.1 Peak receiver output signal and noise levels versus relative input signal level.

Relative Input Signal Power (dB)	Approximate Reference Signal Peak Amplitude	Peak Noise Amplitude Within 30 Hz B.W.	$\left(\frac{\text{Peak Signal}}{\text{Peak Noise}}\right)$ dB
0	76	0.16	54
-10	75	0.49	44
-20	72	0.96	38
-30	66	2.5	28
-40	50	4.6	21
-50	20	7.8	8

Note: All amplitudes are relative.

at the reference signal frequency. This "in-band" noise is directly responsible for frequency measurement error. The information in this table was obtained by using the FFT spectral analysis procedure of Section 5.1. Table 6.1 shows that the signal spectral amplitude decreased very slowly as the input signal power level was reduced in 10 dB steps. This is the result of AGC action in the receiver. On the other hand, the peak noise amplitude approximately doubled for each 10 dB reduction of input signal power. The ratio of the peak amplitudes of signal and noise is also calculated in decibels for each of the input power levels. For the 0 dB relative input level, the output signal was approximately 500 times stronger than the background spectral noise. This factor decreased as the input signal power was reduced.

6.2.3 *Noise in the system.* The second system performance check undertaken was designed to monitor the effects of noise at several locations within the experimental system. The procedure was to use portable equipment to monitor the effect of noise on the instantaneous frequency of the reference signal. The equipment for this purpose is shown in Figure 6.3 where it is seen that the reference signal is first band-pass filtered (BPF) then FM detected followed by a low-pass filter (LPF) and finally spectrum analyzed. The concept that is used by this approach is that any noise within the bandwidth of the BPF causes the instantaneous frequency to vary which is demodulated by the FM detector. Spectral analysis of this detected signal allows for both the identification and classification of any noise present; that is, determine the presence of any noise and whether it is random or periodic. Since the digital data processing provides very narrow bandwidth filtering, only noise within several Hz of dc of the FM detector output are of concern.

For this test the experimental system was also operated in a pre-launch configuration and measurements were made at the transmitter van, launch pad blockhouse, and at the telemetry station. The van measurements were of the reference signal prior to amplification of the two CW carriers. The blockhouse measurements were made from the rocket payload control panel which monitored the receiver output. In the telemetry station, measurements were taken of the signal that was digitally sampled for recording purposes.

Results for the test can be divided into those related to system 1 and system 2. For system 1 no noise was observed at the van but white noise was observed at both the blockhouse and the telemetry station. The magnitude

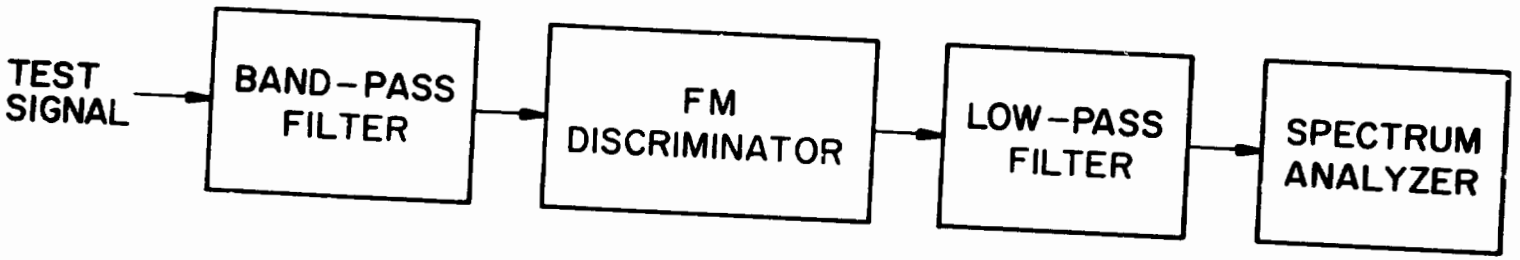

Figure 6.3 Test arrangement for second system check to monitor the effects of noise at various locations within the experimental system.

of the white noise was inversely related to the transmitted signal amplitude. For system 2 white noise was also observed at the blockhouse and telemetry station, but not in the van. In addition, periodic noise was also observed at 40, 60 and 80 Hz at all three locations. The source of noise for the 40 and 80 Hz components was identified as coming from the equipment that generates the 999.75 and 1000.25 kHz carrier signals in system 2; it was observed that the periodic noise frequencies could be moved several hertz by slight adjustments to the carrier signal frequencies. It was also discovered from this test that the system 2 local oscillator, f_o, shown in Figure 4 2 did not have the best type of crystal oven. Instead of using a linear (proportional) oven, a switching type was being used. As detailed in Section 4.1 switching ovens cause transient behavior in the reference frequency; this problem has subsequently been corrected.

Several conclusions can be made from this system test. For system 1, the source of the noise could not be clearly identified; from the previous SNR system test it is clear that the source was located before the receiver output but after the oscillator generating equipment in the van. This conclusion also holds for system 2 but further conclusions are possible. Theoretically, a constant amplitude sinusoid that frequency modulates a carrier generates a spectrum that places sidebands at multiples of the sinusoid frequency around the carrier frequency. The FM modulation from the 40, 60 and 80 Hz frequencies should not interfere with the frequency measurement of the carrier since the sidebands would be outside the narrow signal processing bandwidth. However, since it was demonstrated that the 40 and 80 Hz components could be shifted significantly in frequency, it is possible that they could, under some circumstances, cause interference.

6.2.4 *Conclusions.* As a result of the system tests as well as experience from the data analysis of Nike Apaches 14.533 and 14.534 certain sections of the system can be eliminated as major sources of noise under normal operating conditions. To begin with, the telemetry system does not appear to introduce any noise. This can be seen by observing the magnetometer rocket roll signal which uses the same or identical telemetry and data recording equipment as is used by the receiver channel. The rocket roll rate decreases very slowly once the rocket is free of the atmosphere. In the measurement of the rocket roll rate, using the spectral analysis techniques of Section 5.1, this characteristic was observed; it is shown in Figure 6.4 for Nike Apache 14.534. This

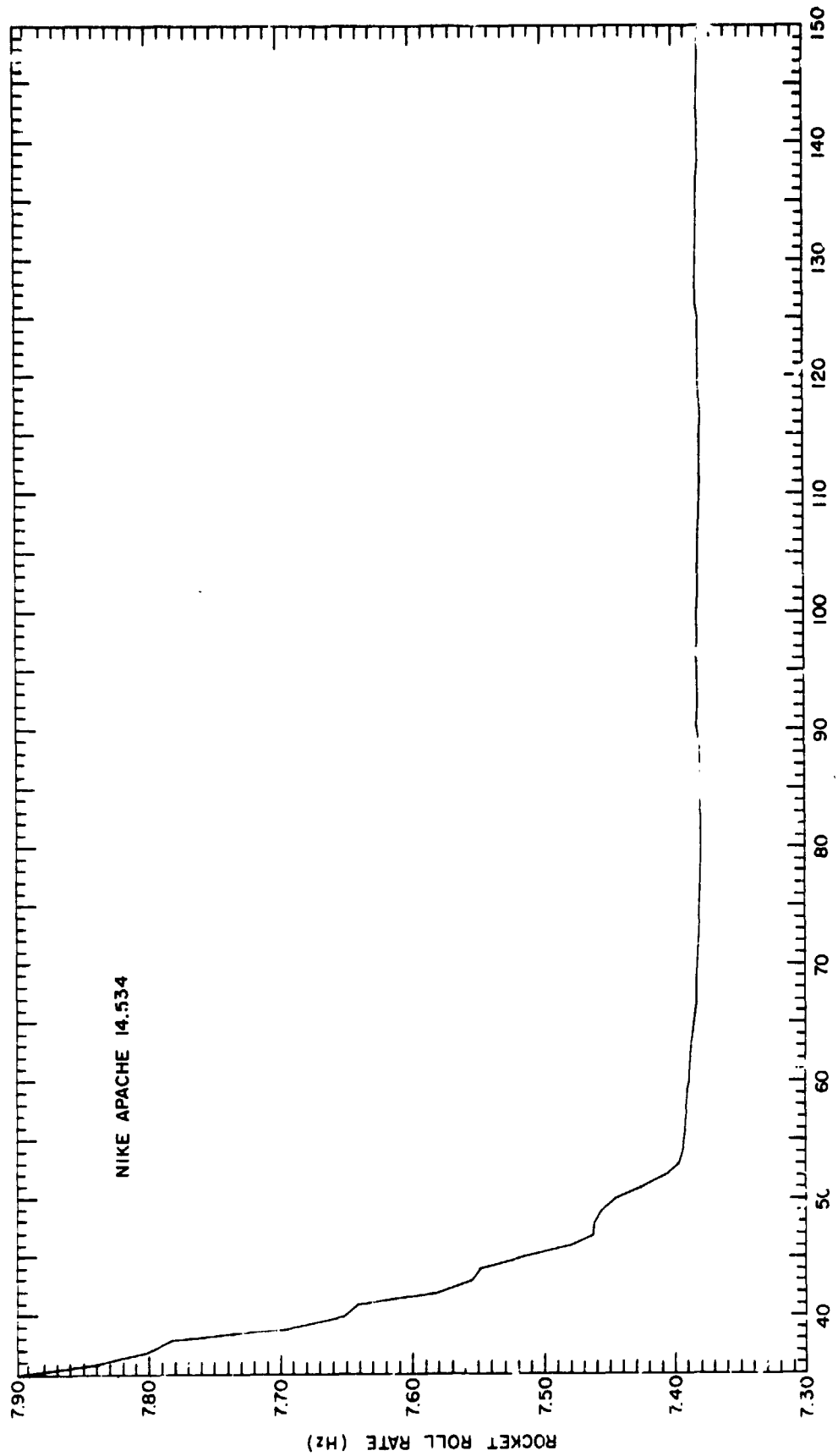

Figure 6.4 Rocket roll rate versus seconds after launch for Nike Apache 14.534.

plot is significant because it does not show any effects attributable to noise. Therefore, it is concluded that the noise introduced in the telemetry system, the A-to-D conversion, and the data recording equipment is negligible.

Some parts of the ground transmitting equipment can also be eliminated as noise sources. This is because it would be expected that any noise generated in the oscillators, mixers, or amplifiers would be most apparent at full power. However, the results of the SNR test of system 1 with full power indicate that no noise of significant amplitude exists. No similar conclusion can be directly made about system 2 from the tests, but it does demonstrate that equipment of this complexity is adequate for experiment requirements, when operating correctly. Further, the analysis of the reference signal channel also indicates no problem with either system with the exception of the frequency jump problem in system 2 due to the switching-type crystal oven.

The combined results and conclusions of the two system tests above indicate that the major source (or sources) of noise involve the receiver and atmospheric noise. It is very likely that at these frequencies of transmission and for moderate signal levels the dominant noise sources would be atmospheric "sky" noise, however, Figure 4.4 indicates that the receiver can contribute significant amounts of noise for low signal levels. Further, the SNR test has shown that at sufficiently large signal levels the experimental system is able to operate with low random error.

6.3 *Measurement of Frequency by Spectral Analysis*

Analysis of system performance is extended in this section to include the computer frequency measurement process of digital data. Several factors have been identified that presently limit the overall accuracy of this procedure. These limitations, which are both theoretical and practical in nature, deal with the definition of average frequency, the problem of frequency measurement overshoot, the effect of Gaussian windowing, and inaccurate rocket roll rate measurements.

6.3.1 *Step changes in frequency.* Section 5.1 presented a Fourier spectral analysis technique for measuring the required frequencies in equation (5.3) to obtain Faraday rotation rate. This procedure requires one second of data for each frequency measurement taken. In general, the signals that are measured for equation (5.3) do not have a constant frequency during the measurement interval and, therefore, some ambiguity exists in

interpreting the resulting measured values. It would be hoped that the values returned by the measurement process would correspond to the frequency time average for that interval. However, it has been established that this is generally not the case.

As an example, the theoretical spectrum of a one-second signal was calculated and the frequency of peak amplitude determined. The signal was a sinusoid at 490.50 Hz from t = 0 to t = 0.5 s and then suddenly changed in frequency to 490.51 Hz for the remainder of the interval: t = 0.5 s to t = 1.0 s. The peak spectral amplitude was found to be at 490.512 Hz. On the other hand, the time-averaged frequency for this signal was only 490.505 Hz. This example shows that the frequency of a spectral peak need not agree with the time-averaged frequency for a signal.

Theoretically, it is expected that the spectral peak frequency and the time-averaged frequency should agree only for a constant frequency sinusoid or a sinusoid whose frequency varies in a purely random fashion [*Taub and Schilling*, 1971]. For an actual electron-density profile the above results imply that reliable data can only be obtained in those regions with constant electron density or those with complex structure. In practice, regions of slowly varying electron density also have been found to give acceptable results. However, for other regions of the profile this ambiguity between measured frequency and actual time-averaged frequency can be a cause of error.

6.3.2 *Varying frequency.* An additional problem has been observed in measuring frequencies which vary during the measurement interval. It has been found that when steep gradients of electron density commence within a measurement window, the measured frequency tends to significantly overshoot or undershoot the actual frequency. Figure 6.5 shows the results of an example that will help clarify this problem. Artificial data was generated from a sinusoid which undergoes an interval of linearly increasing frequency as seen in the figure. The slope of this linear increase in frequency was such that a 30 mHz change occurred in a half second.

As the window was slid across the region of changing frequency the measured frequency significantly overshot the actual value which is also indicated in Figure 6.5. The maximum error between measured and actual frequencies was approximately 66 mHz even though the total actual frequency change was 30 mHz. The corresponding time-averaged value agreed much more

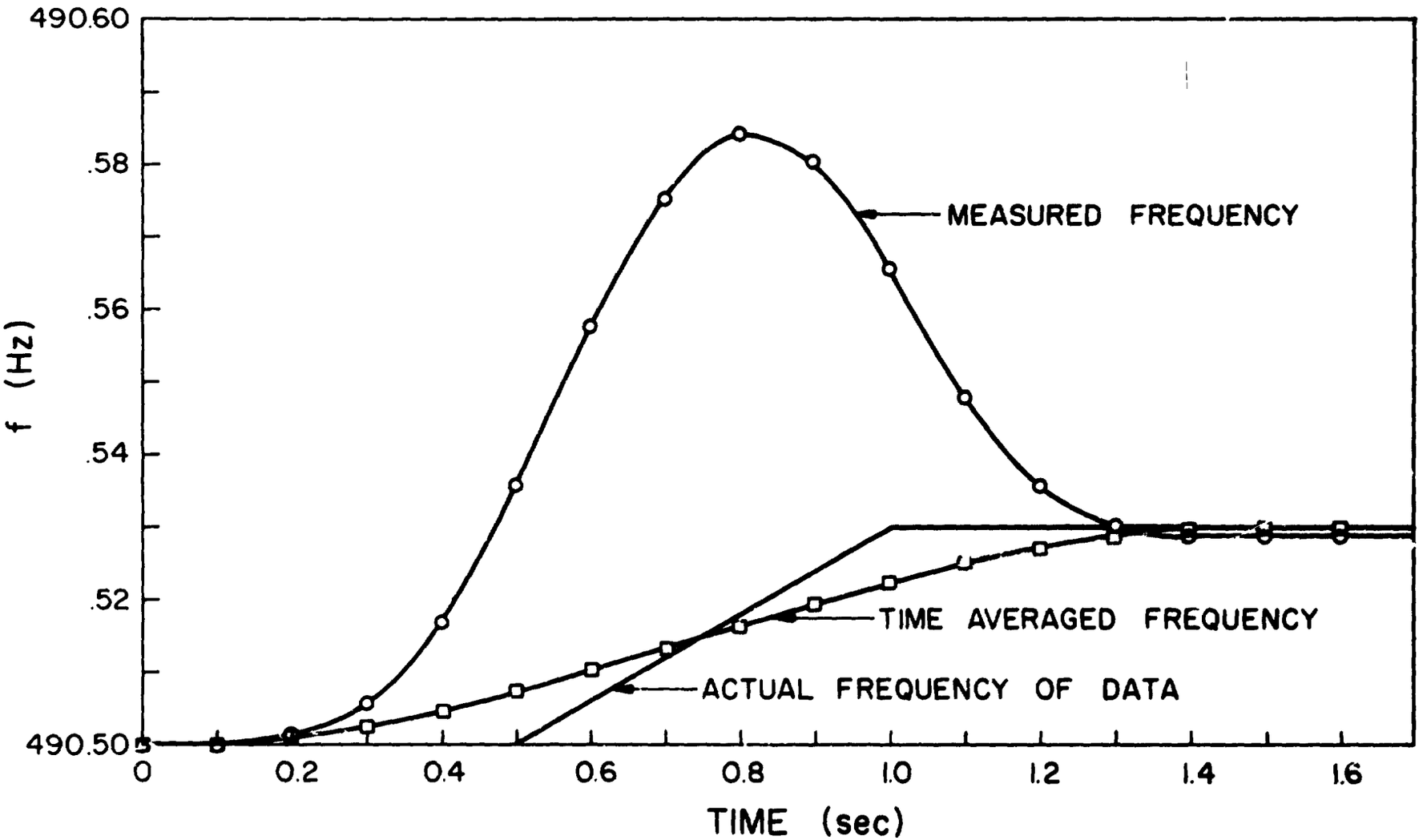

Figure 6.5 Frequency measurement overshoot during an interval of changing signal frequency.

closely as also seen in the figure.

It has been similarly established that a negative frequency slope would cause the measured frequency to undershoot the actual value. The magnitude of this frequency change over a half second is typical of what would be expected to occur at ledges in electron-density profiles. However, the example above may be artificial in that no attempt was made to prevent discontinuities from occurring at the boundaries of the changing frequency interval. Discontinuities in data cause spectral energy to spread over a wide frequency range which can introduce additional error into the measurements. In general, actual data will not have discontinuities such as these. Even so, evidence of overshoot and undershoot effect can be found in the experimental results of Figures 5.6 and 5.7.

6.3.3 *Windowing*. It was also indicated in Chapter 5 that Gaussian windowing was needed to reduce the effects of spectral leakage, however, this process creates a new problem. This problem results from the fact that the amplitude of the Gaussian window function approaches zero near the ends of the measurement window. During data processing that data which is aligned with the ends of the window interval are significantly attenuated due to multiplication with the Gaussian function. The result of this is that the frequency spectrum calculated for each interval is primarily determined from that data in the middle of the interval. Thus the use of windowing functions, such as the Gaussian, introduces the additional complication that some data are lost or greatly attenuated by the windowing process. This is shown in Figure 6.6(a) where the regions of lost data have been indicated. This fact prevents the measured frequencies from truly reflecting the data of the entire window interval.

It is of value at this point, for analysis purposes, to present one possible correction to this problem of lost data. This is done, at the expense of additional computer processing, by inserting new window intervals between the original. Figure 6.6(b) shows these new windows with dotted lines which now overlap the old windows. As is indicated in the figure the new windows would primarily use that data which was lost to the original non-overlapped windows. To prevent the number of subsequent computer processing steps from also increasing, after Faraday rotation calculation, the new data can be averaged into the old using a process known as Hanning filtering. The Hanning filter is essentially a method of calculating running averages. For this application the algorithm

(a) NON-OVERLAPPED WINDOW FUNCTIONS

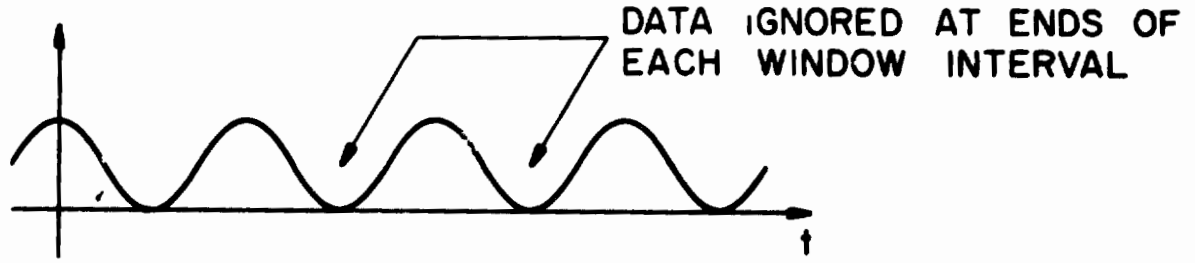

(b) ALTERNATE 50% OVERLAPPED WINDOW FUNCTIONS

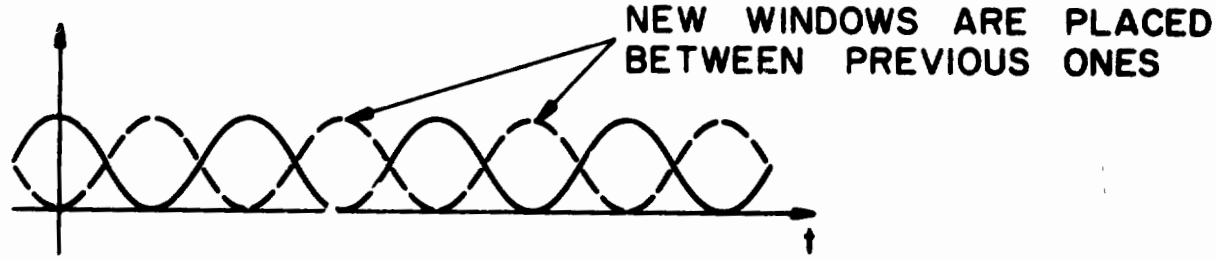

Figure 6.6 Example of window overlapping to provide better use of available data.

appears as

$$(F_j)_{FILTERED} = \frac{1}{4} F_{j-} + \frac{1}{2} F_j + \frac{1}{4} F_{j+}$$

where F_j is the jth Faraday rotation value measured from the jth original non-overlapping window and F_{j-} and F_{j+} represent Faraday rotation values from the new overlapped windows just before and after the jth original window, respectively. Using the above algorithm the number of filtered Faraday rotation values is equal to the number generated for the original non-overlapped windows.

The use of this alternate procedure for calculating Faraday rotation has two basic advantages. Firstly, as discussed above the use of overlapping windows enables all data to be considered in determining Faraday rotation. Secondly, *Harris* [1978] has indicated that measurement variance due to random noise can be reduced by the use of Gaussian windows with 50 percent overlap when the overlapped data is averaged. This latter point is significant because as indicated in Section 6.1 random atmospheric and receiver noise is the major source of error introduced by the experimental system. Therefore, data collected using this method should more closely represent the actual average Faraday rotation desired as well as being less sensitive to the effects of random noise.

Figure 6.7 provides a means of comparison between the use of non-overlapped and the overlapped Hanning filtered measurement procedure. This figure shows both methods, using Faraday rotation data from system 1 for the flight of Nike Apache 14.533. The results seem to substantiate the expected performance: the data derived from the new method tends to have smoother variation between data points when compared with the old method. This behavior is particularly noticeable beyond 90 SAL where the data becomes increasingly noisy (random), a predicted response from the previous section due to degrading SNR which is further substantiated by this figure. As is shown the new method data does not have as large peak variations when compared to the old. Before 90 SAL the data from both methods agree much more closely demonstrating the point that the new method does not simply smooth the old. It is important to remember that the new method uses three measurement values as opposed to one to generate each data point on the graph.

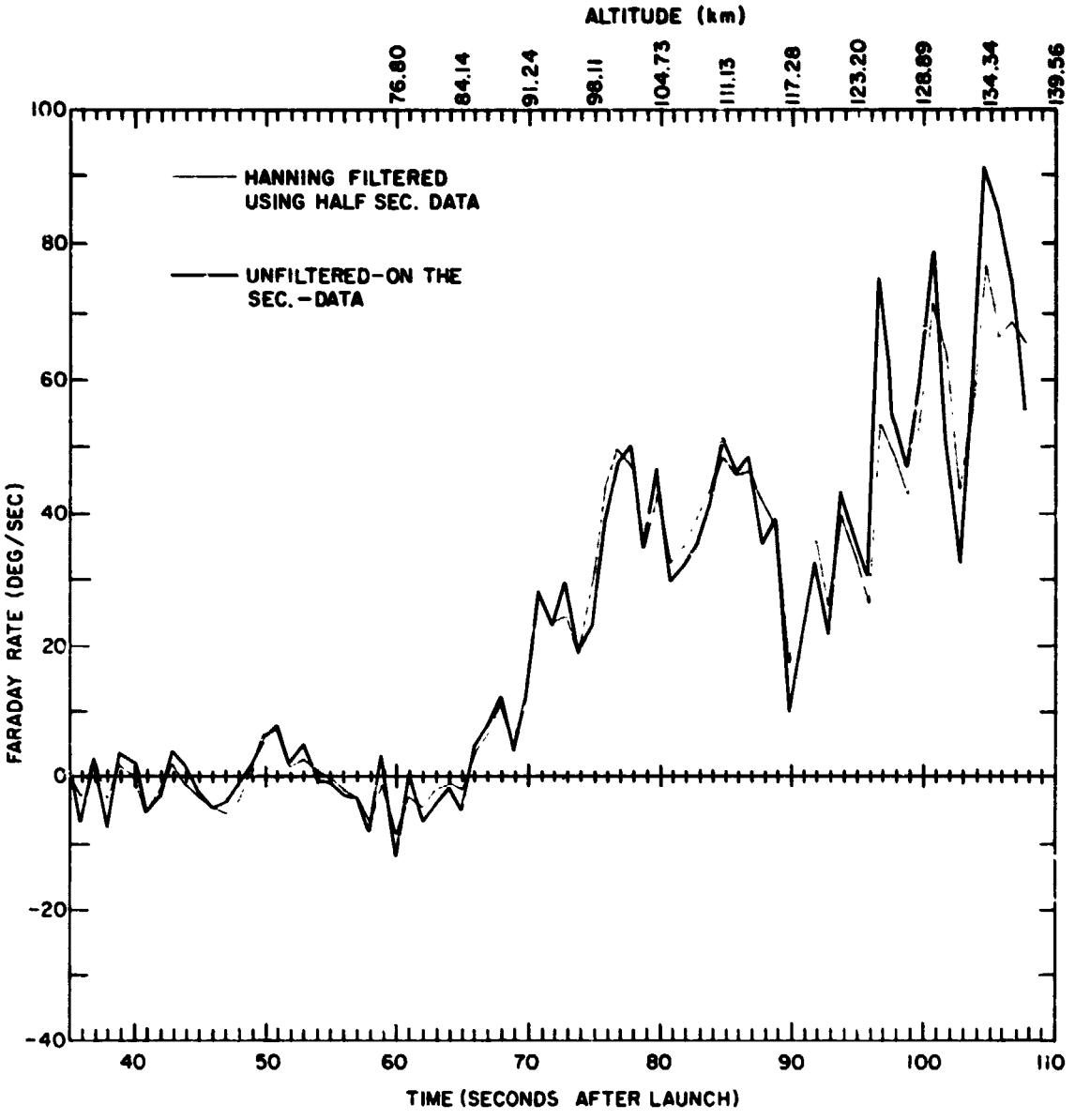

Figure 6.7 Comparison of Hanning filtered and nonfiltered data.

6.3.4 *Rocket roll rate.* The final problem that has been associated with the software data processing is in the measurement of the rocket roll rate. This measurement is particularly important because it is multiplied by 4 in equation (5.3) to determine Faraday rate. Although Faraday rate should be zero below the ionosphere, it has been observed for both Nike Apaches 14.533 and 14.534 (Figures 5.3 and 5.4, respectively) that a periodic error is present (prior to approximately 67 SAL). The error oscillates with a maximum deviation which is typically about 6 degrees per second and is independent of the system measurement frequency (2 or 3 MHz). It is clear that the error is not associated with any ionospheric effect and since the errors from both systems 1 and 2 are well correlated, the error must be caused by a common factor for both systems. It can be further seen in the figures that the oscillating error has a period which slowly increases until ionospheric penetration where any possible continuation of the error becomes obscured by Faraday rotation. This increasing period behavior appears to be related to rocket precessional effects. In general, while the rocket is still in the atmosphere, it has a precessional motion which has a period that slowly increases. Upon leaving the atmosphere (at about 80 km), the precessional period ceases to increase and stabilizes to a nearly constant value. The final values vary from flight to flight apparently dependent on the behavior of the rocket at the moment of exit from the atmosphere. Precessional motion can be observed on the magnetometer signal, which is used to measure rocket roll rate, as an amplitude modulation of a sinusoidal signal; it is also possible that precessional motion effects the frequency of the sinusoid as well. In either case since precession is present throughout the flight and since precessional caused error has been observed prior to ionospheric penetration, it is probable that error is being introduced into electron-density measurements due to precessional motion.

6.3.5 *Conclusion.* Several sources of error in the frequency measurement related to software have been identified in this section. Some, such as the definition of average frequency and the problem of frequency overshoot, are particularly hard to overcome because they are an inherent part of this measurement process. On the other hand the problem of lost data due to windowing can be overcome with the overlapping procedure; this method is also more tolerant to noise. The error due to precessional motion may also be correctable. It would appear that improving system SNR and correcting for

precessional motion effects would be particularly beneficial since SNR is critical and since rocket roll rate errors are magnified in equation (5.3).

7. CONCLUSIONS AND RECOMMENDATIONS FOR FURTHER WORK

The original reason for modifying the radio propagation experiment was to provide an experimental system capable of nighttime operation; the original experiment had not been satisfactory at night. The result of the work that followed was an experiment capable of providing data of sufficient accuracy during the nighttime, with the added advantage of reducing the complexity of the system. This was verified for the flights of Nike Apaches 14.533 and 14.534. However, it was found on those flights that the original experiment was also capable of providing useful nighttime data. No conclusive explanation has been found to explain the original experiment's recent success as opposed to its previous failures. It is possible that measurements on previous flights were made incorrectly or that ionospheric conditions were better for the two recent flights.

The accuracy of the propagation experiment appears to be adequate for its present application: the calibration of the Langmuir probe experiment for electron-density values of 100 cm^{-3} and greater. There are possibilities for further improvement. Based on system performance tests, significant improvements can be expected by improving SNR at the output and by correcting for precessional motion. Further improvement can be expected by dealing with the other error sources described in Chapter 6.

Several approaches exist for improving SNR. The first method would be to increase transmitted signal power. A minimum increase in signal power of 10 dB should be attempted; this will reduce the standard deviation of frequency measurement error by at least one half, as discussed in Section 6.1. Other less costly methods can be used to minimize noise and its effect. For example, the window overlap method described in Section 6.2 appears particularly attractive for noise suppression and complete data utilization. Also noise generated by the payload receiver should be considered. It should be determined whether the amount of noise presently generated by the receiver is significant when compared with typical atmospheric noise levels. If it is, then the receiver can possibly be tuned for minimum noise figure, a procedure not presently followed.

Various other modifications can be considered to improve the accuracy and reliability of the experiment. For example, at present no real-time pre-launch system check exists that can verify the operational readiness of the experiment. The system check would involve confirming adequate signal

strength, frequency stability, spectral purity, and the proper operation of data recording equipment. Semi-portable equipment to monitor the first three of the above items would be particularly helpful for trouble-shooting.

Certain modifications can be directed towards improving spectral leakage interference that occurs during Fourier spectral analysis. As described in Section 5.1 spectral leakage occurs whenever a signal is not periodic within the window interval (of one second), projecting energy over all spectral frequencies. Use of window functions, such as the Gaussian, are designed to reduce this problem. However, the situation can be further improved by reducing the amplitude of any signal which is potentially not periodic within the window interval; this would include any noise or sinusoid that is not exactly at an integer frequency (1, 2, 3, ... Hz). A simple modification for this purpose is to band-pass filter the receiver output signal prior to FFT analysis. This could be accomplished by analog or digital methods.

Another technique directed towards the elimination of unwanted intermodulation signals is the use of a square law detector instead of the envelope detector of the present payload receiver. The desired mixing operation of the detector input signal would be undertaken by a squaring operation. The higher order terms present in the output of the envelope detector generate unwanted components that have the potential of causing spectral leakage interference. A square law detector would not have the higher order components present. Neither of these suggested modifications would require major system alterations. Relatively simple checks could be devised to verify the usefulness of these changes before actually carrying out the modification.

Another problem that should be considered is that of impulse noise. Atmospheric noise due to static discharges from lightning can generate impulsive radio interference that can propagate many hundreds of miles at HF. This impulse noise is often observed in the received signal, particularly at low signal levels. The exact effect of impulse noise on FFT frequency measurements has not yet been determined, but it should be expected that an impulse will generate a white noise power spectrum, thus increasing the error. Some kind of limiter action in the receiver may be able to reduce the effect.

It is hoped that some of the suggested modifications above can be implemented for future nighttime rocket flights. It is expected that improved accuracy and more reliable operation can be obtained while still maintaining overall experimental simplicity.

REFERENCES

Aikin, A. C. and L. J. Blumle [1968], Rocket measurements of the *E*-region electron concentration distribution in the vicinity of the geomagnetic equator, *J. Geophys. Res.*, *73*, 1617-1626.

Allen, J. B. [1977], Short term spectral analysis, synthesis, and modification by discrete Fourier transform, *IEEE Transactions on Acoustics, Speech and Signal Processing*, *ASSP-25*, 235-238.

Allen, J. B. and L. R. Rabiner [1977], A unified approach to short-time Fourier analysis and synthesis, *Proceedings of the IEEE*, *65*, 1558-1564.

Appleton, E. V. [1932], Wireless studies in the ionosphere, *J. Inst. Elec. Eng.*, *71*, 642-650.

Bergland, G. D. [1969], A guided tour of the fast Fourier transform, *IEEE Spectrum*, *6*, 41-52.

Bowhill, S. A. [1964], Electron density measurements by the radio propagation technique, *COSPAR Information Bulletin No. 17, Technique Manual on Electron Density and Temperature Measurements in the Ionosphere*, 7.

Cartwright, D. G. [1964], A 10-kilocycle per second Doppler observation of the intermediate layer of the nighttime ionosphere, *J. Geophys. Res.*, *69*, 1031-4035.

CIRA [1972], *COSPAR International Reference Atmosphere*, Akademie-Verlag, Berlin.

Dickinson, P. H. G., J. E. Hall, and F. D. G. Bennett [1976], Rocket measurements of electron concentration in the lower ionosphere at two European locations, *J. Atmos. Terr. Phys.*, *38*, 163-173.

Fillinger, R. W., E. A. Mechtly, and E. K. Walton [1976], Analysis of sounding rocket data from Punta Chilca, *Aeron. Rep. No. 73*, Aeron. Lab., Dep. Elec. Eng., Univ. Ill. Urbana.

Gooch, J. D., H. V. Krone, and D. O. Skaperdas [1966], Results of sixteen differential absorption and Faraday rotation measurements with Nike Apache rockets, *Internal Rep. R-324*, Coord. Sci. Lab. Univ. Ill., Urbana.

Hall, J. E. and J. Fooks [1965], The electron distribution in the quiet D region from rocket measurements of low frequency propagation, *Planet. Space Sci*, *13*, 1013-1030.

Harris, F. J. [1978], On the use of windows for harmonic analysis with the discrete Fourier transform, *Proceedings of the IEEE, 66,* 51-83.

Hartree, D. R. [1931], The propagation of electromagnetic waves in a refracting medium in a magnetic field, *Proc. Cambridge Phil. Soc., 27,* 143-162.

Hirao, K. and R. Muraoka [1967], Resonance probe, *COSPAR Technique Manual Series, Electron Density and Temperature Measurements in the Ionosphere,* 33.

Kimura, I., R. Nishina, and K. Maeda, Rocket observations of the nighttime ionosphere using the VLF Doppler technique, *Space Res., VIII,* 305-312.

Knight, P. [1972], A classification of nighttime electron density profiles, *J. Atmos. Terr. Phys., 34,* 401-410.

Knoebel, H., D. Skaperdas, J. Gooch, B. Kirkwood, and H. Krone [1965], High resolution radio frequency measurements of Faraday rotation and differential absorption with rocket probes, *Internal Rep. R-273,* Coor. Sci. Lab., Univ. Ill., Urbana.

Knoebel, H. W. and D. O. Skaperdas [1966], Rocket measurements of Faraday rotation and differential absorption, *Rev. Sci. Inst., 37,* 1395-1400.

Lawrence, R. S., C. G. Little, and H. J. A. Chivers [1964], A survey of ionospheric effects upon earth-space radio propagation, *IEEE Proc., 52,* 4-27.

Mechtly, E. A. [1974], Accuracy of rocket measurements of lower ionosphere electron concentrations, *Radio Sci., 9,* 373-378.

Mechtly, E. A., S. A. Bowhill, L. G. Smith, and H. W. Knoebel [1967], Lower ionosphere electron concentration and collision frequency from rocket measurements of Faraday rotation, differential absorption, and probe current, *J. Geophys. Res., 72,* 5239-5245.

Mechtly, E. A., P. E. Monro, N. Golshan, and R. S. Sastry [1970], Fortran programs for calculating lower ionosphere electron densities and collision frequencies from rocket data, *Aeron. Rep. No. 37,* Aeron. Lab., Dep. Elec. Eng., Univ. Ill., Urbana.

Morrison, H. C. [1966], Program media, *Internal Rep. I-134,* Coor. Sci Univ. Ill., Urbana.

Oppenheim, A. V. and R. W. Schafer [1975], *Digital Signal Processing,* Prentice-Hall, Englewood Cliffs, New Jersey.

Ratcliffe, J. A. [1972], *An Introduction to the Ionosphere and Magnetosphere*, Cambridge University Press, 1-256.

Salah, J. E. and S. A. Bowhill [1966], Collision frequencies and electron temperatures in the lower ionosphere, *Aeron. Rep. No. 14*, Aeron. Lab., Univ. Ill., Urbana.

Seddon, J. C. [1953], Propagation measurements in the ionosphere with the aid of rockets, *J. Geophys. Res.*, *58*, 323-335.

Sen, H. K. and A. A. Wyller [1960], On the generalization of the Appleton-Hartree magnetoionic formulas, *J. Geophys. Res.*, *65*, 3931-3950

Slekys, A. G. and E. A. Mechtly [1970], Aeronomy Laboratory system for digital processing of rocket telemetry tapes, *Aeron. Rep. No. 35*, Aeron. Lab., Dep. Elec. Eng., Univ. Ill., Urbana.

Smith, L. G. [1970], A sequence of rocket observations of nighttime sporadic *E*, *J. Atmos. Terr. Phys.*, *32*, 1247-1257.

Smith, L. G., M. A. Geller, and H. D. Voss [1974], Energetic electrons in the midlatitude nighttime *E* region, *J. Atmos. Terr. Phys.*, *36*, 1601-1612.

Smith, L. G., E. K. Walton, and E. A. Mechtly [1978], Vertical incidence absorption calculated using electron density profiles from rocket experiments and comparison with observations during the winter anomaly, *J. Atmos. Terr. Phys.*, *40*, 1185-1197.

Taub, and D. Schilling [1971], *Principles of Communication Systems*, McGraw-Hill, Inc.

Ulwick, J. C., W. Pfister, O. C. Haycock, and K. D. Baker [1967], Standing wave impedance probe, *COSPAR Technique Manual Series, Electron Density and Temperature Measurements in the Ionosphere*, 66.

Voss, H. D. and L. G. Smith [1977], Energetic particles and ionization in the nighttime middle and low latitude ionosphere *Aeron. Rep. No. 76*, Aeron. Lab., Dep. Elec. Eng., Univ. Ill., Urbana.

Yeh, K. C. and C. H. Liu [1972], *Theory of Ionospheric Waves*, Academic Press, New York.

APPENDIX I. PROGRAM FOR READING DIGITAL TAPES

```
FRIES.
SIGNON(?22541553).
[redacted] ←—(CODE WORD GOES HERE)
BILL,CLEC,PS6899.
PRINT,RJE=EE/CC/EJ.
SETTL,30.
FTN,A,L=0.
LABEL,TAPE1,NT,LB=KU,PO=R,VSN=WI543F-A047,F=L.
ATTACH,UOILIB/UN=LIBRARY.
LDSET(LIB=SYMLIB/UOILIB).
LGO.
SKIPTO,X.
EXIT.
ENDSKIP,X
DAYFILE.
   PROGRAM TIMDIS (INPUT,OUTPUT,TAPE1,TAPE2=OUTPUT,TAPE3=INPUT)
* THIS PROGRAM IS INTENDED  TO DISPLAY THE HEADER RECORDS AND DATE
* CODES AND/OR CHECK THE TIME BETWEEN RECORDS ON THE DATA TAPE
* AGAINST THE EXPECTED VALUE FOR NASA DATA TAPES RECORDED AT WALLOPS
* ISLAND VIRGINIA.  THE USER SUPPLIES THE BEGINNING RECORD NUMBER
* AND THE NUMBER OF RECORDS TO BE READ INDICATING IF ALL TIME RECORDS
* IN THAT BLOCK WILL BE PRINTED OR JUST THOSE WITH TIME LENGTHS NOT
* EXPECTED.  MORE THAN ONE DATA CARD CAN BE USED.  DATA CARDS MUST
* HAVE THE FOLLOWING FORMAT:
*
* FIRST DATA CARD
*       COLUMN 1-4          EXPECTED TIME BETWEEN RECORDS, MILLISECONDS*10
* OTHER DATA CARDS
*       COLUMN 1-4          FIRST RECORD IN BLOCK, RIGHTJUSTIFIED
*       COLUMN 5            COMMA
*       COLUMN 6-9          NUMBER OF CONSECUTIVE RECORDS TO CHECK
*       COLUMN 10           COMMA
*       COLUMN 11           1 IF ALL TIME CODES TO BE PRINTED
*                           0 IF ONLY DESCREPENCIES PRINTED
*
* A 789 CARD MUST FOLLOW THE DATA DECK.  THE PROGRAM WILL PRINT HEADERS
* FOR RECORDS OF LENGTH 10, 45, 1005, OR 2008 WORDS.  EACH WORD IS 16
* BITS LONG.
* WRITTEN BY KEITH FRIES    JULY 5, 1978
* AERONOMY LABORATORY - UNIVERSITY OF ILLINOIS
      IMPLICIT INTEGER(A-Z)
      REAL DIFF.DFRSEC,F1
      DIMENSION ARRAY(2008),PARRAY(400)
      DATA (NBLOCK=0)
* THE FOLLOWING LINE LOCATES THE 'FILE ENVIRONMENT TABLE' ADDRESS WHICH
* IS USED LATER IN THE PROGRAM TO BACKSPACE TAPE1.
      NN=FETADR(1)
* SET FLAG FOR PRINTING HEADER WITH FIRST GROUP OF RECORDS
      HEAD=0
* WRITE "NASA" BANNER AT TOP OF OUTPUT.
```

```
      WRITE(2,5)
    5 FORMAT("0"/"0",6X,"N     N   AAAA    SSSS    AAAA",13X,"AERONOMY"
     J/" ",6X,"NN    N  A    A  S    S  A    A"
     J/" ",6X,"N N   N  A    A  S       A    A",10X,"LABORATORY"
     J/" ",6X,"N  N  N  AAAAAA   SSSS   AAAAAA"
     J/" ",6X,"N   N N  A    A       S  A    A",14X,"ROCKET"
     J/" ",6X,"N    NN  A    A  S    S  A    A"
     J/" ",6X,"N     N  A    A   SSSS   A    A",13X,"PROGRAM"
     J/"0",11X,"-- CDC CYBER VERSION --"/"0"/"0")
C READ CARD INFORMATION.
C INPUT STANDARD TIME BETWEEN RECORDS
      READ(3,6) STDSTP
    6 FORMAT(I4)
C INPUT DESIRED RECORD INFORMATION
   10 CONTINUE
      READ(3,20) RECNUM,NUM,ALLPRT
   20 FORMAT(I4,1X,I4,1X,I1)
      IF(EOF(3)) 200,21
C SET FLAG INDICATING FIRST RECORD IN GROUP
   21 START=0
C PRINT NASA WITH FIRST DATA GROUP, ELSE START NEW PAGE
      IF(HEAD.EQ.0) GOTO 300
      WRITE(2,310)
  310 FORMAT("1")
  300 CONTINUE
      HEAD=1
      WRITE(2,22) NUM,RECNUM
   22 FORMAT("0"/"0","SEARCH ",I4," RECORDS BEGINNING WITH RECORD "
     J,I4," .")
      IF(ALLPRT.EQ.1) GOTO 24
      WRITE(2,23)
   23 FORMAT(" ","ONLY RECORDS WHICH HAVE NON-STANDARD TIME ",
     J"BETWEEN RECORDS WILL BE PRINTED")
   24 CONTINUE
      WRITE(2,26)
   26 FORMAT("0"/" ")
C SKIP THE PROPER NUMBER OF RECORDS TO GET TO THE RECORDS DESIRED.
   25 ISKIP=RECNUM-NBLOCK-1
      IF(ISKIP) 30,70,50
   30 ISKIP=-ISKIP
      DO 40 I=1,ISKIP
   40 CALL BACKUP(NN,NBLOCK)
      GOTO 70
   50 DO 60 I=1,ISKIP
   60 CALL FORWRD(1,NBLOCK)
C FILL ARRAY WITH DATA.
   70 DO 190 I=1,NUM
      CALL TPGET(1,ARRAY,1,NWORDS,NBLOCK)
      IF(NWORDS.EQ.2008) GOTO  90
      IF(NWORDS.EQ.1005) GOTO 130
      IF(NWORDS.LE.45)   GOTO 160
      WRITE(2,80) NBLOCK,NWORDS
   80 FORMAT("+","RECORD ",I4," NON-STANDARD LENGTH, ",I4,
     J" WORDS."/"0")
```

```
      GOTO 190
   90 CONTINUE
      CALL CALTIM(ARRAY(2006),ARRAY(2007), ARRAY(2008),DAY,HOUR,MIN,SEC,
     JFRCSEC)
      D1=DAY/100
      D2=(DAY-D1*100)/10
      D3=(DAY-D1*100-D2*10)
      H1=HOUR/10
      H2=HOUR-H1*10
      M1=MIN/10
      M2=MIN-M1*10
      S1=SEC/10
      S2=SEC-S1*10
      F1=FRCSEC*.0001
*  CONVERT TIME TO SECONDS
*  KEEP IN INTEGER VARIABLES TO AVOID ONVERSION ERROR
      DECSEC=864000000*DAY+36000000*HOUR+600000*MIN+10000*SEC+FRCSEC
      IF(START.EQ.0) GOTO 126
      IDIFF=DECSEC-OLDDEC
*  CHECK TIME INTERVAL, IF CORRECT DO NOT PRINT
      IF(IDIFF.EQ.STDSTP) GOTO 126
*  BREAK INTO SINGLE DIGIT VARIABLES IN ORDER TO DISPLAY
*  LEADING ZEROS
*  CONVERT TO REAL TO SIMPLIFY PRINT ROUTINE, CONVERSION ERROR
*  WILL BE ROUNDED VIA PRINT
      DIFF=IDIFF*.0001
      DDAY=DIFF/86400
      DHOUR=(DIFF-DDAY*86400)/3600
      DH1=DHOUR/10
      DH2=DHOUR-DH1*10
      DMIN=(DIFF-DDAY*86400-DHOUR*3600)/60
      DM1=DMIN/10
      DM2=DMIN-DM1*10
      DSEC=DIFF-DDAY*86400-DHOUR*3600-DMIN*60
      DS1=DSEC/10
      DS2=DSEC-DS1*10
      DFRSEC=DIFF-INT(DIFF)
      TEMP=NBLOCK-1
      WRITE(2,124)NBLOCK,TEMP,DDAY,DH1,DH2,DM1,DM2,DS1,DS2,DFRSEC
  124 FORMAT("+",60X,"TIME BETWEEN RECORDS ",I4," AND ",I4,
     J": DAYS ",I3,", ",2I1,":",2I1,":",2I1,F5.4)
      GOTO 127
  126 CONTINUE
      IF(ALLPRT.NE.1) GOTO 129
  127 CONTINUE
      WRITE(2,110)NBLOCK,D1,D2,D3,H1,H2,M1,M2,S1,S2,F1
  110 FORMAT("+","RECORD ",I4,"  TIME: DAY ",
     J3I1,", ",2I1,":",2I1,":",2I1,F5.4," U.T."/"0")
  129 CONTINUE
      START=1
      OLDDEC=DECSEC
      GOTO 190
  130 WRITE(2,140) NBLOCK
  140 FORMAT("+","RECORD ",I4," CONTAINS 1005 WORDS."/"0")
```

```
      GOTO 190
  160 WRITE(2,170) NBLOCK,NWORDS                                          95
  170 FORMAT("+","RECORD ",I4," CONTAINS ",I2," WORDS.")
*  THE FOLLOWING THREE DO-LOOPS ARE NECESSARY TO CONVERT TEXTUAL DATA
*  FROM IBM EBCDIC REPRESENTATION TO CYBER DISPLAY REPRESENTATION.
      DO 173 N=1,NWORDS
      M=2*N-1
  173 CALL GBYTES(ARRAY(N),PARRAY(M),44,8,0,2)
      M=2*NWORDS
      DO 176 N=1,M
  176 PARRAY(N)=CONETD(PARRAY(N))
      DO 178 N=1,M
      IF((PARRAY(N).EQ.00).OR.(PARRAY(N).EQ.42).OR.(PARRAY(N).EQ.50).OR.
     J(PARRAY(N).EQ.63)) PARRAY(N)=45
  178 CONTINUE
      WRITE(2,180)(PARRAY(N),N=1,M)
  180 FORMAT(" ",90R1)
      WRITE(2,182)
  182 FORMAT("0")
  190 CONTINUE
      GOTO 10
  200 STOP
      END

      SUBROUTINE CALTIM(T2006,T2007,T2008,DAY,HOUR,MIN,SEC,FRCSEC)
      IMPLICIT INTEGER(A-Z)
      DIMENSION I(16)
*  SUBROUTINE CALTIM (CALCULATE TIME) CALCULATES TIMES
*  BY DECODING THE NASA DIGITAL TIME DATA IN THE LAST
*  THREE WORDS OF A TAPE RECORD.    THIS IS UNIVERSAL
*  COORDINATED TIME IN DAYS, HOURS, MINUTES, SECONDS,
*  AND DECIMAL FRACTIONAL SECONDS.

*  CONVERT T2006 INTO FRACTIONAL SECONDS.
      CALL BINARY(T2006,I)
      FRCSEC=(8*I(16)+4*I(15)+2*I(14)+I(13))*1000
     1+(8*I(12)+4*I(11)+2*I(10)+I(9))*100
     2+(8*I(8)+4*I(7)+2*I(6)+I(5))*10
     3+(8*I(4)+4*I(3)+2*I(2)+I(1))

*  CONVERT T2007 INTO MINUTES AND SECONDS.
      CALL BINARY(T2007,I)
      MIN=(4*I(15)+2*I(14)+I(13))*10
     1+(8*I(12)+4*I(11)+2*I(10)+I(9))
      SEC=(4*I(7)+2*I(6)+I(5))*10
     1+(8*I(4)+4*I(3)+2*I(2)+I(1))

*  CONVERT T2008 INTO DAYS AND HOURS
      CALL BINARY(T2008,I)
      DAY=(2*I(16)+I(15))*100
     1+(8*I(14)+4*I(13)+2*I(12)+I(11))*10
     2+(8*I(10)+4*I(9)+2*I(8)+I(7))
      HOUR=(2*I(6)+I(5))*10
     1+(8*I(4)+4*I(3)+2*I(2)+I(1))
      RETURN
      END
```

```
      SUBROUTINE BINARY(IINTGR,I)
      INTEGER I(16)
*  SUBROUTINE BINARY GENERATES THE BINARY REPRESENTATION
*  OF THE NUMBER INTGR, FOR USE IN SUBROUTINE CALTIM.

      INTGR=IINTGR
      DO 1 N=1,16
    1 I(N)=0
      DO 2 N=1,16
      J=17-N
      L=2**(J-1)
      IF(INTGR.GE.L) I(J)=1
      IF(INTGR.GE.L) INTGR=INTGR-L
    2 CONTINUE

*  THE ARRAY I(1-16) IS THE BINARY REPRESENTATION OF
*  THE NUMBER INTGR, WITH I(16) BEING THE MOST SIGNI-
*  FICANT BIT,2**15, AND I(1) THE LEAST SIGNIFICANT
*  BIT,2**0.

      RETURN
      END
      SUBROUTINE TPGET(U,ARRAY,M,N,NBLOCK)

*   THIS SUBROUTINE IS USED TO TRANSFER ONE RECORD OF TAPE DATA FROM
*   UNIT 'U' TO 'ARRAY', BEGINNING WITH ARRAY ELEMENT M.  THE NUMBER
*   OF 16-BIT WORDS TRANSFERRED ON EACH CALL IS N (TYPICALLY 10, 45,
*   1005, OR 2008). THE NUMBER OF THE RECORD JUST READ IS NBLOCK.

      IMPLICIT INTEGER(A-Z)
      DIMENSION BUFFER(540), ARRAY(1)
      BUFFER IN (U,1)(BUFFER(1),BUFFER(540))
      NBLOCK=NBLOCK+1
      IF(UNIT(U)) 10,20,40
   10 CALL LENGTHX(U,I,J)
*  I IS THE NUMBER OF 60-BIT WORDS READ.
*  J IS THE NUMBER OF BITS IN THE LAST 60-BIT WORD THAT WERE NOT USED.
      N=(60*I-J)/16
      CALL GBYTES(BUFFER,ARRAY(M),0,16,0,N)
      RETURN
   20 NBLOCK=NBLOCK-1
      WRITE(2,30) NBLOCK
   30 FORMAT(" "/"0","*** END OF FILE ENCOUNTERED. LAST RECORD IS ",I4,
     J". ***")
      STOP 1
   40 WRITE(2,50) NBLOCK
   50 FORMAT(" "/"0","*** PARITY ERROR DETECTED IN RECORD ",I4,". ***")
      STOP 2
      END


      SUBROUTINE FORWRD(U,NBLOCK)
```

```
*  THIS SUBROUTINE IS USED TO FORWARD SPACE ONE RECORD ON TAPE UNIT U.
*  THE NUMBER OF THE RECORD SKIPPED IS NBLOCK.

      IMPLICIT INTEGER(A-Z)
      DIMENSION BUFFER(540)
      BUFFER IN (U,1)(BUFFER(1),BUFFER(540))
      NBLOCK=NBLOCK+1
      IF(UNIT(U)) 10,20,40
   10 RETURN
   20 NBLOCK=NBLOCK-1
      WRITE(2,30) NBLOCK
   30 FORMAT(" "/"0","*** END OF FILE ENCOUNTERED. LAST RECORD IS ",I4,
     J". ***")
      STOP 3
   40 WRITE(2,50) NBLOCK
   50 FORMAT(" "/"0","*** PARITY ERROR DETECTED IN RECORD ",I4,". ***")
      RETURN
      END


      INTEGER FUNCTION FETADR(UNIT)

*  THIS INTEGER FUNCTION RETURNS AS ITS VALUE THE ADDRESS OF
*  THE "FILE ENVIRONMENT TABLE" CORRESPONDING TO THE FORTRAN
*  UNIT NUMBER GIVEN BY "UNIT", OR ELSE 0, IF THAT UNIT WAS NOT
*  DEFINED IN THE "PROGRAM" STATEMENT IN THE MAIN PROGRAM. FOR
*  INSTANCE, IF THE PROGRAM STATEMENT IS
*
*           PROGRAM XYZ(TAPE1,TAPE2,INPUT,TAPE5=INPUT)
*
*  THEN FETADR(1) WILL BE THE MACHINE ADDRESS OF THE "FET" FOR
*  "TAPE1", FETADR(2) WILL BE ADDRESS OF THE FET FOR TAPE2
*  AND FETADR(5) WILL BE THE ADDRESS OF THE FET FOR FILE "INPUT",
*  SINCE UNIT 5 IS EQUATED TO "INPUT" IN THE PROGRAM. FETADR(6),
*  FOR EXAMPLE, WILL BE 0, SINCE TAPE6 DOES NOT APPEAR IN THE
*  PROGRAM STATEMENT.
*
*  THIS FUNCTION IS INTENDED TO WORK ONLY UNDER CDC CYBER FORTRAN.
*  IF YOU TRY TO USE IT IN ANY OTHER CIRCUMSTANCE, YOU DESERVE
*  WHAT YOU GET. ALSO, UNLESS YOU KNOW WHAT A FET IS AND WHAT IT'S
*  FOR, DON'T MUCK WITH THE ROUTINE, BECAUSE OTHER ROUTINES MAY
*  DEPEND ON THIS ONE.
*
*  CODED FEBRUARY 1978 BY STAN KERR AT THE COMPUTING SERVICES OFFICE
*  OF THE UNIVERSITY OF ILLINOIS AT URBANA, FOR BOB ZIMMERMAN OF
*  ELECTRICAL ENGINEERING.

      IMPLICIT INTEGER(A-Z)
      DIMENSION CORE(1)

      IF(UNIT .GE. 10) GOTO 50
         LFN = 4LTAPE + SHIFT(1R0+UNIT,30)
         GOTO 60
50    LFN = 4LTAPE + SHIFT(1R0+UNIT/10,30) +
```

```
     +               SHIFT(IRO+MOD(UNIT,10),24)
60    B = LOCF(CORE(0))
      FETADR = 0

      DO 80 I = 2,64
        IF(CORE(I-B) .EQ. 0) GOTO 100
        IF((CORE(I-B) .AND. -777777B) .EQ. LFN) GOTO 90
80    CONTINUE
90    FITADR = CORE(I-B) .AND. 777777B
      FETADR = CORE(FITADR-B+1) .AND. 777777B

100   RETURN
      END

      SUBROUTINE BACKUP(FETADR,NBLOCK)

*  THIS ROUTINE IS INTENDED MAINLY FOR BACKING UP 1 BLOCK ON
*  A MAGNETIC TAPE BEING READ BY A FORTRAN PROGRAM. IT IS ASSUMED
*  THAT THE TAPE IS ACCESSED BY THE PROGRAM VIA SOME UNIT NUMBER,
*  SAY 5. THE USER OF THIS ROUTINE SHOULD FIRST USE THE INTEGER
*  FUNCTION "FETADR" TO ESTABLISH THE ADDRESS OF THE "FILE
*  ENVIRONMENT TABLE" FOR THE TAPE, AND SAVE THE VALUE (NEVER MIND
*  WHY, JUST DO IT). THEN THIS ROUTINE MAY BE CALLED AT WILL TO
*  BACKSPACE THE TAPE BY ONE BLOCK. THE SECOND PARAMETER IS SUPPOSED
*  TO BE AN INTEGER VARIABLE WHICH THE USER PRESUMABLY USES TO
*  KEEP TRACK OF WHICH BLOCK THE TAPE IS POSITIONED ON; ALL BACKUP
*  DOES WITH "BLOCK" IS SUBTRACT ONE FROM IT.
*
*  IF THE TAPE IS UNIT 5, THEN THE PROCESS OF USING BACKUP WOULD BE
*  SOMETHING LIKE THIS:
*
*      IADDR = FETADR(5)
*
*      .
*      .
*      CALL BACKUP(IADDR,NBLOCK)
*      .
*      .
*      .
*      DO 25 I = 1,10
*25      CALL BACKUP(IADDR,NBLOCK)
*
*      ETCETERA,ETCETERA,ETCETERA
*
*  THIS  ROUTINE IS INTENDED TO RUN ONLY UNDER CYBER FORTRAN AT THE
*  UNIVERSITY OF ILLINOIS. IT USES AN EXTERNAL ROUTINE "SKIPB" FROM
*  SYSTEM LIBRARY SYMLIB TO DO THE ACTUAL BACKSPACE.
*
*  CODED BY STAN KERR AT THE COMPUTING SERVICES OFFICE OF THE UNIVERSITY
*  OF ILLINOIS AT URBANA FOR BOB ZIMMERMAN OF ELECTRICAL ENGINEERING.
*
      IMPLICIT INTEGER(A-Z)
      DIMENSION  CORE(1)
```

```
      BIAS = LOCF(CORE(0))

      IN = CORE(FETADR+1-BIAS) .AND. 777777B
      CORE(FETADR+2-BIAS) = (CORE(FETADR+2-BIAS) .AND. MASK(42)) + IN
      CORE(FETADR+3-BIAS) = (CORE(FETADR+3-BIAS) .AND. MASK(42)) + IN

      CALL SKIPB(CORE(FETADR-BIAS),1,1)
      NBLOCK = NBLOCK-1
      RETURN
      END
```

```
          IDENT  CONETD
((        ENTRY  CONETD
**        CONETD - TABLE ORGANIZATION
*
*         THE CONVERSION TABLE USED BY CONETD IS SET UP WITH
*         8 DISPLAY CODE CHARACTERS PER WORD, LEFT-JUSTIFIED, TO
*         SIMPLIFIY THE ARITHMETIC NECESSARY TO ACCESS A WORD
*         WHICH CONTAINS THE DISPLAY CODE CORRESPONDING TO A GIVEN
*         EBCDIC CHARACTER.

CONETD    EQ     0
          SA1    X1           X1 = I
          SX6    -1           X6=-1, DEFAULT VALUE IF I OUT OF RANGE
          NG     X1,CONETD    RETURN IF I<0
          SX2    256
          IX2    X1-X2
          PL     X2,CONETD    RETURN IF I>255
          BX2    X1
          AX2    3            X2=I/8
          SA2    X2+TABLE     X2 = TABLE WORD WITH CONVERTED VALUE
          MX0    57
          BX1    -X0*X1       X1=MOD(I,8)
          SX1    X1+1         X1=MOD(I,8)+1
          LX1    1
          BX3    X1
          LX3    1
          IX1    X1+X3        X1=6*(1+MOD(I.8))
          SB2    X1
          LX2    B2           SHIFT CONVERTED VALUE TO LOW 6 BITS
          MX0    54
          BX6    -X0*X2       AND OUT EXTRANEOUS AND RETURN
          EQ     CONETD

TABLE     DATA   5562646055525565000OB,5555554556465750000OB
          DATA   3334353655555155000OB,4344555561547371000OB
          DATA   5555555555474277000OB,5555555550067700000B
          DATA   5555415555555553000OB,5555555374055000000B
          DATA   5555555555555555000OB,5555615772514566000OB
          DATA   6755555555555555000OB,5555625347527776000OB
          DATA   4650555555555555000OB,5555755636573710000B
          DATA   5555555555555555000OB,5574006074705464000OB
          DATA   5501020304050607000OB,1011555555555555000OB
          DATA   5512131415161720000OB,2122555555555555000OB
```

```
          DATA    5576232425262730000B,3132555555555550000B
          DATA    5555555555555550000B,5555555555555550000B
          DATA    7201020304050607000B,1011555555555550000B
          DATA    6612131415161720000B,2122555555555550000B
          DATA    7555232425262730000B,3132555555555550000B
          DATA    3334353637404142000B,4344555555555550000B
          END
0800
0644,1356,1
```

APPENDIX II. PROGRAM FOR FREQUENCY DETERMINATION BY FFT

```
//BRIAN JOB
/*ID PS=5184,NAME=BRIAN GILCHRIST
/*ID CODE=MARCI
/*ID PLOT=YES,IOREQ=5000,LINES=5000,TIME=(3,00),REGION=280K
/*SETUP UNIT=TAPE,R=A317,ID=(WI534F,NORING)
// EXEC FORTLDPT,PARM.GO='TIME=10.00,PL=60',REGION.GO=280K
//FORT.SYSIN DD *
C     IWK MUST BE FOUND IN CORE ON A BOUNDRY DIVISIBLE BY 8
C     INTEGER*4 IWK(18050) WILL ONLY WORK HALF THE TIME
C     THIS IS BECAUSE IT IS USED AS A STORAGE AREA FOR A REAL *4 VARIABLE IN FFT
      REAL*8 IWK(9025)
      INTEGER*2 ARRAY(32128)
      REAL*8 DATA(6000)
      COMPLEX*16 GAMN
      REAL*4 DMAG(3000),FREQ(200)
      EQUIVALENCE(DATA,DMAG)
      NAMELIST/PRAMS/NRGO,NSNGO,NELT,NELN
      ASSIGN 999 TO KILL
      CALL TPOPIZ(12)
C     NRGO IS FIRST RECORD NUMBER
C     NSNGO IS FIRST SCAN NUMBER IN RECORD
C     NELT IS ELEMENT NUMBER IN SCAN
C     NELN IS NUMBER OF ELEMENTS TO BE USTD.
C     WARNING - USER MUST  COMPUTEALL OF THESE VALUES CAREFULLY
C     PLOTTING SEQUENCE **********************
      NCRV=35
C     GENERATE FREQ. ARRAY (MINUS TO MOVE DOWN THE PAGE)
      DIMENSION SCA(2),SCF(2)
      DO 8 NF=1,200
8     FREQ(NF)=1-NF
C     FIRST DRAW FREQ. CCALE
C     START AT ZERO, THEN GO AT 20. PER INCH(FOR 8 INCH AXIS)
      SCF(1)=0.0
      SCF(2)=20.
      CALL PLOT(.5,.5,-3)
      CALL CCP5AX(0.,9.,'LOW FREQ(HZ)',-13,2.,-90.,SCF)
      SCF(1)=380
      CALL CCP5AX(0.,7.,'FREQUENCY (HZ)',-14,7.,-90.,SCF)
C     READY SCALE FACTOR FOR FREQ ARRAY
      SCF(1)=-180.0
C     SET UP TIME AXIS.(NCRV = # OF PLOTS TO MAKE)
      SCA(1)= 1.
      SCA(2)=1.
      DIST = NCRV
      CALL CCP5AX(0.,0.,'TIME(RELATIVE)',-14,DIST,0.,SCA)
      CALL CCP5AX(0.,9.,'TIME(RELATIVE)', 14,DIST,0.,SCA)
C     PLOTTING SEQUENCE **********************
43    CONTINUE
      READ (5,PRAMS)
      WRITE(6,889)NRGO,NSNGO,NELT,NELN
```

```
889   FORMAT(1X,9I10)
C     FORMAT DATA CARD &PRAMS NRGO=4000,NSNGO=20,   ETC    ,&END
      IF(NRGO.EQ.0) GO TO 42
C     TAPE HANDLING ROUTINES
      IF(NRGO.EQ.1) CALL TPBSRZ(12)
      IF(NRGO.EQ.1)NSNGO=KNSNGO
      IF(NRGO.EQ.1) GO TO 41
      KSKIP = NRGO -1
      DO 40 N=1,KSKIP
      CALL TPFSRZ(12)
40    CONTINUE
41    FNTOP=FLOAT(NELN+NSNGO)
      NTOP=IFIX(FNTOP/400.)+1
      KNSNGO=IFIX(FNTOP)+400*(1-NTOP)
      WRITE(6,99)FNTOP,NRGO,NSNGO,NTOP,KNSNGO
99    FORMAT('  DEBUG  ',F15.6,4I10)
      DO 50 N=1,NTOP
      M=(N-1)*2008 + 1
      CALL TPGETZ(12,ARRAY(M))
      CALL TPCHKZ(12,NTAPE,KILL)
C     IGO=M+1999
C     ISTOP = IGO+ 8
C     WRITE(6,104)(ARRAY(I),I=IGO,ISTOP)
104   FORMAT(1X,9I10)
C     NTAPE = # OF BYTES TRANSFERRED
50    CONTINUE
      WRITE(6,102) ARRAY(2006),ARRAY(2007),ARRAY(2008) ,NTAPE
102   FORMAT(1H0,'   TIME CODE   ',4I10)
42    N005=2005
      NA=NSNGO*5+NELT
      DO 10 N=1,NELN
      DATA(N)= ARRAY(NA)
      NA=NA+5
      IF(NA.LE. N005 ) GO TO 10
      NA=NA+8
      N005 = N005+2008
10    CONTINUE
      TOTAL=0.0
      DO 26 N=1,NELN
   26 TOTAL=TOTAL+DATA(N)
      TOTAL=TOTAL/NELN
      DO 27 N=1,NELN
   27 DATA(N)=DATA(N)-TOTAL
   25 CONTINUE
C     DC NOW REMOVED
C     AT THIS POINT, "DATA" IS READY FOR WINDOWING
      NELN2=NELN/2
      FLN2=NELN2
      STT=1.+1./FLOAT(NELN)
      GBASE = 0.01111
      DO 20 K=1,NELN2
      DEL = 3.0*(STT-FLOAT(K)/FLN2)
      G=EXP(-0.5*DEL*DEL)-GBASE
```

```
      DATA(K) = G*DATA(K)
      KTP=NELN-K+1
      DATA(KTP) = G*DATA(KTP)
20    CONTINUE
C      **********
      CALL FFTR(DATA,GAMN,NELN,IWK)
C     AT THIS POINT, "DATA " CONTAINS THE COMPLEX SPECTRUM.
C     WRITE IT OUT
C     CONVERT TO MAGNUTUDES.   **************
      DO 30 N=1,NELN2
      NT = N*2
      DMAG(N)=DSQRT(DATA(NT)*DATA(NT)+DATA(NT-1)*DATA(NT-1) )
30    CONTINUE
C     WRITE IT OUT IN SELECTED GROUPS   **********
      DO 31 N=1,70,10
      NFREQ = N-1
      NTP = N + 9
31    WRITE(6,103) NFREQ,(DMAG(K),K=N,NTP)
103   FORMAT(1X,I9,10(1X,E9.2))
      DO 32 N=401,551,10
      NFREQ= N-1
      NTP = N + 9
32    WRITE(6,103) NFREQ,(DMAG(K),K=N,NTP)
C******FIND FREQUENCY OF PEAK******
      K1=3
      K2=16
      MAX=5
   53 AMAX=0.
      DO 52 K=K1,K2
      IF(DMAG(K).LT.AMAX) GO TO 52
      MAX=K
      AMAX=DMAG(K)
   52 CONTINUE
C COMPUTE FREQ. OF SIG. ALOGORITHIM
      MAXM=MAX-1
      MAXP=MAX+1
      RR=ALOG(AMAX/DMAG(MAXP))/ALOG(AMAX/DMAG(MAXM))
      FMAX1=MAX-1
      FSIG=FMAX1+0.5*(1.0-RR)/(1.0+RR)
      WRITE(6,106)FSIG
106   FORMAT(/,'FREQ. OF PEAK=',F10.5)
      K1=5
      K2=70
      XKM1=DMAG(1)
      XKM=DMAG(2)
      XK=DMAG(3)
      XKP=DMAG(4)
      GO TO 6
5     K1=400
      K2=540
      XKM1=DMAG(396)
      XKM=DMAG(397)
      XK=DMAG(398)
```

```
      XKP=DMAG(399)
    6 DO 54 K=K1,K2
      IF(XK.GT.XKM.AND.XKM.GT.XKM1.AND.XK.GT.XKP) GO TO 55
   56 XKM1=XKM
      XKM=XK
      XK=XKP
      XKP=DMAG(K)
      GO TO 54
   55 MAXM=K-3
      RR=ALOG(XK/XKP)/ALOG(XK/XKM)
      FSIG=MAXM+0.5*(1.-RR)/(1.+RR)
      WRITE(6,106)FSIG
      GO TO 56
   54 CONTINUE
      IF(K1.LT.200) GO TO 5
C  DANGER<<<<<DATA CAN (]) GIVE DIVIDE BY 0
C END OF FREQ. COMPUTATION ON SPECTRAL PEAKS
C     PLOTTING SEQUENCE **********************
C     SET UP SCALING FOR ALL PLOTS
C     WARNING*****XLOGZ EXPECTS REF. PT. IN LOWER LEFT<<<<<<<<<<<<<<<<
C     WARNING DMAG SCALE HAS BEEN SET TO "NICE" VALUES< < < < < < < < < < < <
C     WARNING MINIMUM ALLOWED VALUE OF  DIST" IS 2.0 < < < < < < < < < < < < < <
C      SCA WILL NOW BE SET TO FIXED VALUES...
      SCA(1)=1.
      IF(NELT.EQ.5) SCA(1)=0.0
      SCA(2)=2.
      CALL XLOGZ(DMAG,FREQ,40,1,SCA,SCF)
      WRITE(6,101) SCA(1),SCA(2)
  101 FORMAT(1X,2E15.5)
      CALL XLOGZ(DMAG(381),FREQ(41),139,1,SCA,SCF)
       CALL PLOT(1..0.,-3)
C     READY FOR NEXT XLOGZ CALL.
C     PLOTTING SEQUENCE **********************
C     READ NEXT DATA CARD....IF SCAN # = - Z , DO OTHER NELT
C                           ...IF CCAN# = 0, READ NEXT NELN ELEMENTS.
      GO TO 43
999   WRITE (6,998) NTAPE
998   FORMAT('   TAPE ERROR    ',I10)
      STOP
      END
//GO.FT12F001 DD UNIT=TAPE,VOL=(,RETAIN,SER=WI534F),DISP=OLD,
// DCB=(RECFM=U,BLKSIZE=4016),LABEL=(1,BLP,,IN)
//GO.SYSIN DD *
 &PRAMS NRGO=1287,NSNGO=151,NELT=1,NELN=5000,&END
 &PRAMS NRGO=1,NSNGO=1,NELT=1,NELN=5000,&END
 &PRAMS NRGO=1,NSNGO=1,NELT=1,NELN=5000,&END
 &PRAMS NRGO=1,NSNGO=1,NELT=1,NELN=5000,&END
           .
           .
           .
/*
```

APPENDIX III. PROGRAM TO CALCULATE ELECTRON CONCENTRATION FROM FARADAY ROTATION

```
//BRIAN JOB
/*ID PS=5184,NAME=BRIAN GILCHRIST
/*ID CODE=MARCI
/*ID TIME=2
/*ID LINES=4500
//  EXEC  FORTLDGO
//FORT.SYSIN  DD  *
C   ANALYSIS OF FR WITHOUT DA, GIVEN CF MODEL.
C   ENTER PARAMETERS OF OBLATE EARTH
      A=6.378165E6
      A2 =A*A
      A4 = A2*A2
      FLAT=1.-1./298.3
      B2=(A*FLAT)**2
      A2B2=A2*(1.-FLAT**2)
      A4B4=A4*(1.-FLAT**4)
      WRITE(11,41)
   41 FORMAT('-','NOTE THE FOLLOWING ABREVIATIONS AND CONVENTIONS:'/ -',
     *2X,
     *'AZD - LOOK AZIMUTH   - - - - - - - - -   DEGREES'/' ',2X,
     *'ELD - LOOK ELEVATION - - - - - - - - -   DEGREES'/' ',2X,
     *'HT  - HEIGHT   - - - - - - - - - - - - - METERS'/' ',2X,
     *'V   - VELOCITY - - - - - - - - -  METERS/SECOND'/' ',
     *'RLATD - ROCKET LATITUDE- - - - - - - - -   DEGREES'/' ',
     *'RLNGD - ROCKET LONGITUDE - - - - - - - -   DEGREES'/' ',2X,
     *'FRE - FARADAY ROTATION,EXPERIMENTAL -  DEGREES/SECOND'/' ',2X,
     *'DAE - DIFFERENTIAL ABSORBTION,EXPERIMENTAL - DECIBLES'/' ',2X,
     *'P   - PRESSURE - - - - - - - - - - - -   PASCALS'/' ')
C   ENTER PARAMETERS
C
C  RKTNO - ROCKET NUMBER
C  TM    - TIME
C  F     - FREQUENCY (HERTZ)
C  CFM   - COLLISION FREQ. MODEL PARAMETER (HERTZ/PASCAL)
C
      READ (5,50) RKTNO,TM,F,CFM
50    FORMAT (F10.4,F10.1,F10.0,F10.0)
      WRITE(11,42)
   42 FORMAT('-','INPUT DATA DECK:')
      WRITE(11,43) RKTNO, TM,F,CFM
   43 FORMAT('-',F7.4,2X,F6.1,2X,1PE10.3,2X,1PE10.3)
      WRITE(11,40)
   40 FORMAT(' ',2X,'AZIMUTH   ELEVATION ALTITUDE  VEL.  LATITUDE',
     *'  LONGITUDE    FRE.     DAE.')
      CALL COEFF (TM)
      W = 6.2831853*F
      DTR = 1.745329E-2
C   INITIALIZE ELECTRON DENSITY
      ED = 1.E9
C   ENTER VARIABLES
C
```

```
C  AZD   - AZIMUTH (DEGREES)
C  ELD   - ELEVATION (DEGREES)
C  HT    - HEIGHT (METERS)
C  V     - VELOCITY (METERS/SECOND)
C  RLATD - ROCKET LATITUDE (DEGREES)
C  RLNGD - ROCKET LONGITUDE (DEGREES)
C  FRE   - FARADAY ROTATION, EXPERIMENTAL (DEGREES/SECOND)
C  DAE   - DIFFERENTIAL ABSOBPTION, EXPERIMENTIAL (DECIBELS)
C  P     - PRESSURE (PASCALS)
C
    1 READ(5,51,END=30)AZD,ELD,HT,V,RLATD,RLNGD,FRE,DAE
51    FORMAT (8F10.4)
      WRITE(11,44) AZD,ELD,HT,V,RLATD,RLNGD,FRE,DAE
   44 FORMAT(' ',F9.4,2X,F9.4,2X,F7.0,2X,F5.0,2X,F8.4,2X,F9.4,2X,F8.3,2X
     *,F7.4)
      DAE=0.0
      READ (5,52)P
   52 FORMAT (F10.7)
      WRITE(11,45) P
   45 FORMAT(' ',2X,1PE9.2)
      CF = CFM*P
C   CONVERT DEGREES TO RADIANS
      AZ = AZD*DTR
      EL = ELD*DTR
      RLATR = RLATD*DTR
      RLNGR = RLNGD*DTR
      SINLA = SIN(RLATR)
20    SINLA2=SINLA*SINLA
      COSLA2=1.-SINLA2
      SPH = SIN(RLNGR)
      CPH = COS(RLNGR)
C   FIND GEOCENTRIC COORDINATES OF ROCKET
      DEN2=A2-A2B2*SINLA2
      DEN=SQRT(DEN2)
      FAC=(((HT*DEN)+A2)/((HT*DEN)+B2))**2
      CT=SINLA/SQRT(FAC*COSLA2+SINLA2)
      R=SQRT(HT*(HT+2.*DEN)+(A4-A4B4*SINLA2)/DEN2)
21    ST=SQRT(1.-CT**2)
C   CALCULATE GEOMAGNETIC FIELD AT ROCKET
      CALL FIELD (R,ST,CT,SPH,CPH,BR,BT,BP,B)
C   TRANSFORM FIELD COMPONENTS, GEOCENTRIC TO GEODETIC.
      SIND=SINLA*ST-SQRT(COSLA2)*CT
      COSD=SQRT(1.-SIND**2)
      BN=-BT*COSD-BR*SIND
      BD=BT*SIND-BR*COSD
      BW=-BP
      S = -1.758803E11*B
      Y=S/W
C   CALCULATE COSINE OF PROPAGATION ANGLE
      CEL = COS(EL)
      CTH = (CEL*COS(AZ)*BN-SIN(EL)*BD-CEL*SIN(AZ)*BW)/B
      TH=ARCOS(CTH)/DTR
C   CALCULATE FR AND DA COEFFICIENTS
      FV = F*V
```

```
      FC = 6.004153E-7*FV
      AC = 1.820428E-7*FV
C   ITERATE TO MATCH FR
      WRITE (6,67)
67    FORMAT (1H1)
      WRITE (6,68) RKTNO,TM,CFM
68    FORMAT (3X,F10.4,F10.1,1PE10.2,/)
      I = 6
      DO 2 N=1,I
C   CALCULATE REFRACTION AND ABSORPTION INDICES
      CALL SENWYL (ED,CF,S,CTH,W,RIO,RIX,AIO,AIX,ROR,RXR,ROI,RXI)
      FR = FC*(RIO-RIX)
      DA=AC*ABS(AIX-AIO)
      X = 3182.6018*ED/W/W
      Z=CF/W
      WRITE(6,61)AZD,BN,ROR,RIO,F,HT
      WRITE(6,62)ELD,BD,RXR,RIX,FRE,ED
      WRITE(6,63)RLATD,BW,ROI,AIO,FR,X
      WRITE(6,64)RLNGD,B,RXI,AIX,DAE,CF
      WRITE(6,65)V,Y,CTH,TH,DA,Z
61    FORMAT('    AZ ',1PE13.6,'    BN ',1PE13.6,'   ROR ',1PE13.6,
     &       '   RIO ',1PE13.6,'     F ',1PE13.6,'    HT ',1PE13.6)
62    FORMAT('    EL ',1PE13.6,'    BD ',1PE13.6,'   RXR ',1PE13.6,
     &       '   RIX ',1PE13.6,'   FRE ',1PE13.6,'    ED ',1PE13.6)
63    FORMAT('   LAT ',1PE13.6,'    BW ',1PE13.6,'   ROI ',1PE13.6,
     &       '   AIO ',1PE13.6,'    FR ',1PE13.6,'     X ',1PE13.6)
64    FORMAT('   LNG ',1PE13.6,'     B ',1PE13.6,'   RXI ',1PE13.6,
     &       '   AIX ',1PE13.6,'   DAE ',1PE13.6,'    CF ',1PE13.6)
65    FORMAT('     V ',1PE13.6,'     Y ',1PE13.6,'   COS ',1PE13.6,
     &       '    TH ',1PE13.6,'    DA ',1PE13.6,'     Z ',1PE13.6)
      WRITE (6,60)
60    FORMAT (1H )
      ED = FRE/FR*ED
2     CONTINUE
      GO TO 1
   30 WRITE(11,40)
      STOP
      END
      SUBROUTINE COEFF(TM)
      COMMON /COEFFS/TG(11,11)
      DIMENSION G(11,11),GT(11,11),SHMIT(11,11)
C   READ SPHERICAL HARMONIC COEFFICIENTS
C     THE COEFFICIENTS IN THE DATA STATEMENT ARE GSFC(12/66)
C     THIS G ARRAY CONTAINS BOTH G AND H VALUES
      DATA G/
     Z0.,-30401.2,-1540.1,1307.1,949.3,-233.5,49.2,72.2,8.5,10.4,-2.9,
     15778.2,-2163.8,2997.9,-1988.9,803.5,355.7,57.5,-53.7,6.5,5.8,-.9,
     2-1932.,202.9,1590.3,1276.8,502.9,228.4,-.8,7.9,-9.3,7.5,-2.2,
     3-425.4,227.8,-133.8,881.2,-397.7,-28.8,-238.3,15.6,-9.6,-15.1,.8,
     4160.3,-274.3,2.3,-246.6,266.5,-157.9,-1.5,-24.3,-6.1,12.1,-2.8,
```

```
     55.1,117.8,-114.8,-108.9,82.4,-62.2,-2.,-3.6,5.5,4.7,6.4,
     6-12.1,104.4,56.6,-23.4,-14.8,-13.3,-108.9,15.5,-8.1,.2,4.7,
     7-53.7,-27.4,-8.1,7.,24.3,-22.5,-21.4,3.6,13.,1.6,-.2,
     85.4,-11.7,4.2,-15.3,4.6,21.9,-.7,-17.1,7.4,.9,1.8,
     9-22.4,13.8,6.3,-3.,-1.9,9.,11.5,.1,-1.5,.2,2.,
     D-.1,4.5,-1.,2.6,-4.4,-1.3,-3.6,4.,1.,-2.,1.1/
      DATA GT/
     Z0.,14.03,-23.29,-.93,1.45,1.61,-.42,-.57,.35,-.10,-.01,
     1-3.71,8.76,-.09,-10.62,.9,.6,.82,-.34,.5,-.13,-.13,
     2-14.31,-16.62,-4.56,2.31,-1.75,3.34,.82,-1.44,1.7,-1.2,.88,
     35.2,2.53,-6.98,-5.89,.66,-.04,2.35,-.9,-.11,.08,-.18,
     4-2.19,-.14,1.88,-6.52,-3.01,-.6,.83,.03,.34,-.08,.17,
     52.24,1.59,-2.61,.5,-.12,1.76,.01,-.6,-.07,-.39,-.02,
     6.05,.09,2.55,-1.19,.33,.84,.23,-.17,.43,-.36,.05,
     7-.96,.01,.43,.75,-.33,.49,.9,-.64,-.15,.47,.17,
     8-.5,-.21,.03,-.79,.05,.1,-.36,-.43,-.42,.37,.16,
     9.66,.54,.03,.35,-.03,-.01,.45,-.05,.75,-.46,.31,
     D-.61,-.64,.02,.05,-.63,-.07,.07,-.03,-.02,-.45,-.23/
C    CALCULATE NORMALIZATION CONVERSION FACTORS
      SHMIT(1,1)=-1.
      MAXN =11
      DO 15 N=2,MAXN
      SHMIT(N,1)=SHMIT(N-1,1)*FLOAT(2*N-3)/FLOAT(N-1)
      SHMIT(1,N)=0.
      JJ=2
      DO 15 M=2,N
      SHMIT(N,M)=SHMIT(N,M-1)*SQRT(FLOAT((N-M+1)*JJ)/FLOAT(N+M-2))
      SHMIT(M-1,N)=SHMIT(N,M)
15    JJ=1
C    CONVERT COEFFICIENTS, SCHMIDT TO GAUSS
      DO 16 N=2,MAXN
      DO 16 M=1,N
      G(N,M)=G(N,M)*SHMIT(N,M)
      GT(N,M)=GT(N,M)*SHMIT(N,M)
      IF (M.EQ.1) GO TO 16
      G(M-1,N)=G(M-1,N)*SHMIT(M-1,N)
      GT(M-1,N)=GT(M-1,N)*SHMIT(M-1,N)
16    CONTINUE
C    CONVERT COEFFICIENTS TO NEW TIME
17    T=TM-1960.0
      DO 18 N=1,MAXN
      DO 18 M=1,N
      TG(N,M)=G(N,M)+T*GT(N,M)
      IF (M.EQ.1) GO TO 18
      TG(M-1,N)=G(M-1,N)+T*GT(M-1,N)
18    CONTINUE
      RETURN
      END
      SUBROUTINE FIELD (R,ST,CT,SPH,CPH,BR,BT,BP,B)
      DIMENSION P(11,11), DP(11,11), CONST(11,11)
      DIMENSION SP(11), CP(11), FN(11), FM(11)
      COMMON/COEFFS/G(11,11)
      NMAX = 11
1     P(1,1) = 1.
```

```
      DP(1,1) = 0.
      SP(1) = 0.
      CP(1) = 1.
      DO 2 N = 2,11
      FN(N) = N
      DO 2 M = 1,N
      FM(M) = M-1
2     CONST(N,M) = FLOAT((N-2)**2-(M-1)**2)/FLOAT((2*N-3)*(2*N-5))
3     SP(2) = SPH
      CP(2) = CPH
      DO 4 M = 3,NMAX
      SP(M) = SP(2)*CP(M-1)+CP(2)*SP(M-1)
4     CP(M) = CP(2)*CP(M-1)-SP(2)*SP(M-1)
      AOR=6.3712E6/R
      AR = AOR**2
      BT = 0.
      BP = 0.
      BR = 0.
      DO 8 N = 2,NMAX
      AR = AOR*AR
      DO 8 M = 1,N
      IF(M.EQ.N) GO TO 5
      P(N,M)=CT*P(N-1,M)
      DP(N,M)=CT*DP(N-1,M)-ST*P(N-1,M)
      IF(M.EQ.N-1) GO TO 7
      P(N,M)=P(N,M)-CONST(N,M)*P(N-2,M)
      DP(N,M)=DP(N,M)-CONST(N,M)*DP(N-2,M)
      GO TO 7
5     P(N,N) = ST*P(N-1,N-1)
      DP(N,N) = ST*DP(N-1,N-1)+CT*P(N-1,N-1)
7     PAR = P(N,M)*AR
      IF (M.EQ.1) GO TO 9
      TEMP = G(N,M)*CP(M)+G(M-1,N)*SP(M)
      BP = BP-(G(N,M)*SP(M)-G(M-1,N)*CP(M))*FM(M)*PAR
      GO TO 10
9     TEMP = G(N,M)*CP(M)
      BP = BP-(G(N,M)*SP(M))*FM(M)*PAR
10    BT = BT+TEMP*DP(N,M)*AR
8     BR = BR-TEMP*FN(N)*PAR
      BP = BP/ST
      B = SQRT(BT*BT+BP*BP+BR*BR)
      GTT=1.E-9
      BR=BR*GTT
      BT=BT*GTT
      BP=BP*GTT
      B=B*GTT
      RETURN
      END
      SUBROUTINE SENWYL(ED,CF,S,CPH,W,RIO,RIX,AIO,AIX,ROR,RXR,ROI,RXI)
C   GENERALIZED MAGNETO-IONIC THEORY, SEN-WYLLER EQUATIONS.
```

```
      COMPLEX EI,EII,EIII,AA,BB,CC,DD,EE,VC,VD,VE,VF,VG,VH,VO,VX
      COMPLEX CMPLX,CSQRT,BBVA,CCCPH,RO,RX
C     DEFINE BURKE-HARA FUNCTIONS FOR C3/2 AND C5/2.
      C32(X) = (X*(X*(X*(X+24.653115)+113.9416)+11.287513)+.023983474)/(
     1X*(X*(X*(X*(X*(X+24.656819)+120.49512)+289.58085)+149.21254)+9.387
     27372)+.018064126)
      C52(X) = (X*(X*(X+6.6945939)+16.901002)+1.1630641)/(X*(X*(X*(X*(X+
     16.6314497)+35.355257)+68.920505)+64.093464)+4.3605732)
      P2 = 3182.6018*ED
      WPS = W+S
      WMS = W-S
      Q = P2/W/CF
      R = Q/CF
      T = 2.5*Q
      A1 = W/CF
      A2 = WMS/CF
      A3 = WPS/CF
      A = R*W*C32(A1)
      B = T*C52(A1)
      C = R*WMS*C32(A2)
      D = T*C52(A2)
      E = R*WPS*C32(A3)
      F = T*C52(A3)
      EI = CMPLX (1.-A,-B)
      EII = CMPLX (.5*(F-D),.5*(C-E))
      EIII = CMPLX (A-.5*(C+E),B-.5*(F+D))
      AA = 2.*EI*(EI+EIII)
      BB  = EIII*(EI+EIII)+EII**2
      CC = 2.*EI*EII
      DD = 2.*EI
      EE = 2.*EIII
      VB = CPH*CPH
      VA = 1.-VB
      VC = BB*BB*VA*VA-CC*CC*VB
      VD=CSQRT(VC)
      BBVA=BB*VA
      VE=AA+BBVA
      VF = DD+EE*VA
      VG = (VE+VD)/VF
      VH = (VE-VD)/VF
      VO=CSQRT(VG)
      VX=CSQRT(VH)
C     SEPARATE INDICES
      RIO = REAL (VO)
      AIO = -AIMAG(VO)
      RIX = REAL (VX)
      AIX = -AIMAG(VX)
C     CALCULATE WAVE POLARIZATIONS
      CCCPH=CC*CPH
      RO=-((BBVA-VD)/CCCPH)
      ROR=REAL(RO)
      ROI=AIMAG(RO)
      RX=-((BBVA+VD)/CCCPH)
      RXR=REAL(RX)
```

```
      RXI=AIMAG(RX)
      RETURN
      END
//GO.FT11F001 ID SYSOUT=A,DCB=(RECFM=FA,LRECL=133)
//GO.SYSIN  DD *
14.534     1977.7     2225000.0 630000.0
104.8560   80.4478    89685.0    1460.0     37.8055    -75.3202   13.29
0.190
104.8680   80.4203    91113.0    1451.0     37.8049    -75.3172   25.79
0.147
104.8776   80.3932    92532.0    1442.0     37.8042    -75.3142   36.95
0.123
          .
          .
          .
/*
```

APPENDIX IV. PROGRAM TO CALIBRATE PROBE CURRENT

```
//BRIAN JOB
/*ID PS=5184,NAME='GILCHRIST'
/*ID CODE=MARCI
// EXEC FORTLDGO
//FORT.SYSIN DD *
      REAL LNCHSC
      DIMENSION T(120),TIME(600),C(120,5),CRNT(600),AVCRNT(120),
     1EN(100),UT(600),RATIO(100),SEC(100)
C  RN = ROCKET NUMBER
C  LNCHHR = HOUR AND MINUTE OF LAUNCH (UT)
C  LNCHSC = SECOND OF LAUNCH (UT)
      READ(5,90) RN,LNCHHR,LNCHSC
      WRITE(6,900) RN,LNCHHR,LNCHSC
900   FORMAT(1X,F7.4,5X,I4,5X,F5.1)
C  EN = ELECTRON DENSITY
C  READINGS MUST BEGIN AT THE FIRST INTEGER SECOND AFTER CURRENT READINGS START
      READ(5,91) (EN(I),I=1,60)
      WRITE(6,901)(EN(I),I=1,60)
901   FORMAT(1X,6(2X,E13.4))
C  T = TIME ON DATA CARDS
C  C = CURRENT ON DATA CARDS ( 2-DIMENSIONAL ARRAY )
      DO 111 I=1,120
      READ(5,100,END=150) T(I),(C(I,J),J=1,5)
  111 CONTINUE
      WRITE(6,902)(T(I),(C(I,J),J=1,5),I=1,120)
902   FORMAT(1X,F9.2,5E15.4)
      I=121
C
C  CONSTRUCT SINGLE SUBSCRIPTED ARRAYS OF TIME AND CURRENT
C
  150 NCARDS=I-1
C  NCARDS = NUMBER OF CARDS (TIME & CURRENT) THAT HAVE
C           BEEN READ AND WILL BE PROCESSED.
      K=0
C  CRNT = CURRENT ON DATA CARDS ( 1-DIMENSIONAL ARRAY )
C  TIME = ELAPSED TIME IN 0.1 SECOND INTERVALS
C  UT = UNIVERSAL TIME
      DO 210 I=1,NCARDS
      DO 210 J=1,5
      K=K+1
      CRNT(K)=C(I,J)
      TIME(K) = T(1) + (K-1)/10.
      UT(K) = LNCHSC + TIME(K)
C  THERE SHOULD BE (N-1) OF THE FOLLOWING CARDS FOR A MAXIMUM E.T. OF N MINUTES
      IF(UT(K).GE.60.0)UT(K)=UT(K)-60.0
  210 CONTINUE
      KM = K
      J=0
      MARK = 0
      DO 220 I=1,KM
C
C  FIND INTEGER SECONDS
C
```

```
      ITIME=TIME(I)
      TRT=ITIME
      DIF = TIME(I)-TRT
      IF(DIF.GT.0.01  .AND. DIF.LT.0.99 )GO TO 220
      J=J+1
      SEC(J) = TIME(I)
C  AVERAGE CANNOT BE FOUND FOR FIRST AND LAST SECONDS
      IF(J.EQ.1)GO TO 219
      IF(I.GT.(KM-9))GO TO 219
C
C  MULTIPLY CURRENTS BY WEIGHTING FACTORS AND FIND AVERAGE
C
      TCRNT = 0.0
      DO 215 K=1,10
      AK = K
      WCRNT = CRNT(I-10+K)*AK
  215 TCRNT = TCRNT + WCRNT
      DO 216 K=1,9
      AK = K
      WCRNT = CRNT(I+K) * (10.0-AK)
  216 TCRNT = TCRNT + WCRNT
      AVCRNT(J) = TCRNT/100.0
      RATIO(J) =  EN(J)/AVCRNT(J)
      GO TO 220
  219 AVCRNT(J) = 0.0
      RATIO(J) = 0.0
  220 CONTINUE
      JMX1 = J+1
      SEC(JMX1) = 0.05
C
C  FORM ARRAY FOR PRINT OUT
C
      WRITE(6,301) RN,LNCHHR,LNCHSC
      K=0
      XKM = KM
      HAF = XKM/2.
      IHAF = HAF
      HF = IHAF
      IF((HAF-HF).GT.0.001)GO TO 225
      N = IHAF
      GO TO 226
  225 N = IHAF+1
      IF((HAF-HF).GT. 0.99)GO TO 226
      TIME(N*2) = 0.0
      UT(N*2) = 0.0
      CRNT(N*2) = 0.0
      AVCRNT(JMX1) = 0.0
      EN(JMX1) = 0.0
      RATIO(JMX1) = 0.0
  226 JJ = 1
      M = 1
      MM = 50
  231 IF((N*2).GT.(MM+50))GO TO 265
      MARK = 10
```

```
      NTWO = N**2
      IF(NTWO.LE.MM)GO TO 255
      MM50 = MM + 50
C  THIS IS THE PRINTOUT FOR MORE THAN A HALF PAGE BUT LESS THAN A FULL PAGE
      DO 240 II=NTWO,MM50
      TIME(II) = 0.0
      UT(II) = 0.0
      CRNT(II) = 0.0
  240 CONTINUE
      JEND = JMX1 + 5
      DO 250 JI=JMX1,JEND
      SEC(JI) = 0.0
      AVCRNT(JI) = 0.0
      EN(JI) = 0.0
      RATIO(JI) = 0.0
  250 CONTINUE
      GO TO 265
C  THIS IS THE PRINTOUT FOR LESS THAN A HALF PAGE
  255 DO 260  L=M,NTWO
      IF(SEC(JJ).EQ.TIME(L)) GO TO 256
      WRITE(6,650) TIME(L),UT(L),CRNT(L)
      GO TO 260
  256 WRITE(6,651) TIME(L),UT(L),CRNT(L),AVCRNT(JJ),EN(JJ),RATIO(JJ)
      JJ = JJ + 1
  260 CONTINUE
      GO TO 280
C  THIS IS THE PRINTOUT FOR A FULL PAGE
  265 DO 270 L=M,MM
      IF(SEC(JJ).EQ.TIME(L))GO TO 266
      WRITE(6,450) TIME(L),UT(L),CRNT(L),TIME(L+50),UT(L+50),CRNT(L+50)
      GO TO 270
  266 WRITE(6,451) TIME(L),UT(L),CRNT(L),AVCRNT(JJ),EN(JJ),RATIO(JJ),
     1TIME(L+50),UT(L+50),CRNT(L+50),AVCRNT(JJ+5),EN(JJ+5),RATIO(JJ+5)
      JJ = JJ + 1
  270 CONTINUE
      IF(MARK.EQ.10)GO TO 280
      JJ = JJ + 5
      M = M + 100
      MM = MM + 100
      WRITE(6,301) RN,LNCHHR,LNCHSC
      GO TO 231
  280 WRITE(6,700)
      STOP
C
   90 FORMAT(F7.4,5X,I4,F5.1)
   91 FORMAT(6E13.4)
  100 FORMAT(F7.1,5E13.4)
  301 FORMAT(1H1,10X,'PROBE CURRENT AND WEIGHTED AVERAGES FOR FLIGHT NO.
     1 ',F7.4,5X,'LAUNCH TIME = ',I4,':',F4.1,' UT',//,3X,'ET',4X,'UT'
     2,9X,'I',12X,'IA',11X,'N',11X,'N/IA', 8X,'ET',4X,'UT',9X,'I',12X,
     3'IA',11X,'N',11X,'N/IA',/)
  450 FORMAT(1X,2(F5.1,1X),E13.4,42X,2(F5.1,1X),E13.4)
  451 FORMAT(1X,2(F5.1,1X),4E13.4,3X,2(F5.1,1X),4E13.4)
  650 FORMAT(1X,2(F5.1,1X),E13.4)
```

```
  651 FORMAT(1X,2(F5.1,1X),4E13.4)
  700 FORMAT(1H1)
C
      END
//GO.SYSIN DD *
14.534      0501 0.0
    0.0000E00    3.6736E08    7.1275E08    1.0231E09    1.7713E09    1.1056E09
    9.7248E08    1.2378E09    1.7004E09    2.0154E09    1.4876E09    1.7899E09
    7.7521E08    1.3261E09    7.8465E08    5.6499E08    0.0000E00    8.8611E08
    7.9762E08    0.0000E00    9.1819E08    7.1116E08    0.0000E00    1.9516E09
    1.0075E09    1.0114E09    2.3411E09    1.8292E09    1.9388E09    1.9655E09
    1.6734E09    1.8177E09    2.1163E09    1.4362E09    2.2506E09    2.1041E09
    1.4892E09    1.2826E09    1.6694E09    2.3264E09    1.7722E09    2.1993E09
    2.3582E09    1.7651E09    2.3729E09    3.3357E09    1.6570E09    1.8439E09
    1.8721E09    9.8402E08    2.6688E09    0.0000E00    0.0000E00    1.8630E09
    2.3049E09    1.8107E09    2.5580E09    1.3913E09    0.0000E00    1.1381E09
   68.0     .1156E-07    .1115E-07    .1073E-07    .1050E-07    .1047E-07
   68.5     .1146E-07    .1350E-07    .1553E-07    .1704E-07    .2300E-07
   69.0     .3160E-07    .4149E-07    .5120E-07    .5896E-07    .6550E-07
   69.5     .7339E-07    .7703E-07    .7555E-07    .8069E-07    .8908E-07
   70.0     .1031E-06    .1086E-06    .1051E-06    .1047E-06    .1122E-06
   70.5     .1242E-06    .1392E-06    .1602E-06    .1761E-06    .1752E-06
   71.0     .1765E-06    .1717E-06    .1665E-06    .1690E-06    .1666E-06
   71.5     .1587E-06    .1524E-06    .1514E-06    .1506E-06    .1506E-06
   72.0     .1946E-06    .2235E-06    .1590E-06    .1534E-06    .1462E-06
          .
          .
          .
/*
```

APPENDIX V. PROGRAM TO TABULATE AND PLOT ELECTRON CONCENTRATION

```
      PROGRAM GLOBAL(INPUT,OUTPUT,TRJTRY,TAPE1=TRJTRY,PCOUT,TAPE2=PCOUT,
     JECOUT,TAPE3=ECOUT,INTPL,TAPE4=INTPL)
      REAL T(60),ALTI(60),TIM(3500),PC(3500),ALT(3500),ECI(2500)
      REAL ZI(2500)
      REAL BB(9),BD(9),CC(9),DD(9)
      COMMON/Q/T(60),ALTI(60),ITCALL
      REAL NO
      REWIND1
      REWIND2
      REWIND3
      REWIND4
      DATA YES/"Y"/
      DATA NO/"N"/
      DATA EEE/"E"/
      DATA CCC/"C"/
      WRITE 1000
      READ 1001,A,B
      WRITE 1002
      READ 1003,C,D,CD
      WRITE 1004
      READ 1001,E,EE
      WRITE 1006
      READ 1003,F,G,FG
      WRITE 1008
C INPUT TRAJECTORY DATA FROM TAPE1.
      I=0
   10 I=I+1
      READ(1,1009)T(I),ALTI(I)
      IF(EOF(1)) 20,10
C OUTPUT TRAJECTORY DATA ON TERMINAL FOR VERIFICATION.
   20 II=I-1
      WRITE 1010,(T(I),ALTI(I),I=1,II)
      WRITE 1011
   30 READ 1012,H
      IF(H.EQ.YES) GOTO 50
      IF(H.EQ.NO ) GOTO 40
      WRITE 1013
      GOTO 30
   40 WRITE 1014
      STOP
C INPUT PROBE CURRENT DATA FROM FILE PCOUT.
   50 DO 70 I=1,3500,5
      READ(2,1025) TIM(I),(PC(I+J-1),J=1,5)
      IF(EOF(2)) 80,70
   70 CONTINJE
      WRITE 1026
      STOP
   80 JJ=I-1
      JN=I-5
C JJ IS THE INDEX OF THE LAST PROBE CURRENT.
      DO 90 I=1.JN.5
```

```
      DO 90 J=1,4
   90 TIM(I+J)=TIM(I)+.1*J
C ARRAY TIM IS NOW FILLED WITH THE TIME OF EACH PROBE CURRENT.
      IF(TIM(1).LT.T(1)) GOTO 92
      IF(TIM(JJ).LT.T(II)) GOTO 55
      WRITE 1028,TIM(JJ),T(II)
      STOP
   92 WRITE 1027,TIM(1),T(1)
      STOP
   55 WRITE 1015,A,B
   60 READ 1012,H
      IF(H.EQ.YES) GOTO 65
      IF(H.EQ.NO)  GOTO 120
      WRITE 1013
      GOTO 60
   65 WRITE 1017
      READ 1018, AM
      WRITE 1019
      READ 1020, PH
      WRITE 1021
      READ 1022, TAU
      WRITE 1023
      READ 1020, T1
      WRITE 1024
      READ 1020, T2
      DO 110 I=1,JJ
      IF((TIM(I).GE.T1).AND.(TIM(I).LE.T2)) GOTO 100
      GOTO 110
  100 IF(PC(I).EQ.2.0) GOTO 110
      PC(I)=PC(I)*(1.0+AM*COS(2.*3.1416*(TIM(I)-PH)/TAU))
  110 CONTINUE
C ASPECT CORRECTION IS NOW COMPLETE.
      ASPC1=1.0+AM*COS(2.*3.1416*(T1-PH)/TAU)
      ASPC2=1.0+AM*COS(2.*3.1416*(T2-PH)/TAU)
      WRITE 1029,A,B,AM,PH,TAU,T1,T2,T1,ASPC1,T2,ASPC2
  120 WRITE 1030
C CONVERT FROM PROBE CURRENT VERSUS TIME TO VERSUS ALTITUDE.
      ALTMAX=0.0
      DO 130 I=1,JJ
      CALL TRAJ(TIM(I),ALT(I))
      IF(ALTMAX.LT.ALT(I)) MM=I
      IF(ALTMAX.LT.ALT(I)) ALTMAX=ALT(I)
  130 CONTINUE
      WRITE 1031,ALTMAX,TIM(MM)
C CONVERSION TO ELECTRON CONCENTRATION FOLLOWS.
      WRITE 1032,A,B
      READ 1033,NUM
      IF(NUM.EQ.1) GOTO 175
      WRITE 1034
      READ 1035,BD(1)
```

```
  133 IJK=1
      CC(IJK)=0.0
      WRITE 1036, IJK
      READ 1037,BB(1)
  135 IJK=IJK+1
      IF(IJK.EQ.NUM) GOTO 170
      IF(IJK.GT.NUM) GOTO 180
      WRITE 1038,IJK,BD(IJK-1)
      READ 1035,BD(IJK)
  137 WRITE 1039, IJK
  140 READ 1012,H
      IF(H.EQ.EEE) GOTO 160
      IF(H.EQ.CCC) GOTO 150
      WRITE 1040
      GOTO 140
  150 CC(IJK)=0.0
      WRITE 1036, IJK
      READ 1037,BB(IJK)
      GOTO 135
  160 WRITE 1041,IJK
      READ 1037,BB(IJK)
      WRITE 1042
      READ 1035,CC(IJK)
      WRITE 1043
      READ 1035,DD(IJK)
      GOTO 135
  170 WRITE 1044,IJK,BD(IJK-1),ALTMAX
      BD(IJK)=ALTMAX+.0048
      GOTO 137
  175 CC(1)=0.0
      BD(1)=ALTMAX+.0048
      WRITE 1053
      READ 1037,BB(1)
C DISPLAY N/I CALIBRATION FACTORS ON THE SCREEN.
  180 WRITE 1045,A,B
      WRITE 1046,BD(1),BB(1)
      IF(NUM.EQ.1) GOTO 195
      DO 190 IJK=2,NUM
      IF(CC(IJK).GT.1.0) GOTO 185
      WRITE 1047,BD(IJK-1),BD(IJK),IJK,BB(IJK)
      GOTO 190
  185 WRITE 1048,BD(IJK-1),BD(IJK),IJK,BB(IJK),CC(IJK),DD(IJK)
  190 CONTINUE
C CONVERSION FROM PROBE CURRENT TO ELECTRON CONCENTRATION.
  195 DO 230 LMN=1,JJ
      DO 200 NOP=1,NUM
      IF(BD(NOP).GE.ALT(LMN)) GOTO 210
  200 CONTINUE
      STOP
  210 IF(PC(LMN).EQ.2.0) GOTO 230
      IF(CC(NOP).GT.1.0) GOTO 220
      PC(LMN)=PC(LMN)*BB(NOP)
      GOTO 230
  220 PC(LMN)=PC(LMN)*BB(NOP)*EXP((ALT(LMN)-CC(NOP))/DD(NOP))
```

```
  230 CONTINUE
C PROBE CURRENTS HAVE BEEN CHANGED TO ELECTRON CONCENTRATIONS.
C
C LINEAR ALTITUDE INTERPOLATION FOLLOWS.
      WRITE 1049
C FIND THE LOWEST-ALTITUDE ELECTRON CONCENTRATION.
      I=1
  240 IF(PC(I).NE.2.0) GOTO 250
      I=I+1
      GOTO 240
  250 IZT=ALT(I)*10.+.001
      RIZT=IZT+1
      J=1
      ZI(J)=RIZT/10.
C ZI(1) IS THE LOWEST ALTITUDE FOR WHICH AN ELECTRON
C CONCENTRATION CAN BE COMPUTED. READY TO INTERPOLATE.
  255 IP=I+1
  260 IF(IP.GT.JJ) GOTO 295
      IF(ALT(IP).LT.ALT(IP-1)) GOTO 295
      IF(PC(IP).EQ.2.0)  GOTO 265
      GOTO 270
  265 IP=IP+1 $ GOTO 260
  270 IF(ALT(IP).LT.ZI(J)) GOTO 275
      GOTO 280
  275 I=IP $ GOTO 255
C COME HERE FOR INTERPOLATION.
  280 AI=ZI(J)-ALT(I)
      BI=PC(IP)-PC(I)
      CI=ALT(IP)-ALT(I)
  285 EI=BI*(AI/CI)
      ECI(J)=PC(I)+EI
  286 ZI(J+1)=ZI(J)+.1
      J=J+1
      IF(ZI(J).GT.ALT(IP)) GOTO 290
      AI=AI+.1 $ GOTO 285
  290 I=IP $ GOTO 255
C COME HERE WHEN INTERPOLATION FOR ASCENDING PORTION OF FLIGHT IS
C COMPLETED.
  295 IEND=IP-1
      JEND=J-1
C JEND IS THE INDEX OF THE LAST ECI TO BE PRINTED FOR ASCENT.
C ECI STANDS FOR INTERPOLATED ELECTRON CONCENTRATION.
C
C IEND IS THE INDEX OF THE LAST PC USED IN THE INTERPOLATION ROUTINE
C FOR ASCENT. IN THIS PORTION OF THE PROGRAM PC IS THE UNINTERPOLATED
C ELECTRON CONCENTRATION (NOT THE PROBE CURRENT).
C
C OUTPUT THE ASCENDING ELECTRON CONCENTRATION TABLE TO TAPE 4.
      WRITE(4,1050)A,B,C,D,CD,E,EE,F,G,FG
      WRITE(4,1051)
      WRITE(4,1052)
      KM=ZI(1)+.001
      KMD=10*KM
      LD=ZI(1)*10.+.001
```

```
      ITEST=10-(LD-KMD)
C ITEST IS THE NUMBER OF  VALUES TO BE PRINTED IN THE FIRST LINE.
      GOTO(301,302,303,304,305,306,307,308,309,310),ITEST
  301 WRITE(4,1061)KM,ECI(1) $ GOTO 325
  302 WRITE(4,1062)KM,(ECI(J),J=1,ITEST) $ GOTO 325
  303 WRITE(4,1063)KM,(ECI(J),J=1,ITEST) $ GOTO 325
  304 WRITE(4,1064)KM,(ECI(J),J=1,ITEST) $ GOTO 325
  305 WRITE(4,1065)KM,(ECI(J),J=1,ITEST) $ GOTO 325
  306 WRITE(4,1066)KM,(ECI(J),J=1,ITEST) $ GOTO 325
  307 WRITE(4,1067)KM,(ECI(J),J=1,ITEST) $ GOTO 325
  308 WRITE(4,1068)KM,(ECI(J),J=1,ITEST) $ GOTO 325
  309 WRITE(4,1069)KM,(ECI(J),J=1,ITEST) $ GOTO 325
  310 WRITE(4,1070)KM,(ECI(J),J=1,ITEST) $ GOTO 325
C PRINT ALL BUT THE LAST LINE.
  325 INDEX=ITEST+1
  330 KM=KM+1
      IF((INDEX+9).GT.JEND) GOTO 340
      INDEX9=INDEX+9
      WRITE(4,1070) KM,(ECI(J),J=INDEX,INDEX9)
      IF((INDEX+9).EQ.JEND) GOTO 350
      INDEX=INDEX+10
      GOTO 330
C PRINT LAST (PARTIAL) LINE OF DATA.
  340 ITEST=JEND-INDEX+1
C ITEST IS THE NUMBER OF VALUES TO BE PRINTED IN THE LAST LINE.
      GOTO(341,342,343,344,345,346,347,348,349),ITEST
  341 WRITE(4,1081)KM,ECI(JEND) $ GOTO 350
  342 WRITE(4,1082)KM,(ECI(J),J=INDEX,JEND) $ GOTO 350
  343 WRITE(4,1083)KM,(ECI(J),J=INDEX,JEND) $ GOTO 350
  344 WRITE(4,1084)KM,(ECI(J),J=INDEX,JEND) $ GOTO 350
  345 WRITE(4,1085)KM,(ECI(J),J=INDEX,JEND) $ GOTO 350
  346 WRITE(4,1086)KM,(ECI(J),J=INDEX,JEND) $ GOTO 350
  347 WRITE(4,1087)KM,(ECI(J),J=INDEX,JEND) $ GOTO 350
  348 WRITE(4,1088)KM,(ECI(J),J=INDEX,JEND) $ GOTO 350
  349 WRITE(4,1089)KM,(ECI(J),J=INDEX,JEND)
  350 WRITE(4,1080)
C TABLE OF ASCENDING ELECTRON CONCENTRATION VALUES IS COMPLETE.
C234567890123456789012345678901234567890123456789012345678901234567890123456789012
      WRITE 1090,ZI(1),ZI(JEND)
C OUTPUT ELECTRON CONCENTRATION TO FILE 3.
      WRITE(3,1092)A,B,C,D,CD,E,EE,F,G,FG
      WRITE(3,1093)(ZI(N),ECI(N),N=1,JEND)
C CLOSING REMARKS ARE PRINTED ON SCREEN.
      WRITE 1091
 1000 FORMAT(" "/" "/" "/"  GGGG    L",8X,"OOOO",4X,"BBBBB",5X,"AAAA",4X
     *,"L",17X"AERONOMY"/" G    G   L",7X,"O    O   B    B   A    A   L"
     */" G",8X,"L",7X,"O    O   B    B   A    A   L",15X,"LABORATORY"/
     *" G  GGG   L",7X,"O    O   BBBBB    AAAAAA   L"/
     *" G    G   L",7X,"O    O   B    B   A    A   L",19X,"ROCKET"/
     *" G    G   L",7X,"O    O   B    B   A    A   L"/
     *"  GGGG    LLLLLL   OOOO    BBBBB    A    A   LLLLLL",13X,
     *"PROGRAM"/" "/" "/"* PROGRAM GLOBAL PERFORMS THE FOLLOWING TASKS:"
     *  /"   A.THE PROBE CURRENT PROFILE IS ASPECT CORRECTED IF NEEDED."
     *   / "   B.TRAJECTORY DATA IS USED TO CREATE A FILE OF PROBE CURRE
```

```
    *NT VERSUS ALTITUDE."/    "   C.N/I CALIBRATION FACTORS ARE USED TO
    * CREATE A FILE OF ELECTRON"/  5X,"CONCENTRATION VERSUS ALTITUDE."/
    *  "   D.A LINEAR ALTITUDE INTERPOLATION ROUTINE IS EMPLOYED TO PRO
    *DUCE A TABLE OF"/ 5X,  "ELECTRON CONCENTRATION IN 1/10 KILOMETER I
    *NCREMENTS."/" "/"* ENTER ROCKET TYPE AND NUMBER BELOW.")
1001 FORMAT(2A10)
1002 FORMAT(" "/"* ENTER LAUNCH DATE AND TIME.")
1003 FORMAT(3A10)
1004 FORMAT(" "/"* ENTER ZENITH ANGLE.")
1006 FORMAT(" "/"* ENTER LAUNCH SITE LOCATION.")
1008 FORMAT(" "/    "* GLOBAL USES TRAJECTORY DATA FROM FILE TRJTRY. TH
    JESE DATA ARE PRINTED BELOW TO"/    "  INSURE THEY HAVE BEEN INPUT
    JTO THE SYSTEM CORRECTLY.    (F5.1,4X,F7.3)")
1009 FORMAT(F7.1,F10.3)
1010 FORMAT(F5.1,4X,F7.3)
1011 FORMAT(" "/"* IS THE TRAJECTORY DATA CORRECT AS SHOWN?")
1012 FORMAT(1A1)
1013 FORMAT("* PLEASE RESPOND WITH YES OR NO.")
1014 FORMAT(/"* PLEASE RETYPE THE DATA IN FILE TRJTRY USING THE FORMAT
    J(F5.1,4X,F7.3)")
1015 FORMAT(" "/"* PART A - ASPECT CORRECTION."/"  IS ASPECT CORRECTION
    J NEEDED FOR ",2A10,"?")
1017 FORMAT(   /"* ASPECT CORRECTION IS ACCOMPLISHED BY MULTIPLYING THE
    J PROBE CURRENT PROFILE BY"/"  THE FUNCTION F(T)=1.0+AM*COS(2.0*PI*
    J(T-PH)/TAU)."/  "  WHAT IS THE AMPLITUDE CORRECTION FACTOR AM? (X.
    JXX)")
1018 FORMAT(1F4.2)
1019 FORMAT(" "/"* WHAT IS THE PHASE (PH) IN SECONDS? (XXX.X)")
1020 FORMAT(1F5.1)
1021 FORMAT(" "/"* WHAT IS THE PRECESSION PERIOD (TAU) IN SECONDS? ",
    J"(XX.X)")
1022 FORMAT(1F4.1)
1023 FORMAT(" "/"* AT WHAT TIME (SECONDS AFTER LAUNCH) SHOULD ASPECT ".
    J"CORRECTION BEGIN? (XXX.X)")
1024 FORMAT(/"* AT WHAT TIME SHOULD ASPECT CORRECTION STOP? (XXX.X)")
1025 FORMAT(F7.1,5E13.4)
1026 FORMAT(" THIS PROGRAM IS DESIGNED TO HANDLE ONLY 3500 PROBE ",
    J"CURRENT VALUES.")
1027 FORMAT(/"* THE PROBE CURRENT PROFILE BEGINS BEFORE THE FIRST TRAJE
    JCTORY DATA POINT. MORE"/"TRAJECTORY DATA IS NEEDED. THE FIRST PROB
    JE CURRENT OCCURRED AT ",F5.1," SECONDS"/"AFTER LAUNCH. THE FIRST T
    JRAJECTORY DATA POINT IS AT ",F5.1," SECONDS AFTER LAUNCH.")
1028 FORMAT(/"* THE PROBE CURRENT PROFILE EXTENDS PAST THE LAST ENTRY",
    J" IN THE TRAJECTORY"/"DATA. MORE TRAJECTORY DATA IS NEEDED. THE ",
    J"LAST PROBE CURRENT OCCURRED AT ",F5.1/"SECONDS AFTER LAUNCH. ",
    J"THE LAST TRAJECTORY DATA POINT IS AT ",F5.1," SECONDS AFTER"/
    J"LAUNCH.")
1029 FORMAT(" "/"* O.K. ASPECT CORRECTION FOR ",2A10/"  F(T)=1.0+",
    JF4.2,"*COS(2.0*PI*(T-",F5.1,")/",F4.1,")"/"  FOR T BETWEEN ",
    JF5.1," AND ",F5.1," SECONDS AFTER LAUNCH."/"  F(",F5.1,")=",
    JF5.3/"  F(",F5.1,")=",F5.3)
1030 FORMAT(/"* PART B - CONVERSION FROM TIME TO ALTITUDE PROFILE")
1031 FORMAT("  IS COMPLETE.   APOGEE = ",F7.3," KILOMETERS AT ",F7.3,
    J" SECONDS AFTER LAUNCH.")
```

```
1032 FORMAT(/"* PART C - CONVERSION FROM PROBE CURRENT TO ELECTRON ",
    J"CONCENTRATION PROFILE."/"  HOW MANY N/I CALIBRATION FACTORS ARE "
    J,"NEEDED FOR ",2A10,"?")
1033 FORMAT(1I1)
1034 FORMAT(/"* O.K. CALIBRATION FACTOR 1 GOES FROM GROUND LEVEL TO ",
    J"WHAT ALTITUDE?  (XXX.XX)")
1035 FORMAT(1F6.2)
1036 FORMAT(/"* WHAT IS THE VALUE OF N/I(",I1,")?  (X.XXEXX) OBSERVE ',
    J"FORMAT")
1037 FORMAT(1E7.2)
1038 FORMAT(/"* CALIBRATION FACTOR ",I1," GOES FROM ",F6.2," TO WHAT ",
    J"ALTITUDE?  (XXX.XX)")
1039 FORMAT(/"* SHOULD CALIBRATION FACTOR ",I1," BE A CONSTANT OR ",
    J"EXPONENTIAL FACTOR?  (C OR E)")
1040 FORMAT("  PLEASE COOPERATE BY RESPONDING WITH C OR E.")
1041 FORMAT(/"* N/I(",I1,")=BB*EXP((Z-CC)/DD)"/"  WHAT IS BB?  ",
    J"(X.XXEXX)")
1042 FORMAT(/"* WHAT IS CC?  (XXX.XX)")
1043 FORMAT(/"* WHAT IS DD?  (XXX.XX)")
1044 FORMAT(/"* CALIBRATION FACTOR ",I1," GOES FROM ",F6.2," TO ",F7.3,
    J" KM.  (APOGEE).")
1045 FORMAT(/"* THE N/I CALIBRATION FACTORS FOR ",2A10," ARE:")
1046 FORMAT("   00.00 TO ",0PF6.2,"  KM.  N/I(1)=",1PE8.2)
1047 FORMAT(2X,0PF6.2," TO ",0PF6.2,"  KM.  N/I(",I1,")=",1PE8.2)
1048 FORMAT(2X,0PF6.2," TO ",0PF6.2,"  KM.  N/I(",I1,")=",1PE8.2,"*EXP(
    J(Z-",0PF6.2,")/",0PF6.2,")")
1049 FORMAT(/"* PART D - ALTITUDE INTERPOLATION.")
1050 FORMAT(//13X,2A10/13X,3A10/13X,"SOLAR ZENITH ANGLE=",2A10/13X,
    J3A10)
1051 FORMAT(/2X,"ALTITUDE !",30X,"ELECTRON CONCENTRATION (CM-3) ASCENT
    J DATA",41X,"!")
1052 FORMAT(4X,"(KM)   !",113X,"!"/11X,"!",T17,"+.0",T28,"+.1",T39,
    J"+.2",T50,"+.3",T61,"+.4",T72,"+.5",T83,"+.6",T94,"+.7",T105,
    J"+.8",T116,"+.9",T126,"!"/2X,9("-"),"!",113("-"),"!")
1053 FORMAT(/"* O.K. CALIBRATION FACTOR 1 GOES FROM GROUND LEVEL ",
    J"TO APOGEE."/"  WHAT IS THE VALUE OF N/I(1)?  (X.XXEXX) ",
    J"OBSERVE FORMAT")
1061 FORMAT(6X,I3,2X,"!",99X,1P1E11.2,3X,"!")
1062 FORMAT(6X,I3.2X,"!",88X,1P2E11.2,3X,"!")
1063 FORMAT(6X,I3,2X,"!",77X,1P3E11.2,3X,"!")
1064 FORMAT(6X,I3,2X,"!",66X,1P4E11.2,3X,"!")
1065 FORMAT(6X,I3,2X,"!",55X,1P5E11.2,3X,"!")
1066 FORMAT(6X,I3,2X,"!",44X,1P6E11.2,3X,"!")
1067 FORMAT(6X,I3,2X,"!",33X,1P7E11.2,3X,"!")
1068 FORMAT(6X,I3,2X,"!",22X,1P8E11.2,3X,"!")
1069 FORMAT(6X,I3,2X,"!",11X,1P9E11.2,3X,"!")
1070 FORMAT(6X,I3,2X,"!",1P10E11.2,3X,"!")
1080 FORMAT(2X,124("-"))
1081 FORMAT(6X,I3,2X,"!",1P1E11.2,9(11X),3X,"!")
1082 FORMAT(6X,I3,2X,"!",1P2E11.2,8(11X),3X,"!")
1083 FORMAT(6X,I3,2X,"!",1P3E11.2,7(11X),3X,"!")
1084 FORMAT(6X,I3,2X,"!",1P4E11.2,6(11X),3X,"!")
1085 FORMAT(6X,I3,2X,"!",1P5E11.2,5(11X),3X,"!")
1086 FORMAT(6X,I3,2X,"!",1P6E11.2,4(11X),3X,"!")
```

```
 1087 FORMAT(6X,I3,2X,"!",1P7E11.2,3(11X),3X,"!")
 1088 FORMAT(6X,I3,2X,"!",1P3E11.2,2(11X),3X,"!")
 1089 FORMAT(6X,I3,2X,"!",1P9E11.2,1(11X),3X,"!")
 1090 FORMAT("  MINIMUM ALTITUDE=",F5.1/"  MAXIMUM ALTITUDE=",F5.1)
 1091 FORMAT(" "/" PROGRAM GLOBAL IS NOW FINISHED. REMEMBER THAT THE",
     J" TWO OUTPUT FILES ARE"/"  LOCAL FILES AND MUST BE SAVED OR ",
     J"REPLACED. OUTPUT FILE INTPL IS THE"/"  FILE WHICH CONTAINS ",
     J"THE INTERPOLATED ELECTRON CONCENTRATION IN CHART"/"  FORM. ",
     J"OUTPUT FILE ECOUT CONTAINS ALTITUDE/CONCENTRATION PAIRS IN A",
     J" FORMAT"/"  4(0PF10.2,1PE10.2) SUITABLE FOR PLOTTING.")
 1092 FORMAT(2A10/3A10/"SOLAR ZENITH ANGLE=",2A10/3A10)
 1093 FORMAT(4(0PF10.2,1PE10.2))
      STOP
      END
      SUBROUTINE TRAJ(TIME,HEIGHT)
C COMPUTES INTERPOLATED ALTITUDE VALUE FOR ANY TIME AFTER LAUNCH.
C MODIFIED FOR USE WITH PROGRAM GLOBAL. ALTITUDE AND TIME VALUES
C AT 10 SECOND INTERVALS MUST BE PROVIDED VIA ARRAYS T AND ALTI
C FOR ENTIRE PERIOD OF FLIGHT. GLOBAL READS THESE ARRAYS FROM FILE
C TRJTRY.
C INPUT  ARGUMENT:   TIME = TIME IN SECONDS AFTER LAUNCH.
C OUTPUT ARGUMENT: HEIGHT = ALTITUDE IN KILOMETERS.
C
      COMMON/Q/T(60),ALTI(60),ITCALL
      INCR=0
C IF FIRST CALL TO TRAJ, INITIALIZE VARIABLES. IF NOT SKIP TO 10.
      IF(ITCALL.GT.0) GOTO 10
      I=3
      ITCALL=1
    5 INCR=1
      IM1=I-1
      IM2=I-2
   10 IF(TIME.LT.T(IM2))WRITE 801,TIME
  801 FORMAT(" "/"TIME LESS THAN LOWEST TRAJECTORY POINT,  TIME=",F7.3)
C LOCATE TIME VALUES WHICH BRACKET PRESENT INPUT TIME VALUE.
      IF(TIME.LE.T(I)) GOTO 15
      I=I+1
      GOTO 5
C IF PRESENT TIME VALUE IS IN SAME INTERVAL AS PREVIOUS ONE,
C COMPUTE ALTITUDE WITH OLD COEFFICIENTS. IF NOT, COMPUTE NEW
C COEFFICIENTS FIRST.
   15 IF(INCR.EQ.1) GOTO 25
   20 HEIGHT=A*TIME*TIME+B*TIME+C
      RETURN
   25 BRAC1=(T(I)-T(IM1))*(ALTI(IM1)-ALTI(IM2))
      BRAC2=(T(IM1)-T(IM2))*(ALTI(I)-ALTI(IM1))
      TOP=BRAC1-BRAC2
      BRAC1=(T(IM1)-T(IM2))*(T(I)*T(I)-T(IM1)*T(IM1))
      BRAC2=(T(I)-T(IM1))*(T(IM1)*T(IM1)-T(IM2)*T(IM2))
      BOTTOM=BRAC2-BRAC1
      A=TOP/BOTTOM
      B=(ALTI(IM1)-ALTI(IM2))-A*(T(IM1)*T(IM1)-T(IM2)*T(IM2))
      B=B/(T(IM1)-T(IM2))
      C=ALTI(IM2)-A*T(IM2)*T(IM2)-B*T(IM2)
      GOTO 20
      END
```